T.C.
REPUBLIC OF TURKEY
HACETTEPE UNIVERSITY
INSTITUTE OF HEALTH SCIENCES

EVALUATION OF T CELL RESPONSES IN THE CO-CULTURES ESTABLISHED WITH NEUTROPHILS, MONOCYTES, AND LUNG ADENOCARCINOMA CELLS

M.Sc. Feyza Gül ÖZBAY

Tumor Biology and Immunology Program

M.Sc. THESIS

ANKARA

2019

T.C.
REPUBLIC OF TURKEY
HACETTEPE UNIVERSITY
INSTITUTE OF HEALTH SCIENCES

EVALUATION OF T CELL RESPONSES IN THE CO-CULTURES ESTABLISHED WITH NEUTROPHILS, MONOCYTES, AND LUNG ADENOCARCINOMA CELLS

M.Sc. Feyza Gül ÖZBAY

Tumor Biology and Immunology Program
M.Sc. THESIS

ADVISOR OF THE THESIS
Prof. Dr. Güneş ESENDAĞLI

ANKARA
2019

APPROVAL PAGE

Evaluation of T Cell Responses in the Co-Cultures Established with Neutrophils, Monocytes, and Lung Adenocarcinoma Cells

Feyza Gül ÖZBAY

Supervisor: Prof. Dr. Güneş Esendağlı

This thesis study has been approved and accepted as a Master dissertation in "Tumor Biology and Immunology Program" by the assesment committee, whose members are listed below, on 29 July 2019.

Chairman of the Committee :	*Assoc. Prof. Dr.* *İbrahim Çağatay Karaaslan* *Hacettepe University*
Advisor of the Dissertation :	*Prof. Dr. Güneş Esendağlı* *Hacettepe University*
Member :	*Assoc. Prof. Dr. Füsun Özmen* *Hacettepe University*
Member :	*Assoc. Prof. Dr. İrem Doğan Turaçlı* *Ufuk University*
Member :	*Assist. Prof. Dr. Neşe Ünver* *Hacettepe University*

This dissertation has been approved by the above committee in conformity to the relatedissues of Hacettepe University Graduate Education and Examination Regulation.

05 Ağustos 2019

Prof. Diclehan ORHAN, MD, PhD

Institute Manager

YAYIMLAMA VE FİKRİ MÜLKİYET HAKLARI BEYANI

Enstitü tarafından onaylanan lisansüstü tezimin/raporumun tamamını veya herhangi bir kısmını, basılı (kağıt) ve elektronik formatta arşivleme ve aşağıda verilen koşullarla kullanıma açma iznini Hacettepe Üniversitesine verdiğimi bildiririm. Bu izinle Üniversiteye verilen kullanım hakları dışındaki tüm fikri mülkiyet haklarım bende kalacak, tezimin tamamının ya da bir bölümünün gelecekteki çalışmalarda (makale, kitap, lisans ve patent vb.) kullanım hakları bana ait olacaktır.
Tezin kendi orijinal çalışmam olduğunu, başkalarının haklarını ihlal etmediğimi ve tezimin tek yetkili sahibi olduğumu beyan ve taahhüt ederim. Tezimde yer alan telif hakkı bulunan ve sahiplerinden yazılı izin alınarak kullanılması zorunlu metinlerin yazılı izin alınarak kullandığımı ve istenildiğinde suretlerini Üniversiteye teslim etmeyi taahhüt ederim.
Yükseköğretim Kurulu tarafından yayınlanan ***"Lisansüstü Tezlerin Elektronik Ortamda Toplanması, Düzenlenmesi ve Erişime Açılmasına İlişkin Yönerge"*** kapsamında tezim aşağıda belirtilen koşullar haricince YÖK Ulusal Tez Merkezi / H.Ü. Kütüphaneleri Açık Erişim Sisteminde erişime açılır.

- Enstitü / Fakülte yönetim kurulu kararı ile tezimin erişime açılması mezuniyet tarihimden itibaren .... yıl ertelenmiştir. [1]
- Enstitü / Fakülte yönetim kurulunun gerekçeli kararı ile tezimin erişime açılması mezuniyet tarihimden itibaren 6 ay ertelenmiştir. [2]
- Tezimle ilgili gizlilik kararı verilmiştir. [3]

5/8/19

Feyza Gül ÖZBAY

[1] *"Lisansüstü Tezlerin Elektronik Ortamda Toplanması, Düzenlenmesi ve Erişime Açılmasına İlişkin Yönerge"*

*(1) Madde 6. 1. Lisansüstü tezle ilgili patent başvurusu yapılması veya patent alma sürecinin devam etmesi durumunda, tez **danışmanının** önerisi ve **enstitü anabilim dalının** uygun görüşü üzerine **enstitü** veya **fakülte yönetim kurulu** iki yıl süre ile tezin erişime açılmasının ertelenmesine karar verebilir.*

*(2) Madde 6. 2. Yeni teknik, materyal ve metotların kullanıldığı, henüz makaleye dönüşmemiş veya patent gibi yöntemlerle korunmamış ve internetten paylaşılması durumunda 3. şahıslara veya kurumlara haksız kazanç imkanı oluşturabilecek bilgi ve bulguları içeren tezler hakkında tez **danışmanının** önerisi ve **enstitü anabilim dalının** uygun görüşü üzerine **enstitü** veya **fakülte yönetim kurulunun** gerekçeli kararı ile altı ayı aşmamak üzere tezin erişime açılması engellenebilir.*

*(3) Madde 7. 1. Ulusal çıkarları veya güvenliği ilgilendiren, emniyet, istihbarat, savunma ve güvenlik, sağlık vb. konulara ilişkin lisansüstü tezlerle ilgili gizlilik kararı, **tezin yapıldığı kurum** tarafından verilir *. Kurum ve kuruluşlarla yapılan işbirliği protokolü çerçevesinde hazırlanan lisansüstü tezlere ilişkin gizlilik kararı ise, **ilgili kurum ve kuruluşun önerisi** ile **enstitü** veya **fakültenin** uygun görüşü üzerine **üniversite yönetim kurulu** tarafından verilir. Gizlilik kararı verilen tezler Yükseköğretim Kuruluna bildirilir.*

(4) Madde 7.2. Gizlilik kararı verilen tezler gizlilik süresince enstitü veya fakülte tarafından gizlilik kuralları çerçevesinde muhafaza edilir, gizlilik kararının kaldırılması halinde Tez Otomasyon Sistemine yüklenir

** Tez **danışmanının** önerisi ve **enstitü anabilim dalının** uygun görüşü üzerine **enstitü** veya **fakülte yönetim kurulu tarafından karar verilir.***

ETHICAL DECLARATION

In this thesis study, I declare that all the information and documents have been obtained in the base of the academic rules and all audio-visual and written information and results have been presented according to the rules of scientific ethics. I did not do any distortion in data set. In case of using other works, related studies have been fully cited in accordance with the scientific standards. I also declare that my thesis study is original except cited references. It was produced by myself in consultation with supervisor (Prof. Dr. Güneş ESENDAĞLI) and written according to the rules of thesis writing of Hacettepe University Institute of Health Sciences.

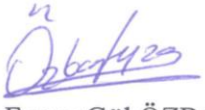

Feyza Gül ÖZBAY

ACKNOWLEDGEMENTS

I would like to express my sincere gratitude to my advisor Prof. Güneş Esendağlı for the enlightened counselling, guiding insight, his patience, motivation, and immense knowledge. His guidance steered me in the right direction throughout this study.

I would also like to thank all the faculty members, technicians, and staffs in the department of Basic Immunology for their valuable support and goodwill.

I greatly appreciate the scientific support, valuable friendship, and perpetual encouragement received by Ece Tavukçuoğlu. I would also like to thank Utku Horzum, Süleyman Can Öztürk, and Alper Kurşunel for their scientific support and help. I extend my appreciations to the other Esendagli lab members including, Diğdem Yöyen Ermiş, Sakine Ulusoy, Hamdullah Yanık, Sibel Gökşen, Sefa Özdemir, Kerim Bora Yılmaz, and Gözde Bilir who provide positive, warm and supportive atmosphere.

I owe a profound gratitude to İlker Burak Kurt for providing me unfailing support, never ending encouragement, and devoted advices.

Words are incommensurate to verbalize my thanks to my beloved parents, Yaşar and Günnur Özbay, sister Elif, brother-in-law Burhan, and my little nephew Ali Mert for their endless love, moral motivation, and always being there for me.

ABSTRACT

Özbay F.G. Evaluation of T cell responses in the co-cultures established with neutrophils, monocytes and lung adenocarcinoma cells. Hacettepe University Graduate School of Health Sciences, Tumor Biology and Immunology Master of Science Program, Ankara, 2019. $CD4^+$ and $CD8^+$ T cells are critical mediators in anti-tumor immunity. Together with neutrophils, they have been shown to dominate the immune landscape of the non-small cell lung cancer (NSCLC). A number of studies have estimated the prognostic significance of neutrophil-to-lymphocyte ratio in NSCLC. However, immune regulatory role of neutrophils has not yet been fully elucidated. Hence, this study aims to evaluate T cell responses in the presence of neutrophils, monocytes and lung adenocarcinoma cell lines, *in vitro*. Peripheral blood neutrophils, $CD14^+$ monocytes, and $CD8^+$ or $CD4^+$ T cells were purified from the healthy volunteers. In order to optimize the co-cultures, different combinations of these cell types were employed under various stimuli. Neutrophils were stimulated with different combinations of IFN-γ, G-CSF, N-acetylcysteine (NAC), and N-Formylmethionine-leucyl-phenylalanine (fMLP). At different ratios, pre-stimulated or freshly isolated neutrophils were co-cultured with NSCLC cell lines media (A549, NCI-H1299, or NCI-H441) or their conditioned with or without monocytes. Soluble anti-human CD3 mAb was added in order to test the antigen-independent influences on T cells. Proliferation, viability, activation, ROS production capacity, cytokine secretion, and expression of co-stimulatory molecules were tested on specific cell types. Based on TIM-3 expression, $CD8^+$ T cells were recovered from the co-cultures and re-stimulated to test whether the $TIM\text{-}3^{mod/high}$ subpopulation is exhausted. G-CSF and NAC stimulation promoted the PMN longevity, diminished the ROS production, and enhanced the stimulatory capacity of PMNs on T cell proliferation. The presence of lung cancer cells and monocytes prolonged the survival of neutrophils. In co-cultures, neutrophils swiftly acquired an activated state with decreased CD62L. Besides, ROS production by neutrophils was decreased in the co-cultures. The presence of monocytes, neutrophils, and lung cancer cells enhanced $CD8^+$ T proliferation and the expression of inhibitory receptors. Under certain conditions lacking monocytes as major supporters of T-cell proliferation, the presence of neutrophils together with lung adenocarcinoma cells, barely supported $CD8^+$ T cell responses. $TIM\text{-}3^{mod/high}$ $CD8^+$ T cells recovered from NSCLC co-cultures were not exhausted and displayed high proliferation and IFN-γ secretion. NAC stimulation did not modulate the $CD8^+$ T cell proliferation or TIM-3/LAG3 expression in co-cultures. Expression of 4-1BBL, OX40L and B7-2 costimulatory genes were increased in the PMNs co-cultured with lung cancer cells, monocytes and $CD8^+$ T cells. Consequently, in a co-culture setup employing neutrophils, monocytes, $CD8^+$ T cells and lung cancer cells, which was established to partially model the tumor microenvironment, our findings indicate the importance of neutrophils as a critical modulator for $CD8^+$ T cell responses.

Keywords: T cells, neutrophils, lung cancer, monocytes, costimulation

This study was supported by Hacettepe University Scientific Research Projects Coordination Unit (BAB, Grant Number, THD-2018-17436

ÖZET

Özbay F.G. T lenfosit yanıtlarının nötrofil, monosit ve akciğer adenokarsinom hücrelerini içeren ko-kültürlerde analizi. Hacettepe Üniversitesi Sağlık Bilimleri Enstitüsü, Tümör Biyolojisi ve İmmünoloji Yüksek Lisans Programı, Ankara, 2019. $CD4^+$ ve $CD8^+$ T hücreleri, anti-tümör immün yanıtlarında kritik aracılardır. Nötrofillerle beraber, küçük hücreli dışı akciğer kanserinin (KHDAK) tümör mikroçevresinde fazla miktarlarda bulundukları gösterilmiştir. Ayrıca, bir dizi çalışma, akciğer kanserinde nötrofil/lenfosit oranının prognostik önemini göstermiştir. Bununla birlikte, nötrofillerin immün düzenleyici rolü henüz tam olarak açıklanamamıştır. Bu nedenle, bu çalışma, nötrofiller, monositler ve akciğer adenokarsinom hücrelerinin varlığında T hücre yanıtlarını değerlendirmeyi amaçlamaktadır. Periferik kan nötrofilleri, $CD14^+$ monositler ve $CD8^+$ ve $CD4^+$ T hücreleri sağlıklı bireylerden toplanan kanlardan izole edilmiştir. Ko-kültürleri optimize etmek için, bu hücre tiplerinin farklı kombinasyonları ile ve çeşitli uyaranlar varlığında ko-kültürler oluşturulmuştur. Nötrofiller IFN-γ, G-CSF, NAC ve fMLP ile uyarılmıştır. Farklı oranlarda, önceden uyarılmış veya yeni izole edilmiş nötrofiller, KHDAK hücre hatları (A549, NCI-H1299 veya NCI-H441 ve/veya monositler) ile birlikte ko-kültür edilmiştir. T hücreleri üzerindeki antijenden bağımsız etkileri test etmek için çözünür anti-human CD3 monoklonal antikoru eklenmiştir. İmmün hücrelerin proliferasyonu, canlılığı, aktivasyonu, ROS üretim kapasitesi, sitokin üretimi, ve kostimülatör gen ekspresyonu belirli hücre tiplerinde test edilmiştir. TIM-$3^{mod/high}$ alt popülasyonun yorulmuş olup olmadığını anlamak için, TIM-3 ekspresyonuna göre, $CD8^+$ T hücreleri ko-kültürlerden toplanarak yeniden uyarılmıştır. G-CSF ve NAC ile uyarılan nötrofillerde, ROS üretimi düşerek canlılık süresi artmıştır ve bu nötrofillerin T hücre proliferasyonunu da desteklediği görülmüştür. Kanser hücrelerinin ve monositlerin varlığı, nötrofillerin yaşam sürelerini uzatmış, üzerlerindeki CD62L ekspresyonunu düşürmüş ve ROS üretim kapasitelilerini azaltmıştır. Monositlerin, nötrofillerin ve akciğer kanseri hücrelerinin varlığı, $CD8^+$ T hücre çoğalmasını ve üzerlerindeki inhibitör reseptörlerinin ekspresyonunu arttırmıştır. T hücre proliferasyonunun ana destekçileri olarak monositlerden yoksun olan belirli koşullar altında, akciğer kanseri hücreleri ile birlikte nötrofillerin varlığında $CD8^+$ T hücre proliferasyonu ve aktivasyonu engellenmemiştir. KHDAK ko-kültürlerinden toplanan TIM-$3^{mod/high}$ $CD8^+$ T hücreleri yüksek proliferasyon ve IFN-γ üretimi kapasitesine sahip olup yorulmamış hücre oldukları gösterilmiştir. NAC eklenen ko-kültürlerde $CD8^+$ T hücre proliferasyonu veya TIM-3/LAG3 ekspresyonu değişmemiştir. Akciğer kanseri hücreleri, monositler ve $CD8^+$ T hücreler ile birlikte kültürlenen nötrofillerde 4-1BBL, OX40L ve B7-2 kostimülatör genlerinin ekspresyonu artmıştır. Nötrofiller, monositler, $CD8^+$ T hücreleri ve akciğer kanseri hücrelerini kullanarak tümör mikroçevresini kısmen modellemek için kurulan bir ko-kültür düzeninde, bulgularımız nötrofillerin $CD8^+$ T hücre yanıtları için kritik bir modülatör olarak önemini göstermektedir.

Anahtar Kelimeler: T hücre, nötrofil, akciğer kanseri, monosit, kostimülasyon.

Bu çalışma Hacettepe Üniversitesi Bilimsel Araştırmalar Birimi tarafından desteklenmiştir. (Proje No: THD-2018-17436)

CONTENTS

APPROVAL PAGE iii
YAYIMLAMA VE FİKRİ MÜLKİYET HAKLARI BEYANI iv
ETHICAL DECLARATION v
ACKNOWLEDGEMENTS vi
ABSTRACT vii
ÖZET viii
CONTENTS ix
LIST OF ABBREVIATIONS xii
FIGURES xv
TABLES xviii
1. INTRODUCTION 1
2. LITERATURE OVERVIEW 4
2.1. Polymorphonuclear Leukocytes (PMNs) 4
2.1.1. Origin and Maturation of PMNs 4
2.1.2. Migration of PMNs 11
2.1.3. Functions of PMNs 15
2.1.4. Subsets of PMNs 17
2.1.5. Influence of PMNs on T cell responses 20
2.2. Lung Cancer 22
2.2.1. Classification of Lung Cancer 23
2.3. Immune Response in NSCLC 24
2.3.1. PMNs in NSCLC 27
2.3.2. T Cell Responses in NSCLC 28
2.3.3. Tumor-associated Macrophages in NSCLC 31
2.3.4. Other immune cells in NSCLC 31
3. MATERIALS AND METHODS 35
3.1. Materials Used in This Study 35
3.2. Buffers and Solutions 36
3.3. Cell Culture and Purification 37
3.3.1. Cell Culture 37
3.3.2. Freezing and Thawing of Cell Lines 38

3.3.3. Cell Counting 39
3.3.4. Isolation of the cells and Cell Sorting 40
3.3.5. Establishment of Co-cultures: 45
3.3.6. 3-(4, 5-dimethylthiazolyl-2)-2, 5-diphenyltetrazolium bromide (MTT) cell viability assay: 46
3.4. Immunological Techniques 47
3.4.1. Flow Cytometry Analysis 47
3.5. Molecular Techniques 51
3.5.1. Total RNA isolation and spectrophotometric analysis 51
3.5.2. cDNA synthesis 51
3.5.3. Polymerase chain reaction (PCR) 52
3.5.4. Real-time PCR (RT-PCR) 54
3.5.5. Agarose gel electrophoresis 56
3.6. Statistical analysis 57
4. RESULTS 58
4.1. Preliminary analyses on PMN for the establishment of co-culture conditions 58
4.1.1. Assessment of the PMN viability 58
4.1.2. Assessment of PMN activation 66
4.1.3. The influence of PMNs on T cell proliferation 71
4.2. Assessment of $CD8^+$ T cell responses in the co-cultures of PMNs, monocytes and NSCLC cells 77
4.2.1. $CD8^+$ T cell proliferation in the co-cultures 77
4.2.2. $CD8^+$ T cell activation in the co-cultures 78
4.2.3. $CD8^+$ T cell-related cytokine production in the co-cultures 83
4.2.4. $CD8^+$ T cell exhaustion in the co-cultures 85
4.3. Potential influence of PMN in the co-cultures 88
4.3.1. ROS production and $CD8^+$ T cell responses 88
4.3.2. The costimulatory gene expression in PMNs 91
5. DISCUSSION 93
6. RESULTS AND RECOMMENDATION 106
7. REFERENCES 108
8.APPENDICES

APPENDIX 1: Ethics Committee Approval

APPENDIX 2: Scientific meetings where the data of this thesis were presented.

APPENDIX 3: Thesis Orijinality Report.

APPENDIX 4: Digital Receipt

9. CURRICULUM VITAE

LIST OF ABBREVIATIONS

αCD3	anti-CD3 monoclonal antibody
APC	Antigen presenting cells
BAFF	B-cell activating factor
BALTs	Bronchus-associated lymphoid tissues
BaP	Basophil lineage-committed progenitor
BM	Bone marrow
CD	Cluster of differentiation
C/EBP	CCAAT/enhancer binding protein
CLP	Common lymphoid progenitor
CM	Conditioned media
CMP	Common myeloid progenitor
COX-2	Cyclooxygenase-2
CTLA-4	Cytotoxic T-lymphocyte antigen-4
DAMPs	Damage associated molecular patterns
DC	Dendritic cell
EoP	Eosinophil-lineage committed progenitor
FACS	Fluorescence-activated cell sorting
FBS	Fetal bovine serum
FGL1	Fibronogen-like protein 1
fMLP	N-Formylmethionine-leucyl-phenylalanine
FoxP3	Forkhead box protein 3
Gal-9	Galectin-9
G-CSF	Granulocyte colony-stimulating factor
Gfi-1	Growth factor independence 1
GM-CSF	Granulocyte-macrophage colony-stimulating factor
GMPs	Granulocyte-monocyte progenitors
HSC	Hematopoietic stem cells
ICAM-1	Intercellular adhesion molecule-1
ICOS	Inducible T cell co-stimulator
ICOS-LG	Inducible T cell co-stimulator ligand
IDO	Indoleamine 2,3-dioxygenase

IFN	Interferon
IL	Interleukin
JAK	janus-activated kinase
LAG3	Lymphocyte activation gene
LAMP	Lysosome associated membrane protein
LEF-1	Lymphoid enhancer-binding protein
MDSC	Myeloid-derived suppressor cells
MEP	Megakaryocyte-erythroid progenitors
MFI	Mean fluorescence intensity
MHC	Major histocompatibility complex
MPO	Myeloperoxidase
MPPs	Multipotent progenitors
NAC	N-acetylcysteine
NE	Neutrophil elastase
NET	Neutrophil extracellular traps
NF-κB	Nuclear factor-κB
NK	Natural killer
NO	Nitric oxide
NSCLC	Non-small cell lung cancer
PAMPs	Pathogen-associated molecular patterns
PGE	Prostaglandin E
PD-1	Programmed-cell death-1
PD-L1	Programmed-cell death ligand-1
PI	Propidium iodide
PMN	Polymorphonuclear leukocyte
PSGL1	P-selectin glycoprotein ligand 1
PRRs	Pattern recognition receptors
PU.1	PU box binding-1
ROS	Reactive oxygen species
Runx1	Runt-related transcription factor 1
SCLC	Small cell lung cancer
STAT	Signaling transducers and activators of transcription

TAM	Tumor-associated macrophages
TAN	Tumor-associated neutrophils
TAP1	Transporter associated with antigen processing type 1
TCR	T cell receptor
TGF-β	Transforming growth factor beta 1
TIL	Tumor-infiltrating lymphocyte
TIM-3	T-cell immunoglobulin and mucin domain-containing protein-3
TRAIL	Tumor necrosis factor-related apoptosis-inducing ligand
Treg	Regulatory T cell
VEGF	Vascular endothelial growth factor

FIGURES

Figure		Page
2.1.	Major steps in the hematopoiesis.	6
2.2.	Proteins and transcription factors involved in terminal granulopoiesis.	10
2.3.	Mature segmented neutrophils. May-Grünwald-Giemsa stain.	11
2.4.	The neutrophil recruitment cascade. a) paracellular transmigration, b) transcellular transmigration.	14
2.5.	Neutrophil antimicrobial activities after it migrates into the injured tissue.	15
2.6.	Three phases of immune responses against tumor cells: elimination, equilibrium, and escape.	25
2.7.	Schematic demonstration of anti-tumor and pro-tumor responses in NSCLC.	33
3.1.	Schematic drawing of Fuchs-Rosenthal Counting Chamber (Hausser Scientific, USA) through microscope.	39
3.2.	PBMC and PMN separation by biphasic density gradient centrifugation.	40
3.3.	The gating strategies for the purification of $CD4^+$ and $CD8^+$ T cells from the isolated PBMCs of healthy volunteers by FACS.	42
3.4.	The gating strategies for the purification of $CD15^+$ PMNs from the co-cultures containing $CD8^+$ T cells, monocytes and lung adenocarcinoma cells by FACS.	43
3.5.	$CD8^+$ T cells were back-sorted from the co-cultures containing monocytes, PMNs and lung adenocarcinoma cells according to TIM-3 surface expression levels.	43
3.6.	Confirmation of the purity of $CD14^+$ monocytes isolated by MACS.	44
3.7.	Confluency of the A549, NCI-H1299 and NCI-H441 after 72h of incubation.	45
3.8.	Optical densities (OD) of A459, NCI-H1299 and NCI-H441 cells seeded at different numbers.	47
3.9.	50 bp DNA ladder.	57
4.1.	24, 48, and 72h PMN viability upon exposure to G-CSF, NAC, fMLP and IFN-γ.	59
4.2.	At 48h, PMN viability upon exposure to G-CSF, NAC, fMLP and IFN-γ.	60
4.3.	The effect of the removal of stimulants on PMN viability after PMNs were exposed to these stimulants for 24h.	62
4.4.	PMN viability in PBMC co-cultures.	63
4.5.	PMN viability in the presence of lung cancer cells.	65

4.6. Representative flow cytometry histograms showing the PI and DRAQ7 staining of PMNs cultured with monocytes and lung cancer cells. 66

4.7. ROS levels in PMNs treated with G-CSF and fMLP in the presence or absence of NAC. 67

4.8. ROS production of PMNs in response to monocytes and lung cancer cells. 68

4.9. CD66b, CD62L and CD11b expression on PMNs in the co-cultures with lung cancer cells. 69

4.10. Representative histograms showing the expression of CD66b, CD62L, and CD11b on PMNs. PMNs 70

4.11. Proliferation of T cells amongst PBMCs co-cultured with PMNs. 72

4.12. Proliferation of αCD3-stimulated PBMCs in the presence of freshly isolated and 24h cultured PMN. 73

4.13. Proliferation of $CD4^+$ and $CD8^+$ T cells in the co-cultures established with lung cancer cells or their conditioned media with or without PMNs and monocytes. 75

4.14. Proliferation of $CD8^+$ cells in the co-cultures established with different ratios of PMNs and monocytes. 76

4.15. Proliferation of $CD8^+$ T cells co-cultured with pre-confluent lung cancer cells, PMN and monocytes at PMN:monocyte:T cell 1:0.125:1 ratio. 78

4.16. Expression of CD137, CD69, CD25 and CD107a on $CD8^+$ T cells co-cultured with PMN, monocytes and lung cancer cells. 80

4.17. Expression of inhibitory receptors on $CD8^+$ T cells from 72h of co-cultures with PMNs, monocytes and lung cancer cells. 81

4.18. Representative histograms showing the expression of CD137, CD69, CD25, CD107a, TIM-3, CTLA-4 and PD-1 expression on $CD8^+$ T cells from different co-culture settings. 82

4.19. Schematic demonstration of CD137, CD69, CD25, CD107a, TIM-3, LAG3, CTLA-4, and PD-1 expression on $CD8^+$ T cells from different co-culture settings. 83

4.20. IFN-γ, IL-4, and IL-6 cytokine levels in the supernatants collected from the 72h co-cultures of PMN, monocytes and lung cancer cells under 25ng/mL αCD3 stimulation. 84

4.21. Schematic demonstration of IFN-γ, IL-4, IL-6, Granzyme A, Granzyme B, IL-17, and IL-10 production from different co-culture settings. 85

4.22. The change in the TIM-3 expression on $CD8^+$ T cells in the lung cancer cells containing co-cultures at 72h in the presence of different PMN ratio under αCD3 mAb (25 ng/ml) stimulation. 86

4.23. Re-stimulation capacity of $CD8^+$ T cells recovered from the co-cultures. 87

4.24. Cytokine levels secreted by TIM-$3^{-/lo}$ and TIM-$3^{mo/h}$i $CD8^+$ T cells induced by PMA (5ng/mL) and ionomycin (2 μg/mL) for 16h were assessed by Multiplex bead-based flow cytometric array 88

4.25. ROS levels of PMNs co-cultured with monocytes, $CD8^+$ T cells and lung cancer cells under 25ng/mL αCD3 stimulation. 89

4.26. Effect of NAC on $CD8^+$ T cell proliferation and TIM-3/LAG3 expression in PMN containing co-cultures. 90

4.27. Expression of the co-stimulatory molecules in PMNs purified from co-cultures with monocytes, $CD8^+$ T cells and lung cancer cells under 25 ng/mL αCD3 stimulation was studied with RT-PCR. 92

TABLES

Table		Page
3.1.	Antibodies used in flow cytometric analysis.	48
3.2.	cDNA synthesis reaction set-up.	52
3.3.	Forward and reverse primer sequences of the genes and related information.	52
3.4.	PCR components and reaction mixture.	53
3.5.	Gradient PCR program for B7-1, B7-2, B7-H2, TNSFS9, TNFSF4 and TNFSF14.	54
3.6.	Specific annealing temperatures assessed after gradient PCR.	54
3.7.	Real-time PCR components and related information.	55
3.8.	Real-time PCR Thermal Cycling Protocol.	56

1. INTRODUCTION

The interplay between tumor cells and their local environment determines the outcome of the immune responses in cancer (1-3). In non-small cell lung cancer (NSCLC), T cells and neutrophils have been shown to prevail in the tumor microenvironment (4). Besides, a number of studies have estimated the prognostic significance of neutrophil-to-lymphocyte ratio in lung cancer (5-6). However, immune regulatory role of neutrophils has not yet been fully elucidated. Neutrophils were long thought to be the principal innate immune cells. More recently, they were identified with the capacity to shape adaptive immunity through secretion of soluble mediators or contact-dependent mechanisms (7-8). Both pro-tumor and anti-tumor roles of neutrophils have been reported (9). Thus, investigating the interaction of neutrophils and other immune cells, especially T cells found in the tumor microenvironment may help to better understand tumor immunology and may have implications for the immunotherapy approaches.

Anti-tumor immune responses primarily rely on $CD4^+$ and $CD8^+$ T cells. A triumphant cytotoxic activity against tumor cells is mediated by effective antigen presentation either from antigen presenting cells (APCs) (mainly macrophages and/or dendritic cells) or tumor cells through MHC molecules (1). In NSCLC, high levels of $CD4^+$ and $CD8^+$ T cells in the lung tumor microenvironment are associated with improved survival. On the other hand, APCs were shown to display reduced MHC II expression (2). Inhibitory cytokines produced in the tumor microenvironment can promote Treg differentiation and hinder effector functions of $CD8^+$ lymphocytes (3). After recognition of an antigen, a second signal for T cell activation is mediated by the interaction between co-stimulatory molecules expressed on APCs and cognate receptors on the T cells. For efficient clonal expansion and differentiation of T cells autocrine and paracrine cytokine signaling is also required (4). The fate of T cells function is determined by costimulatory receptors expressed on T cells. Following activation, co-inhibitory receptors (i.e. PD-1, CTLA-4, TIM-3, and LAG3) emerge on the surface of T cells in order to limit aberrant and autoreactive T cell responses (5). Tumor cells, which express ligands for these receptors can escape from the immune attack by inhibiting T cell activation. For instance; in NSCLC, high levels of PD-L1 expressing tumors are associated with decreased numbers of tumor-associated T

lymphocytes (TILs) and better response to anti-PD-1 therapy (6). The frequent detection of inhibitory ligands in NSCLC and upregulation of the receptors on TILs emphasize the potential usage of checkpoint blockade therapies (7, 8).

Recent studies have reported that neutrophils can influence the functions of T cells. They can act as an antigen presenting cells (APCs) for Th cells or cross-present antigens to $CD8^+$ T cells (9, 10). Under physiological conditions, neutrophils are rarely found in the lung environment; however, upon inflammation or infection they can recruit in large numbers. There are conflicting results about the function of neutrophils in NSCLC. Although high neutrophil infiltration is often associated with poor prognosis, some studies reported their anti-tumor function, as well (11). Recent studies have also found a link between the accumulation of myeloid derived suppressor cells (MDSC)-like immature cells and tumor progression. High amount of PMN-MDSCs often correlates with poor survival in NSCLC (12).

This study aims to establish an *in vitro/ex vivo* co-culture model employing neutrophils, monocytes, $CD8^+$ T cells and NSCLC cell lines that may be a suitable in vitro system to determine the role of neutrophils in $CD8^+$ T cell responses. Preliminary optimizations were performed on PMNs for the establishment of co-culture conditions. G-CSF was used to enhance the survival of PMNs. Inflammatory factor IFN-γ and antigenic factor fMLP were used to give adaptive and innate immunity-related stimuli, respectively, In order to reduce the effects of ROS, PMNs were also stimulated with NAC. A549, NCI-H1299, and NCI-H441 cell lines were used in this study as a model for NSCLC. Viability and activation of PMNs were evaluated in the presence of NSCLC cell lines or their conditioned media. $CD4^+$ and $CD8^+$ T cell proliferation were determined in the co-cultures containing lung cancer cells, monocytes, and neutrophils in the presence of αCD3 mAb as the first signal for T cells. The expression of activation and exhaustion-related markers, cytokine production capacities of co-cultured $CD8^+$ T cells were investigated. Next, the potential role of PMNs in $CD8^+$ T cells' responses was investigated in terms of ROS production and costimulatory gene expression.

Here, the viability of PMNs was supported in the presence of G-CSF, lung cancer cells or their conditioned media. ROS production of PMNs were diminished with NAC stimulation and in the presence of lung cancer cells or their conditioned

media. When G-CSF- and NAC-stimulated-PMNs co-cultured with allogenic PBMCs, they significantly facilitate the T cell proliferation. On the other hand, PMNs stimulated with IFN-γ and fMLP did not alter the T cell proliferation. PMNs became spontaneously activated after 24h incubation with decreased CD62L. In the presence of lung cancer cells or their conditioned media delayed but not inhibit the activation of PMNs. Intriguingly, in the co-cultures with PMNs, monocytes, and lung cancer cells, T cell responses were enhanced in a contact-dependent manner. In the absence of myeloid cells, lung cancer cells did not promote T cell proliferation. $CD8^+$ T cell and PMN co-cultures positively influenced T cells, albeit not reaching to the level of monocyte-stimulated T cells. In the co-cultures, increased expression of CD137, CD69, CD25, and CD107a was observed on $CD8^+$ T cells even if when together with lung cancer cells. High levels of IL-6, IL-4, and IFN-γ was detected in the co-cultures; however heterogeneity was observed according to the NSCLC cell lines included. Upregulation of inhibitory receptors (PD-1, CTLA4, TIM-3, and LAG3) were detected on $CD8^+$ T cells; particularly TIM-3 levels were prominent but it was not associated with T cell exhaustion. ROS production was diminished in lung cancer cells-co-cultured PMNs. Further inhibition of ROS by NAC treatment, did not alter T cell stimulatory capacity of PMNs. Upregulation of CD86, OX40L, and 4-1BBL mRNA in PMNs purified from the co-cultures of monocytes, $CD8^+$ T cells, and lung cancer cells was also detected as a possible mechanism promoting PMNs' influence on T cells.

All in all, a co-culture setup employing neutrophils, monocytes, $CD8^+$ T cells and lung cancer cells was created to partially model the tumor microenvironment in NSCLC, the current data indicate considerable role of neutrophils in the modulation of $CD8^+$ T cell responses in anti-tumor immunity.

2. LITERATURE OVERVIEW

2.1. Polymorphonuclear Leukocytes (PMNs)

Polymorphonuclear leukocytes (PMNs), also knowns as granulocytes, constitute the vast majority of white blood cells in human (13). Morphologically, they have multi-lobed nuclei and varying cytoplasmic granules (14). PMNs are comprised of eosinophils, basophils and neutrophils. PMNs are named according to their distinctive staining patterns with hematoxylin and eosin. Mature resting PMNs in human blood express CD15, CD66b, CD16, CD62L, CD11b, CD11a, CD11c and CD68 on their surfaces, while mouse PMNs are characterized with CD11b, Gr-1/Ly6G, Ly6C surface markers (15). PMNs are the key mediators of the innate immune system. They generally patrol the body, seek out foreign invaders and provide the first line of defense. Their principal role in the innate immune responses is to act as guards: recognizing foreign invaders and eliminating them. Eosinophils and basophils are the major effectors against parasitic infections and allergic responses. On the other hand, neutrophils are rapidly recruited to the infected or injured tissues, in which they destroy invaders by multiple mechanisms both intra- and extracellularly (16, 17). In human, neutrophils account for 40-75% of leukocytes, whereas eosinophils and basophils occupy a minority of leukocyte population. (18, 19). Due to their abundance and short life-span, around 10^{11} neutrophils are continuously generated in human bone marrow daily (20). Identification of distinct subsets of PMNs and the network between PMNs and adaptive immunity emerge as novel concepts driving the attention of immunologists (21-23).

2.1.1. Origin and Maturation of PMNs

PMNs are considered as short-lived cells in the circulation and they must be replenished. Thus, they have to be continuously generated in the bone marrow from myeloid precursors. A complex process called Haematopoiesis is comprised of multiple proliferation and differentiation events, occurs during embryonic development and throughout an individual's life. (19). Three organs (liver, spleen and bone marrow) are haematopoietically active in the prenatal period. Soon after the birth, this process becomes restricted to bone marrow (24). Hematopoietic stem cells (HSC)

reside in the bone marrow are capable of self-renewal and produce daughter stem cells; meanwhile, they give rise to a pool of differentiating cells. Progenitor cells produced by HSC eventually become mature blood cells (25).

Once HSCs differentiate into multipotent progenitors (MPPs), MPPs can go through either lymphoid lineage (CLP, common lymphoid progenitor) or myeloid lineage (CMP, common myeloid progenitor). T and B lymphocytes, NK cells and dendritic cells are generated from CLP. Granulocyte-monocyte progenitors (GMPs) and Megakaryocyte-erythroid progenitors (MEPs) branch from CMP. Afterwards, MEPs differentiate into either erythroid/red blood cells or megakaryocytes. On the other hand, GMPs lead to monocytes (further macrophages), PMNs and mast cells (26). Primitives of PMNs originated from GMPs further differentiate into functionally active cells, this process is known as granulopoiesis. Since PMNs account for the vast majority of white blood cells, granulopoiesis makes up the greatest percentage of hematopoiesis. In myeloblast to promyelocyte transition, a switch from proliferation into differentiation is observed (26-28). After promyelocyte stage, cells can no longer divide, rather differentiate into their matured form. Myeloblasts and promyelocytes derived from GMPs are the first elements of granulopoiesis. Subsequently, these cells lead to myelocyte, metamyelocyte, band cell and eventually segmented mature neutrophils (Figure 2.1) (29). Granulopoiesis encompasses series of maturational steps during which granulocytic differentiation and morphological changes occur. Primary azurophilic granules are formed during promyelocyte stage, secondary specific granules in myelocyte stage, tertiary gelatinase granules in metamyelocyte and secretory vesicles in the last stages of differentiation. Large and round nucleus morphs into a kidney-like nucleus during the transition of myelocytes into metamyelocytes. A band-like nucleus are further produced in band neutrophils and ultimately band shaped nucleus shades into the segmented nucleus in mature neutrophils (Figure 2.2) (14).

Eosinophils and basophils undergo similar stages of differentiation with neutrophils; however, they are less frequent in the bone marrow. In mouse, eosinophils are derived from eosinophil-lineage committed progenitor (EoP) which is a population downstream of the GMP. Likewise, basophil lineage-committed progenitor (BaP) derived from GMP branch into Basophils. In contrast, EoP and BaP (derivates of eosinophil and basophils) are directly derived from CMP in human hematopoiesis

(30). Eosinophils have secondary specific granules and two-lobed nucleus. Basophils have secondary specific granules and bean-shaped nucleus. (31, 32).

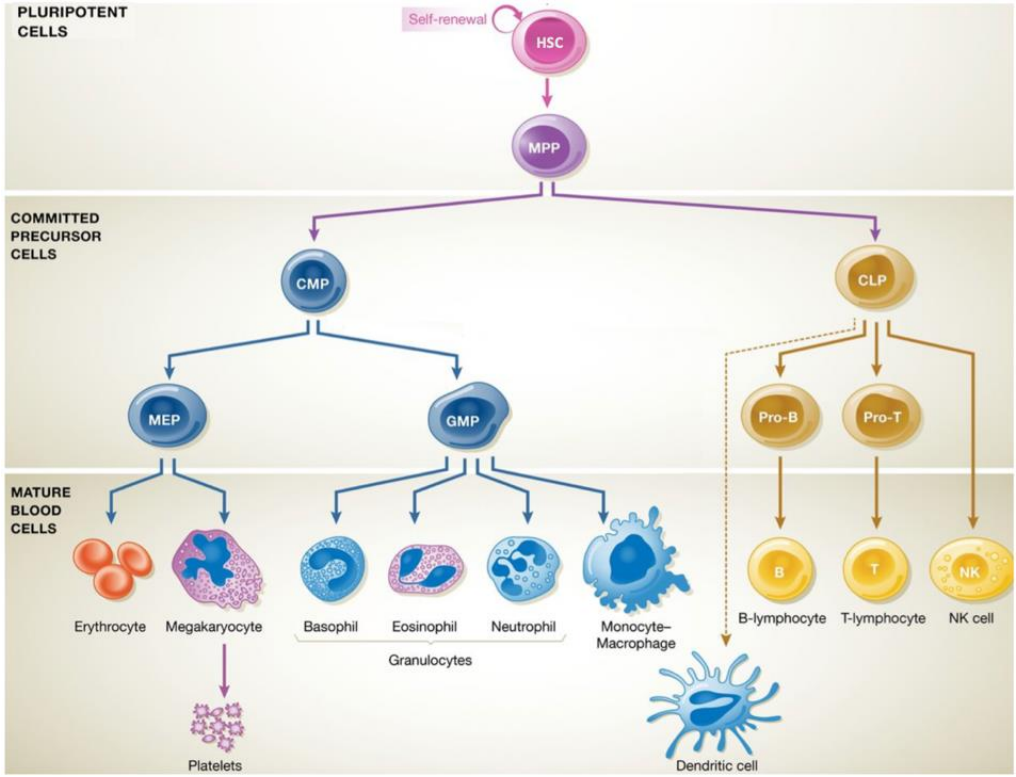

Figure 2.1. Major steps in the hematopoiesis **(33).**

Hematopoiesis is modulated by several growth factors (colony stimulating factors CSFs) including granulocyte-macrophage colony stimulating factor (GM-CSF), granulocyte colony stimulating factor (G-CSF), macrophage colony stimulating factor (M-CSF), multipotential colony stimulating factor (Multi-CSF), and erythropoietin (34). These growth factors are heavily involved in the differentiation of specific blood cells. For instance, G-CSF and GM-CSF are responsible for the generation of PMNs. The blockade of either G-CSF or its receptor G-CSFR in mice leads to neutropenia (35). Moreover, administration of G-CSF results in expansion of neutrophils. Nowadays, G-CSF is used to treat cyclic, acquired and congenital neutropenia and chemotherapy-related neutropenia (36).

Cytokines are critical modulators for hematopoiesis. Interleukin 1 (IL-1) and tumor necrosis factor (TNF) are some of these modulators. Following a pathogen

challenge, many proinflammatory cytokines are produced. IL-1 and TNF-α are critical proinflammatory cytokines (32). When emergency granulopoiesis orchestrates the recruitment of an elevated number of neutrophils from the bone marrow into blood circulation, neutrophilia emerges. Neutrophilia is mediated by inflammatory cytokines such as GM-CSF and G-CSF (37). Under the influence of IL-3, hematopoietic progenitor cells or bone marrow stromal cells may produce IL-6, GM-CSF, and G-CSF which further assist granulopoiesis (36). It was shown that loss of IL-6 aggravates neutropenia resulted from the loss G-CSFR. In addition, IL-6 is involved in primary granule formation in the myeloblast/promyelocyte transition stage of neutrophil granulopoiesis (38).

Granulopoiesis is regulated by the actions of specific transcription factors (Figure 2.2). PU box binding-1 (PU.1), CCAAT/enhancer binding protein α (C-/EBP-α), runt-related transcription factor 1 (Runx1), growth factor independence 1 (Gfi-1) and CCAAT enhancer-binding protein 8 (C/EBP-ε) are the major transcription factors in granulopoiesis (39). PU.1 has a major modulator role in lineage choice of myeloblasts towards granulocytes or monocytes. Decreased PU.1 expression and increased C-/EBP-α favor granulocytic differentiation. Depletion of Runx1 gene in the bone marrow gives rise to disruption of granulopoiesis (40). C-/EBP-α targets the other transcription factors involved in granulopoiesis. Gfi-1 is one of these transcription factors and was shown to be critical in neutrophil maturation at the promyelocyte stage related to formation of secretory vesicles and gelatinase granules. Gfi-1 also promotes the secretion of monocyte lineage promoting factors such as M-CSF (41). Another transcription factor affected by C-/EBP-α is C/EBP-ε, which has an essential role in promyelocyte to myelocyte transition and its expression peaks in myelocytes and metamyelocytes (Figure 2.2). Loss of C/EBP-ε does not affect initial steps of granulopoiesis, rather leads to a failure in terminal differentiation and maturation (42). GCSF receptor gene and myeloperoxidase (MPO) is also induced by C-/EBP-α (43). Cytokines in granulopoiesis have been shown to activate signal transducers and activators of transcription proteins (STATs) which are latent transcription factors involved in growth factor and cytokine receptor signaling. STATs are essential for cell survival, growth, motility, and differentiation. STAT5 can be

activated by IL-3 and GM-CSF; STAT3, STAT1, and STAT5 can be activated by G-CSF. (44, 45).

Neutrophil elastase (NE) is a serine proteinase found in neutrophils, mast cells, and monocytes. NE is synthesized in the early stages of granulopoiesis and stored in azurophilic granules. Mature neutrophils do not produce NE, but rather keep them in their granule contents. In response to various stimuli, they release NE together with other granule contents. NE plays role in breaking down the proteins released from foreign invaders and recruiting many inflammatory cytokines into this site (46).

Lymphoid enhancer-binding protein (LEF-1) is a crucial transcription factor in granulopoiesis. Its target genes such as c-Myc, C/EBP-alpha, cyclin, and survivin are critical for the survival and proliferation of neutrophils. c-Myc induces proliferation but inhibits cell differentiation. With decreased C/EBP-α levels and increased c-Myc expression, granulocytic differentiation is diminished (47).

In terminal granulopoiesis, as the cells become mature, cell size and nuclear volume decrease, cell mobilization is enhanced. Distinct granule subsets are formed during terminal neutrophil granulopoiesis. These granules share a common matrix that contains proteins responsible for exocytosis and a phospholipid bilayer membrane; however, they differ in their protein content at which stage they are produced (29). Sequential formation of granules during granulopoiesis is initiated at myeloblast/promyelocyte transition. Azurophilic (primary), secondary (specific) and tertiary (gelatinase) granules are formed respectively (Figure 2.2). Early produced granules known as primary granules are characterized by high amounts of myeloperoxidase (MPO) (48). Transcription factors involved in azurophilic granule formation are GATA-binding factor 1 (GATA-1) and CCAAT/enhancer binding protein. Moreover, cell proliferation inducer and cell differentiation blocker transcription factors such as c-Myc and acute myeloid leukemia-1 (AML-1) impair azurophilic granule formation. In addition to MPO, various proteins constitute azurophilic granules such as serine proteases (elastase, proteinase 3, cathepsin G) and microbicidal peptides (defensin, azuracidin, and bacterial permeability increasing protein) (Figure 2.2) (49).

MPO production is terminated at the later stages of granulopoiesis. Simultaneously, specific granules and gelatinase granules are formed after primary

granules. They are known as peroxidase-negative granules. Specific granules reside in myelocytes and metamyelocytes. These granules are rich in proteins which participate in microbicidal activities (50). Lactoferrin has a direct bactericidal activity by disrupting and destabilizing bacterial cell membrane. Additionally, releasing lactoferrin from the granules intensifies cathepsin G and serine proteases activation, thereby fostering innate immune responses during inflammation (51). C/EBPε is a transcription factor specific for specific granules and its expression peaks in myelocyte sand metamyelocytes (Figure 2.2). In C/EBPε deficient mice, neutrophils are defective in nucleus shape, respiratory burst production and bacterial activity (42). Moreover, decreased expression of c-Myc and AML-1 blocks azurophilic granule formation and thus accelerates specific granule formation (52).

Gelatinase granule formation is initiated by the transition of metamyelocytes to band nucleus. Cell proliferation halts at metamyelocytes wherein neutrophil differentiation begins. Gelatinase granules are highly enriched for gelatinases (26). Arginase 1(Arg1) is a major gelatinase protein, which metabolizes nitric oxide (NO). NO modulates various functions of neutrophils such as phagocytosis, generation of respiratory burst and neutrophil extracellular traps (NET) formation. After ARG1 metabolizes NO, it can no longer be a substrate for nitric oxide synthase (NOS). Thus, this reaction gives rise to loss of NO, thereby hindering proinflammatory responses (53). In gelatinase granule formation, expression of several antiproliferative genes, AML-1, C/EBP-γ, and CDP are pronounced, whereas expression of various proliferative genes, C/EBP-δ and C/EBP-ζ, is inhibited. Additionally, C/EBP-ε levels, which is a key modulator for secondary granule formation, are decreased, as C/EBP-β, C/EBP-δ and C/EBP-ζ levels are elevated (Figure 2.2) (42).

At the last stage of terminal granulopoiesis, secretory vesicles are formed in segmented neutrophils (Figure 2.2). In these secretory vesicles, the expression of several membrane-associated receptor is elevated. Some of these membrane-associated receptors are CD16, CD15, CD10, CD35, CD11b, CD18, LFA-1 and MMP-25 (54). These receptors are critical for neutrophils to retain firm contact with the vascular endothelium, enter into inflamed tissue, migrate through the inflammation site by chemotaxis and finally eliminate the pathogens. Once the neutrophils become fully matured, they acquire exocytosis capacity. In neutrophils, secretory vesicles are

designated most exocytosed organelles. (55). Mature segmented peripheral blood neutrophils are depicted in Figure 2.3.

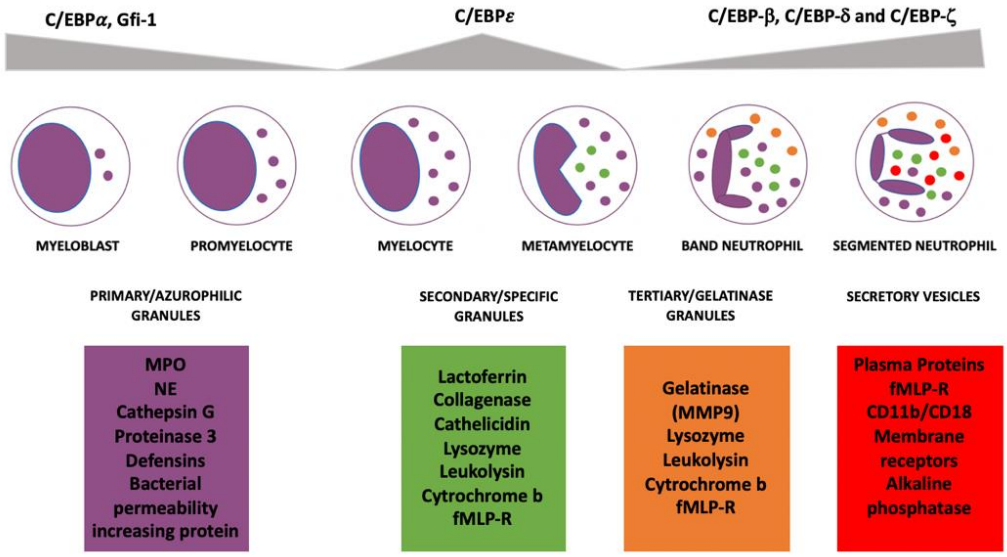

Figure 2.2. Proteins and transcription factors involved in terminal granulopoiesis.

There are two types of granulopoiesis: steady-state granulopoiesis and emergency granulopoiesis. Under physiological conditions, neutrophils are maintained from hematopoietic stem cells and progenitor cells in bone marrow by steady-state granulopoiesis. During infection or inflammation, there is a higher demand for neutrophils for host defense. Since a high number of neutrophils is consumed and should be replenished during the immune responses, granulopoiesis is switched from steady state granulopoiesis to emergency granulopoiesis (35, 56). Since C/EBP-β exerts less inhibitory control towards cell cycle, C/EBP-β is latent in emergency granulopoiesis, while C/EBP-α is a key modulator in steady state granulopoiesis (28). In emergency granulopoiesis, both mature and immature neutrophils enter the circulation. Thus, the heterogeneity in circulating neutrophils of an infected patient can result from emergency granulopoiesis (57).

In the bone marrow, C-X-C Motif Chemokine Ligand 12 (CXCL12) also known as stromal derived factor-1 (SDF-1) is constitutively expressed by osteoblasts and perivascular cells. The receptor for CXCL12 is C-X-C chemokine receptor type 4 (CXCR4) is expressed on neutrophils. CXCR4-CXCL12 interaction retains the

neutrophils in the bone marrow and plays a significant role in maintaining their homeostasis (58). CXCR2 is also expressed on neutrophils. CXCR2 and CXCR4 together exerts opposing actions in regulating the migration and mobilization of neutrophils. Along with the maturation, CXCR2 expression on neutrophils are augmented and CXCR4 expression is declined simultaneously. Thus, neutrophils display less affinity to CXCL12 and are released from the bone marrow (58).

G-CSF is a major mediator of polymorphonuclear neutrophil production in both steady state and emergency granulopoiesis. G-CSF known as a critical survival factor upregulates CXCR2 expression on neutrophils and downregulate SDF-1 in bone marrow cells. Thus, it stimulates neutrophil release from bone marrow (59).

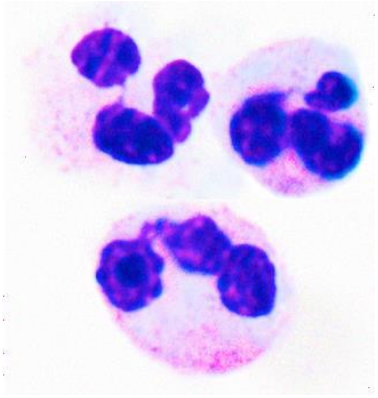

Figure 2.3. Mature segmented neutrophils. May-Grünwald-Giemsa stain.

2.1.2. Migration of PMNs

In response to inflammation or injury, circulating neutrophils, which are in a resting state in healthy individuals are recruited rapidly into the stressed tissue (19). Damage associated molecular patterns (DAMPs) released from injured tissue are recognized by neutrophils generally through G-protein coupled receptors (GPCRs). DAMPs contain histones, DNA, N-formyl peptide, high mobility group protein B1 (HMGB1), interleukin-1α (IL-1α), adenosine triphosphate (ATP) and many other proteins. Surrounding tissues are activated by DAMPs and production of lipid mediators such as leukotriene B_4 (LTB4) and chemokines such as CXCL8 is enhanced. DAMPs can activate nuclear factor-κB (NF-κB), which leads to the production of a

plethora of bioactive mediators (60, 61). On the other hand, IL-1α induces the production of CXCL1, which stimulates the neutrophil migration (62). CXCL8 is produced by both immune cells and non-hematopoietic cells, becomes deposited around the cells, and creates an appropriate environment for chemotaxis (63).

Leukocyte recruitment in most tissues is maintained by: tethering, rolling, adhesion, crawling and transmigration, which are sequentially proceeded. Migration of neutrophil across the endothelium is also a multistep process (tethering, rolling, slow rolling, arrest, adhesion, and transmigration) (Figure 2.4) (64). Adhesion molecules are critical effectors in this process. Bone marrow sinusoidal endothelium cells constitutively express intercellular adhesion molecule-1 (ICAM-1), vascular cell adhesion molecule-1 (VCAM-1), E-selectin, and P-selectin. Alternatively, under inflammatory conditions, the expression of these adhesion molecules is enhanced at the sites of inflammation, as well (65). High levels of CD18 integrins (LFA-1 and Mac-1) on the neutrophils mediate firm adhesion to ICAM-1; however, they are not critical for neutrophil mobilization. VCAM-1 is specifically upregulated during inflammatory responses, whereas in the bone marrow it is constitutively found on stromal cells and sinusoidal endothelium (66). Expression of E-selectin and P-selectin on the endothelial cells is enhanced by DAMP related reactions. With their overlapping functions, these selectins facilitate neutrophil recruitment (67). Once expressed by endothelial cells, they bind circulating neutrophils that express and mediate capturing and tethering of these cells. Neutrophils further roll along the vessel directed by blood flow. L-selectin (CD62L) is one of the adhesion molecules expressed on the surface of neutrophils. CD62L plays a role in neutrophil rolling along the endothelium. Upon activation, neutrophils rapidly shed CD62L, which is a prerequisite for neutrophil mobilization (68). Pro-inflammatory cytokines, in particular, TNFα and IL-1β, pathogen-associated molecular patterns (PAMPs) or growth factors and chemoattractants participate in the recruitment and activation of neutrophils. CXCL8, CXCL2 and CXCL5 signal via CXCR2 and promote neutrophil adhesion to the endothelium.

While rolling along the inflamed endothelium, neutrophils encounter with high shear stress urged by blood flow. Therefore, a robust adhesive bond between neutrophil and endothelium is required (69). Neutrophil rolling is primarily mediated

by creating long membrane bonds known as tethers. When the microvillus resides on the surface of neutrophils is tugged by flow force, tethers are formed. With their surface ligand P-selectin glycoprotein ligand 1(PSGL1), these tethers bind to endothelial P-selectin. Rolling is maintained by the formation and rapidly dissociation of this bond at the center and rear of neutrophils (67). Due to their positive charge, chemokines bind to negatively charged heparan sulfates which obviates the shear forces pushing the cells forward. When LFA1 on neutrophils interacts with ICAM-2, the interaction between neutrophils and endothelium is strengthened. Thus, neutrophils roll slower, eventually, get arrested and enter the tissue (69). During the transmigration process, neutrophils need to pass through the endothelium, then the basement membrane (Figure 2.4). Integrins, CAMs (ICAM-1 and 2, VCAM1), CD99, junctional and epithelial cell adhesion molecules (JAM, ECAM) are involved in the transmigration. Neutrophils are localized between endothelial cells via the interaction between MAC1 and endothelial ICAM1. Using several adhesion molecules, neutrophils can pass through the endothelium (70). The endothelial basement membrane is composed of extracellular matrix proteins, in particular laminins and collagens. Neutrophils are transmitted through some regions poor in extracellular matrix proteins (paracellular transmigration) (Figure 2.4 a) (71, 72), and/or through the basement membrane via releasing proteases such as matrix metalloproteases (MMP) (transcellular transmigration) (Figure 2.4 b) (73).

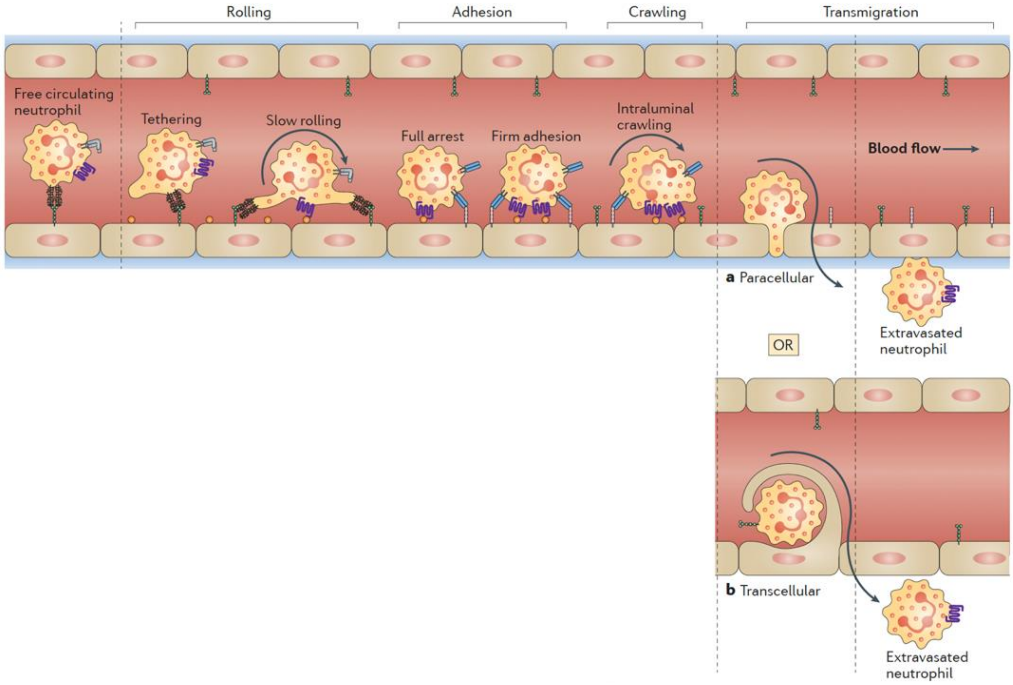

Figure 2.4. The neutrophil recruitment cascade. a) paracellular transmigration, b) transcellular transmigration **(73).**

In the absence of inflammation or infection, neutrophils swiftly undergo apoptosis; however, their lifespan can be prolonged by several days in the presence of inflammatory signals (74). In neutrophils, receptor expression patterns are altered

dynamically to rapidly respond to the pathogens. With the help of altered receptor expression and downregulation of junctional adhesion molecules, neutrophils can undergo reverse migration.

Aged neutrophils can be cleared from the circulation in the liver, spleen and bone marrow (75). As neutrophils get older, expression of CXCR4 is increased and CXCR2 is decreased on their surface. Thus, aged neutrophils become more responsive to SDF-1α and their migration to bone marrow is promoted. Large proportions of aged neutrophils are cleared in the bone marrow by bone marrow macrophages (76). On the other hand, some studies reported that most neutrophils die in the tissue during inflammation and becomes target for macrophages phagocytosis (77). Neutrophils can also be cleared with a process involving breaking down of their nuclear contents in the formation of neutrophil extracellular traps (NETs) (78).

2.1.3. Functions of PMNs

Even though neutrophils' functions are primarily recognized as killing of infectious microorganisms and phagocytosis, these cells widely contribute to both regulation and resolution of inflammation. By producing diverse cytokines, they modulate neighboring cells' activities and stimulate other immune cells (73). Neutrophils employ intracellular and extracellular mechanisms to kill microbes such as phagocytosis, neutrophil extracellular traps (NETs) formation and production of reactive oxygen species. Once a pathogen is phagocytosed, neutrophils release their granule contents into a vacuole called phagosome and reactive oxygen species (ROS) are generated through the activation of NAPDH oxidase system (79, 80). Besides phagocytosis, NET formation may also be promoted by releasing chromatin DNA and granular proteins like neutrophil elastase and MPO and histone proteins (for example, cathepsin and lactoferrin). NETs can catch and immobilize the pathogen, and promote its eradication by either facilitating the phagocytosis or direct proteolytic digestion by antimicrobial histones (Figure 2.5) (81, 82).

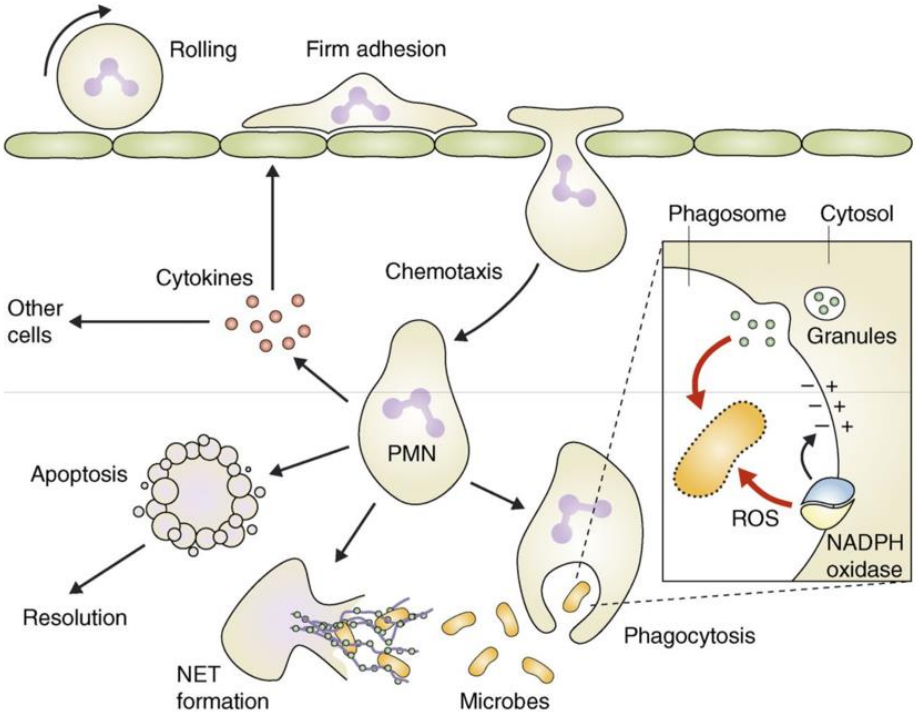

Figure 2.5. Neutrophil antimicrobial activities after it migrates into the injured tissue **(83).**

Epithelial surfaces provide first line of defense against infections. They can either serve as physical barriers or produce microbicidal substances. Once microorganisms cross the epithelial barrier and propagate in host tissues, they will be recognized by tissue-resident immune cells including macrophages (84). PAMPs and DAMPs released during injury and inaugurate the inflammation. PAMPs are composed of bacterial products, whereas DAMPs are host-derived molecules (85). Pattern recognition receptors (PRRs) on resident immune cells like macrophages and mast cells are activated by these molecules. Several signaling pathways are culminated in the activation of transcription factor NF-κB and further production of proinflammatory cytokines such as IL-1β, TNF-α and interferons. Cytokine release recruits to the site of infection (86). Neutrophil recruitment and migration are amplified in the presence of LTB4 and CXCL8 (63).

Upon engagement with the pathogen, neutrophils engulf them in phagocyte membrane and internalize into membrane-bound vesicles called phagosomes, which further merge with lysosomes to form phagolysosomes (87). The lysosomal contents including the enzymes released into the phagolysosome (MPO, NE, MMP-9, etc.) contribute to the destruction of the engulfed pathogen (72). These enzymes' production lasts longer in the presence of infection-related proinflammatory cytokines such as TNF-α (48).

In addition, neutrophils produce toxic hydrogen- and nitrogen-derived molecules such as hydrogen peroxide (H_2O_2), the superoxide anion (O_2^-), and nitric oxide (NO). These reactive species are formed in response to proinflammatory factors or triggered upon recognition and phagocytosis of foreign bodies (85). NADPH oxidase, which is responsible for ROS production produce O_2^- by shuttling electrons across the phagosome membrane. O_2^- is converted to H_2O_2 by superoxide dismutase (SOD). Hydrogen peroxidase is further converted to hypochlorous acid, which is critical for microbial effects in PMN (88). On the other hand, NO is produced by oxidative deamination of L-arginine by nitric oxide synthase (NOS). Upon neutrophil priming with TNF-α, IFN-γ or IL-1β and foreign antigens, inducible nitric oxide synthase (iNOS) produces NO (89).

To protect the host from tissue damage and prevent amplification of acute inflammatory response towards chronicity, inflammation must be strictly regulated. In

the early stages of inflammation, proinflammatory cytokines reach to the highest level in inflamed tissue. In the later stages, anti-inflammatory mediators are produced to halt neutrophil recruitment (90). In the absence of proinflammatory cytokines, neutrophils undergo senescence. Upregulation of CXCR4 and downregulation of CXCR2 and ICAM1 are observed in senescent neutrophils that are prone to reverse migration towards bone marrow. (60).

In addition to innate immune reactions, neutrophils can also modulate adaptive immune cells (91): It has been demonstrated that neutrophils can acquire antigen presenting capacity to helper T cells (Th) through upregulation of major histocompatibility complex (MHC) class II expression (92).

Neutrophils can also interact with dendritic cells (DCs) through NETs. In mice, NETs have inhibitory influence on cytokine production of DCs and lipopolysaccharide (LPS) induced DC maturation. DCs treated with NETs can hamper T cell proliferation and favor type 2 Th (Th2) polarization (93).

Neutrophils can influence survival, proliferation and IFN-γ production capacity of NK cells via their granular components (94). Through the production of survival inducing factors such as B-cell activating factor (BAFF) and the proliferation inducing factor A (APRIL), neutrophils can also shape B cell responses. Human spleen derived neutrophils, which release BAFF, APRIL, and IL-21 can induce T cell-independent antibody response in B cells (95, 96).

2.1.4. Subsets of PMNs

Numerous studies suggested that different neutrophil subsets exist and each have a distinct role in inflammation, infection, and cancer (16, 73). Neutrophils gain different phenotypes throughout their life cycle. Under physiological conditions, they leave the bone marrow and enter the circulation as mature neutrophils and are cleared as they become senescent. This shift in their phenotype results in different surface molecule expression and distinct neutrophil subsets. Migrating neutrophils express a distinct activated phenotype with $CD11b^{high}$, $CXCR2^{low}$, $CD62L^{low}$ (97), whereas aged neutrophils can be found in the circulation with a phenotype of $CD62L^{low}CXCR4^{high}CD49^{high}CD11b^{high}$ (98).

The microenvironment in which they are led to acquisition of diverse functional phenotypes (99). PMNs localized in cystic fibrosis airways exhibit a distinct exocytic phenotype. Elevated number of proteases released from neutrophils' primary granules are involved in tissue damage in cystic fibrosis airway (100). These neutrophils acquire capacity to present antigens through MHC II and B7-1 molecules (101).

In the context of cancer, disease progression is enhanced by tumor-associated inflammation which is consistent with high immune cell infiltration. In many cancer types, tumor-associated neutrophils (TANs) have been shown to dominate the immune cell infiltrate in the tumor microenvironment (102). In the presence of tumor derived proinflammatory factors such as IFN-y, IL-6, GM-CSF, and IL-8, TANs can survive longer than circulating neutrophils. TANs are classified into anti-tumorigenic N1 and pro-tumorigenic N2 subsets. Although there are numerous studies about murine N1 and N2 neutrophils, regulation of their counterparts in human has not been extensively clarified yet (103). TAN polarization is basically mediated by TGF-β and type-I IFNs. N2 polarization is mediated by high TGF-β and low IFN-β, whereas N1 polarization is characterized with low TGF-β and high IFN-β. In a murine study, blockade of TGF-β shifted the polarization towards N1 (104). N1-polarized TANs display increased tumor cytotoxicity, high NET formation, express high levels of ICAM1 and TNF-α (105). TANs produce a large amount of IL-8, thereby recruiting more neutrophils to the tumor microenvironment (106). Nevertheless, regulation of T cell responses by TANs largely depends on the type of tumor and its progression stage (107).

Neutrophils with a phenotype of $CXCR4^{high}VEGFR^{high}CD49^{+}$ have been identified in the circulation as well. Due to their high MMP9 activity, they can promote angiogenesis (108).

Neutrophil populations found amongst the peripheral blood mononuclear cells (PBMCs) separated by density (density < 1.077 g/mL) gradient centrifugation is called low-density neutrophils (LDN). These neutrophils, also known as granulocytic myeloid-derived suppressor cells (G-MDSCs or PMN-MDSCs), have been identified in circulation of pregnant women, neonates, patients with chronic diseases such as cancer and autoimmune diseases (109-111). In mice, PMN-MDSCs are defined as $Ly6G^{+}$ $Ly6C^{low}$ $CD11b^{+}$. Nevertheless, distinct phenotypic markers validated for

human PMN-MDSC is still lacking (112). On the contrary, lectin-type oxidized LDL receptor 1 (LOX-1) was found to be a strong candidate among several markers to identify PMN-MDSCs in human (113). Main feature of PMN-MDSC is to exert immune suppression, which could be revealed by and functional analyses (114).

Healthy neutrophils accumulate on top of erythrocyte layer after density gradient separation of the peripheral blood. In case of inflammation, neutrophils are immediately generated and egress from bone marrow. These newly generated cells have lower density; thus, they can be found in PBMC fraction as well (115). In emergency granulopoiesis, neutrophils with different maturation states are swiftly released into the circulation. Thus, it can give rise to heterogeneity in circulating neutrophil population. This heterogenous neutrophil population exerts either proinflammatory or immunosuppressive function (16). On the other hand, CD10 has been reported to be a specific phenotypic marker to discriminate mature neutrophils from immature ones. In the blood of G-CSF treated donors, one study has demonstrated that mature $CD10^{+}CD66b^{+}$ neutrophils display an activated phenotype, whereas immature $CD10^{-}CD66b^{+}$ neutrophils promote T cell proliferation and IFNγ production (110).

CD177, which is a glycoprotein exclusively expressed in intracellular granules and plasma membrane, has a critical role in mediating neutrophil adherence to the endothelium (116). During pregnancy, sepsis, or G-CSF therapy, CD177 expression on neutrophils is augmented. (117, 118).

Olfactomedin 4 (OLFM4) is largely expressed in prostate, bone marrow and gastrointestinal tract (119). Increased number of circulating neutrophils which carry OLFM4 in their specific granules is associated with autoimmune diseases (120).

Another subset of circulating human neutrophils has been reported to carry T cell receptor variants (121). In addition, neutrophils with a phenotype of $CD11c^{bright}$ $CD11b^{bright}$ $CD16^{bright}$ $CD62L^{dim}$ leads to ROS-mediated T cell suppression (122).

Although they are largely studied in antimicrobial type 1 responses, neutrophils can also be involved in type 2 immune responses. A distinct subset has been found in the site of helminth infections. With an excessive production of IL-13, this subset has been found to favor M2 macrophage polarization (123).

Upon infection and inflammation, IL-17 producing neutrophils have been observed in the circulation. These neutrophils express high levels of IL-6 and IL-23 receptors and have increased ROS production and fungal killing capacity (124).

2.1.5. Influence of PMNs on T cell responses

Neutrophils were long thought to be the principal innate immune cells. More recently they were identified with the capacity to shape adaptive immunity through secretion of cytokines or contact-dependent mechanisms. In both humans and mice, neutrophils can influence the functions of many T cell subsets including Th1, Th2, Th17, regulatory T cells (Treg) and γδ T cells (125).

Th17 is one of the T cell subsets which involves in host protection against extracellular and intracellular bacterial infections. IL-17 is a critical mediator under inflammatory conditions (126). IL-23, which is a differentiation factor for Th17 subtype is suppressed by phagocytosis of aged neutrophils. Reduced IL-23 secretion results in downregulation of IL-17 production from T cells. Thus, decreased IL-17 level reduces the production of new neutrophils (127). IL-17 production from neutrophils can induce Th17 differentiation. Likewise, IL-17 together with CXCL8, IL-1, IL-6, and TNF-α secreted from Th17 cells directly induce the neutrophil recruitment (127). The direct crosstalk between Treg and neutrophils has been demonstrated for human neutrophils. Through the production of CCL17 and anti-inflammatory lipoxin A4, neutrophils can recruit Treg cells into the tumor tissue. On the other hand, there are controversial observations reported on the interaction between γδ T cells and neutrophils both in mice and human. Immune suppressive LDNs or PMN-MDSCs were shown to suppress the activation of γδ T cells in a human study (128). Alternatively, another mice study reported that through secretion of IL-1β during the initial phase of infection, neutrophils can bolster IL-17 production from γδ T cells (129).

They can act like an antigen presenting cell (APC) for Th cells or cross-present antigens to $CD8^+$ T cells (9, 10). Neutrophils were reported to present antigen to memory $CD4^+$ T cells through upregulation of the costimulatory molecules (CD86 and CD80) and MHC II expression. In a mouse study, it was demonstrated that cultured together with T cells, neutrophils express MHC II and costimulatory receptors or

ligands (92). Another study reported that cross-talk between TANs recovered from lung tissue and activated T cells results in upregulation of CD86, OX40-L, and 4-1BBL costimulatory molecules on neutrophils (10, 107).

In cancer, there is an unclear role of neutrophils in the modulation of T cell responses. While some studies demonstrated neutrophils as enhancers of T cell responses in many cancers, others suggested their suppressor role on effector functions of T cells (12, 107, 130). Many mechanisms can be responsible for neutrophil-mediated T cell suppression; for instance, overproduction of ROS and NO, elimination of key nutrients for T cell proliferation such as L-arginine, L-cysteine or tryptophan. PMN-MDSCs can also produce immunosuppressive cytokines including TGF-β and IL-10 to direct immune suppression and induce Treg cells (131, 132). Excessive ROS production is one of the major mechanisms through which PMN-MDSCs suppress T cells (133). A state of oxidative stress is derived from the accumulation of ROS molecules. This state gives rise to several inflammatory and pathologic conditions (134). PMN-MDSCs produce superoxide which rapidly reacts with molecules to form ROS and then disrupts lipids, nucleic acids, proteins and accelerate inflammation and apoptosis. ROS molecules derived from PMN-MDSCs modify TCR and CD8 molecules. Thus, $CD8^+$ T cell-peptide-MHC interaction is hindered. (135). Amino acids including arginine, cysteine, and tryptophan are required for T cell effector functions (proliferation, maintenance of genomic integrity, survival etc.). Under antigenic stimulation, activated T cells consume an excessive amount of amino acids, glucose and fatty acids (136). L-Arginine is catabolized by Arg1 and inducible nitric oxide synthase (iNOS). As a final product, iNOS generates NO from L-arginine. Afterwards, Arg1 converts L-Arginine into L-ornithine and urea. PMN-MDSCs produce high levels of Arg1. Depletion of Arginine leads to the reduced expression of CD3ζ and CD3*ε* on T cells. Downregulation of CD3ζ and CD3*ε* expression inhibits TCR transduction pathway, and therefore blocks T cell proliferation and reduces cytokine production (137). Additionally, T cells do not have an enzyme to convert methionine to cysteine, therefore obtain cysteine from extracellular sources. Antigen presenting cells (APCs), including DCs and macrophages can synthesize cysteine and transport them to T cells. Similar to T cells, PMN-MDSCs cannot synthesize cysteine l and consume higher concentrations of L-cysteine for glutamate uptake. As a result,

T cells are deprived from cysteine, therefore cannot synthesize critical proteins for their effector functions. (138). Tryptophan is metabolized by indoleamine 2,3-dioxygenase (IDO). Upregulation of IDO in MDSCs within the tumor microenvironment results in tryptophan depletion, that hinders T cell effector functions (139).

2.2. Lung Cancer

Mortality rates are thought to be the major indicator of cancer progression. As the most frequently diagnosed cancer, lung cancer is the leading cause of cancer-related deaths worldwide (140). Turkey has been found in the top 25 countries with the highest lung cancer incidence rate. A high number of cancers are directly related to the tobacco smoking and air pollution. In terms of incidence and mortality rates, in Turkey, lung cancer ranks first in men (with 21.9 incidence rate in men and 5.3 incidence rate in women). However, in recent years, its incidence has been also increasing in women (141). In addition, most of lung cancer cases has been diagnosed at late stage (142).

Lung cancer is a very heterogenous disease. Based on the histopathological studies, it is classified as: small cell lung cancer (SCLC) and non-small cell lung cancer (NSCLC). Clinically, according to WHO criteria, lung cancer is categorized wherein Stage 1, the tumor cells are located in the lung and has not spread to any lymph nodes yet; stage 2, the tumor cells spread to lymph nodes inside the lung, but not found in any distant organs; stage 3, the tumor cells spread to lymph nodes at the center of chest; and, in Stage 4, tumor cells are found in distant organs (143).

Epithelial cells constitute the vast majority of lung cells. Upon infection, inflammation, resection or exposure to toxic materials, the lung swiftly adopts an extensive proliferative state that includes a variety of epithelial cell types. Type 2 epithelial cells proliferate and differentiate into non-proliferating type 1epithelial cells in the alveolar region. They also contribute to the replacement of injured epithelial cells (144). Lung alveoli are located at the end of bronchial airways. Alveoli encompass type 1 and type 2 squamous epithelial cells. Gas exchange is enabled through the extremely thin alveolar wall comprised of type 1 squamous epithelial cells (145). Proliferation and differentiation of epithelial cells lining the respiratory tract are

affected by the pathogen or toxic agent exposure. Alterations in the respiratory epithelium are associated with many acute and chronic lung diseases such as goblet cell hyperplasia leading to chronic obstructive lung disease, cystic fibrosis and asthma (146). Likewise, repetitive exposure to pathogens, endotoxin or any toxic agents such as cigarette smoke causes goblet cell hyperplasia or metaplasia in the respiratory epithelium. Moreover, squamous cell metaplasia can be seen in acute or chronic lung injury (147).

Cellular origins of lung cancer remain largely unclear and a matter of debate. Tissue-resident stem cells are strong candidates, since they surround the lung and are vital for tissue repair and maintenance (148). Due to their long lifespan, they can accumulate genetic mutations which may further lead to tumorigenesis. With their self-renewing and differentiation capability, type 1 and type 2 cells are thought to be the major stem or progenitor cell in the alveoli (149). Type 2 cells are generally accepted as initiators of KRAS- mediated adenocarcinoma (150). Neuroendocrine cells and cells of hematopoietic origin are also found in the lung tissue. SCLC is thought to originate from neuroendocrine cells (151).

2.2.1. Classification of Lung Cancer

NSCLC accounts for approximately 80% of lung cancer incidence, whereas SCLC makes up the minority (~20%) (152). SCLC is strongly associated with tobacco smoking and most patients with SCLC are diagnosed at an advanced stage of disease. Therefore, patients with SCLC have very low overall survival rate (153).

The majority of NSCLC is histopathologically categorized as squamous cell carcinoma (SCC, 40%) and adenocarcinoma (ADC, 50%). SCCs often emerge in the proximal airways, while ADCs are generally located in the distal airways. Chronic inflammation and smoking are the main causes of SCCs (154). With glandular histology, in general ADCs express cytokeratin 7 and thyroid transcription factor 1(TTF1) as biomarkers. In contrast, with squamous metaplasia or dysplasia, SCCs are separated from ADCs by expressing cytokeratin 5 and 6 or transcription factors p63 and SRY-box 2 (155). Large cell carcinoma composes a small portion of NSCLC. If the tumor cells do not have squamous or glandular shape or do not express biomarkers

specific to SCC or ADC, these tumors are generally classified as large cell carcinoma (152).

Tobacco consumption is reported to be the primary cause of lung cancer, followed by environmental carcinogens such as air pollution, viral infection, arsenic and genetic factors (156). Together with these factors, inflammatory mediators and ROS cause oxidative DNA damage and genomic instability. Many studies suggested that carcinogens including tobacco can activate nuclear factor kappa B (NFκB) pathway, which maintains cell survival and proliferation (150).

In Turkey, according to Turkish ministry of health cancer statistics, NSCLC incidence is 66% whereas patients with SCLC account for 14.1% of the patients diagnosed with lung cancer (157).

2.3. Immune Response in NSCLC

In the respiratory system, mucus coated upper respiratory tract provide the first line of defense against pathogens attacking the lung. This mucus is exclusively generated by goblet cells and deported by epithelial cells lining the respiratory tract. Through expression of PRRs, epithelial cells can recognize the pathogens and they can direct immune cells via cytokine secretion (158). The following steps of defense against pathogens rests upon immune cells in the lung. Tissue resident macrophages are responsible for phagocytosis. Resident macrophages, neutrophils and dendritic cells are capable to recruit immune cells for effective pathogen clearance (159).

Composition of tumor microenvironment represents a factor determining in both malignant tumor progression and overall response to the therapy. The heterogeneity in the NSCLC microenvironment, especially in terms of function and distribution of tumor infiltrating immune cells, has been acknowledged to be critical in therapy responsiveness. (160-162). Recent studies on cancer immunotherapy focused on characterization of immune cells in tumors, has reported that numerous types of immune cells including neutrophils, T cells, B cells, macrophages, NK cells and DCs surround the NSCLC tumors (163). Among them, neutrophils and T cells prevail (164).

The interplay between immune system and tumor cells leads to the acquisition of numerous anti-inflammatory and regulatory mechanisms by the tumor cells (165).

The immune responses to tumors are recognized to have three phases: elimination, equilibrium and escape. Tumor cells are eliminated by immune surveillance (tumor elimination), and yet remaining tumor cells acquire ability to remain silent and coexist with immune cells (equilibrium), however they eventually improve mechanisms to evade immune reactions (escape) (Figure 2.6) (166).

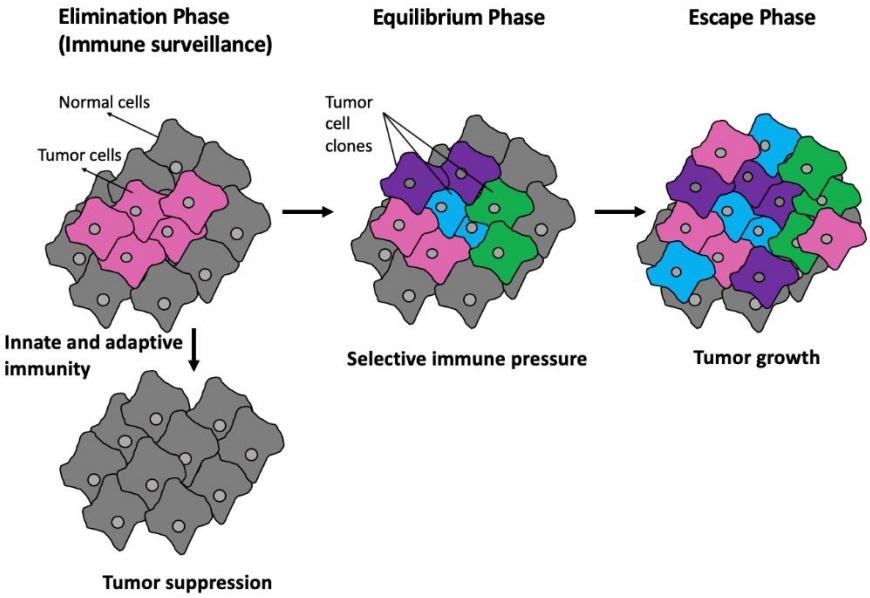

Figure 2.6. Three phases of immune responses against tumor cells: elimination, equilibrium, and escape**.**

In the tumor nest, $CD8^+$ cytotoxic lymphocytes cannot exert robust antitumor response (167). In contrast, the presence of stromal $CD8^+$ and $CD4^+$ T cells are correlated with enhanced survival. Moreover, one study has demonstrated that tumor infiltrating lymphocytes (TILs) are not capable of producing proinflammatory cytokines in vivo; however, they retain their ability to produce these cytokines when they are isolated from tumors (ex vivo) (168). In parallel with these, opposite survival effects of $CD68^+$ tumor associated macrophages (TAMs) infiltration was observed in the tumor stroma and islets in NSCLC. While $CD68^+$ TAMs found in the tumor nest correlate with extended survival, they correlate with poor survival when they are found in the tumor stroma (169). Moreover, the high levels of $CD163^+$ TAMs both in the tumor stroma and nest was found to be correlated with poor prognosis (170).

Harboring distinct molecular signatures and histological subtypes, NSCLC has been described as a very heterogenous disease in terms of tumor biology and immune responses. The type of driver mutations such as KRAS, BRAF, and EGFR and exogenous influences such as tobacco smoke may be in NSCLC biology (171). Tumor cells in the lung or other organs inevitably interact with extracellular matrix (ECM), infiltrating immune cells, fibroblasts, vasculature, and other stromal cells (172). In some cases, this microenvironment provides essential supplies for the tumor establishment. Accordingly, as in all solid tumors, in the lung tumor microenvironment, newly generated lymphatic and blood vessels bring vital nutrients for tumor growth and provide the infiltration of numerous myeloid and lymphoid cells into the tumor site (173).

Tumor antigens displayed on the surface of APCs (such as macrophages and dendritic cells) through major histocompatibility complex class II (MHC II) leads to the activation of $CD4^+$ T helper cells. This further bolsters the activation of $CD8^+$ cytotoxic lymphocytes. Besides, $CD8^+$ cytotoxic lymphocytes are also able to be activated by directly tumor cells via MHC I. Mature dendritic cells efficiently present tumor derived antigens on MHC molecules to $CD8^+$ T cells. This process termed cross-presentation and has critical role in the generation of immune response against tumors (174). Regardless of the activation mechanism, cytotoxic lymphocytes can kill the targeted tumor cells via perforin-/granzyme- or Fas/FasL-mediated pathways (175). In contrast, tumor cells that loose tumor specific antigen and diminish cell surface expression of MHC become hard to be detected by immune cells (176). MHC II expression of APCs is also altered in cancer patients. In NSCLC samples, APCs were shown to display reduced MHC II expression (2). Inhibitor cytokines including IL-10 and TGF-β secreted by tumor cells reduce MHC II expression on APCs. These cytokines can promote Treg differentiation and suppress cytotoxic killing mediated by $CD8^+$ T cells (3).

Tertiary lymphoid structures can arise at the site of inflammation. Bronchus-associated lymphoid tissues (BALTs) are found in human fetus and infant, but they disappear in the normal adult lung. On the other hand, their existence has been reported in NSCLC and they are named as tumor-induced bronchus-associated lymphoid tissue (Ti-BALT) (177). The effector immune cell colocalization in Ti-BALT has been

emphasized. T cells and B cells together with $LAMP^+$ mature dendritic cells colocalized along Ti-BALT are related to long-term survival in NSCLC (178).

The immune cell composition has been recognized as a prognostic biomarker for NSCLC. High neutrophil-to-lymphocyte ratio (NLR) has been found to be associated with poor prognosis (179, 180). Elevated frequency of Tregs and high IL-17 level in tumor microenvironment is correlated with poor overall survival (181, 182). High TGF-β level is associated with angiogenesis and tumor progression (183). On the other hand, high Th1-to-Th2 ratio and $CD8^+$ T cell infiltration are significantly correlated with extended survival (184, 185). Additionally, high infiltration of M1 macrophages and low infiltration of M2 macrophages are significantly correlated with extended survival in NSCLC (186).

2.3.1. PMNs in NSCLC

Under physiological conditions, PMNs are rarely found in healthy lung tissue (20). However, following disruption of this steady state, neutrophils rapidly localize in the stressed areas of the lung. Neutrophil infiltration is often associated with poor prognosis in NSCLCs (11). However, there are conflicting results about the function of neutrophils in NSCLC (9, 187). Neutrophils can directly destroy the tumor cells by producing ROS (Figure 2.7). Neutrophils have been shown to exhibit immune stimulatory activities; when cultured with T cells, tumor-infiltrating neutrophils (TANs) promoted T cell proliferation through the expression of costimulatory molecules such as OX40L, 4-1BBL, ICAM-1 and CD86 (107, 188). Several studies have also reported the antigen presentation capacity of PMNs (Figure 2.7) (10). In a study, neutrophils were shown to reinforce immune responses in early stages of lung cancer. On the other hand, immune suppressive capacity of neutrophils was also reported. Suppression of T cell proliferation was attributed to mechanisms involving the accumulation of Arg1 and ROS production (Figure 2.7) (187).

In NSCLC, N1 and N2 phenotypes of TANs have been described mostly in mouse studies. TGF-β has been accepted as a key mediator on polarization of TANs. High levels of TGF-β induces protumor N2, whereas blockade of TGF-β results in antitumor N1 polarization (Figure 2.7). Depletion of N1 neutrophils leads to increased tumor growth (103). Based on the function and immunophenotype of N2 neutrophils

in a mouse model of NSCLC, number of reports define these cells as PMN-MDSCs. In parallel to this, recent studies found a link between the accumulation of immature myeloid cells during chronic inflammation and the MDSC-like immature cells in the early stages of tumor progression. Furthermore, number of studies showed that the mature neutrophils can also acquire suppressive characters (12). A number of features can be used to differentiate PMN-MDSCs from other neutrophils such as high Arg1, iNOS activity, and ROS production (Figure 2.7) (133).

Cytokines released in response to injury, infection, and cellular stress can determine the outcome of antitumor response in the lung microenvironment (161). Tumor cell growth, invasion and metastasis can be promoted through continuous cytokine secretion in the lung with unresolved inflammation. IL-17A is one of the frequently found cytokines in the lung cancer microenvironment. By inducing IL-6 production and recruiting neutrophils into the tumor site, it plays a key role in the tumor progression (189, 190). High levels of neutrophils recruited by IL-17A was reported to be associated with poor prognosis (191). On the other hand, another study showed that PMN population was inversely correlated with T cell density in the tumor microenvironment of NSCLC. Same study also reported the heterogeneous distribution of PMNs in malignant lung tissue (192).

2.3.2. T Cell Responses in NSCLC

In the battle between tumor cells and immune system, tumor infiltrating lymphocytes (TILs) play a crucial role. Many studies have suggested a correlation between the T cell subsets and disease progression (193). Classically, cytotoxic T lymphocytes (CTLs) and IFN-γ secreting Th1 cells elicit anti-tumor immunity, $Foxp3^+$ and IL-10 secreting Tregs dampen the immune responses and promote tumor growth (Figure 2.7) (194). Through the secretion of suppressive mediators such as cyclooxygenase-2 (COX-2) and prostaglandin E2 (PGE2), tumor cells can directly promote Treg infiltration (Figure 2.7). In NSCLC, a high number of $CD4^+$ and $CD8^+$ T cells in the lung tumor microenvironment are associated with improved survival, whereas high levels of Foxp3 in the lung stroma correlated with higher recurrence risk (195).

Anti-cancer immune responses primarily rely on $CD4^+$ T cells and $CD8^+$ cytotoxic lymphocytes. A triumphant cytotoxic activity against tumor cells is promoted by effective antigen presentation either from APCs or tumor cells (1). This is mainly attained by macrophages and/or dendritic cells. Activation of T cells which recognized the antigens presented requires a second signal mediated by the interaction between co-stimulatory molecules expressed on APCs and cognate receptors on the lymphocytes (4). Final signal for the efficient clonal expansion and differentiation of T cells is promoted by autocrine and paracrine cytokine signaling. Costimulatory receptors expressed on T cells determine the fate of T cell function. The delivery of the second signal prevent activated T cell from undergoing anergy (196). Costimulatory receptor CD28 is constitutively expressed on naïve T cells. Through the interaction with B7-1 (CD80) and B7-2 (CD86) on APCs, it provides an essential second signal for T cell survival and proliferation (197).

In order to limit aberrant and autoreactive T cell responses, co-inhibitor molecules emerge on the surface of T cells following activation. Cytotoxic T lymphocyte associated antigen-4 (CTLA-4) coinhibitory molecule compete with CD28 for ligand binding with its higher binding affinity for both B7-1 and B7-2 (198). This interaction further induces the expression of IDO, which impairs conventional T cell activation and favors Treg functions (199). Besides CTLA-4, programmed cell death-1 (PD-1) is also a major inhibitory receptor upregulated on activated T cells. It delivers negative signal through the interaction with its ligand PD-L1 and PD-L2. PD-1 predominantly restricts effector T cell activity within tumors, whereas CTLA-4 mainly regulates the early activation of T cells (5).

PD-L1 expression by tumor cells lead to direct inhibition of immune responses and correlates with poor clinical outcomes in a numerous number of cancers including lung cancer. The frequent detection of PD-L1 in NSCLC and upregulation of PD-1 on TILs emphasize the potential usage of checkpoint blockade therapies (7, 8). Monoclonal antibodies against PD-1, PD-L1, and CTLA-4 constitutes the majority of checkpoint inhibitor therapies. The checkpoint inhibitors were found to be more effective in the smokers, in which somatic gene mutations are frequent (200). PD-L1 and PD-1 can be augmented in cancers with KRAS and EGFR mutations (201). Based on these studies, expression of PD-L1 and PD-1 molecules may differ with respect to

the molecular pattern of NSCLC (202). Although during the past decades new therapeutic strategies have been emerged for lung cancer, the overall 5-year survival of lung cancer patients remains very poor, especially in the advanced stages (203). As a first checkpoint inhibitor approved in NSCLC, antibody to PD-1 receptor activates T cells, NK cells, B cells, and DCs. Its ligand PDL-1 can be expressed on the surface of myeloid cells and tumor cells. When PD-1 and PD-L1 interacts, effector T cell activity is inhibited (Figure 2.7) (204). High levels of PD-L1 expressing tumors are associated with decreased numbers of TILs and better response to anti-PD1 therapy (6). Recent studies suggested that anti-CTLA-4 therapy in mice cannot promote T cell activation, rather deplete Tregs (163, 205).

Under immune checkpoint inhibitor therapy, certain patient' tumors may regress remarkably, whereas some tumors may retain their aggressiveness. Low response rate towards immunotherapy can be explained by immune escape mechanisms established by tumor cells. Tumor cells can hijack the immune system by altering the expression of checkpoint molecules. Inhibitors to these checkpoint molecules, therefore may not be effective (206). Poor outcomes of immunotherapy can be also explained by adaptive resistance gained by tumor cells. After an extensive time of therapy, patients with NSCLC can develop therapeutic resistance. Most research currently has been focusing on acquired resistance. One study has revealed that upon EGFR inhibitor therapy, initial sensitive cells have begun to adapt to the inhibitor drug within days and these cells have started to regain proliferation capacity (207).

Depending on the cytokines produced by $CD8^+$ cytotoxic lymphocytes, they can confer different responses against tumor cells. IFN-γ-secreted Type 1 $CD8^+$ T cells (Tc1) elicit anti-tumor responses through perforin- or Fas-mediated mechanisms. IL-5, IL-4, and IL-10 producing Tc2 cells can kill the tumor cells principally through perforin mediated mechanism. In addition, IL-17, IL-21, and IL-22-secreting Tc17 cells also possess anti-tumor activity (208). However, the mechanism behind this activity remains controversial (209, 210). While some studies have demonstrated that both Tc1 and Tc17 elicit anti-tumor responses, Tc1 cells possess superior capacity and higher cytotoxicity. Nevertheless, overproduction of IL-17 in the tumor microenvironment has been reported to promote tumor growth through inflammation (211). Not only CD8+ T cells, but also Th17 and $\gamma\delta$T cells are responsible for the IL-

17 found in NSCLC. Additionally, TGF-β and IL-6 secreted by tumor cells or the tumor-infiltrating immune cells favor Th17 differentiation (212). Several cytokines, growth factors and chemokines produced in chronic immune reactions become survival and proliferation signals for malignant tumor cells. Thus, survival, motility and invasiveness of tumor cells are supported by the environment created by inflammation (213, 214).

2.3.3. Tumor-associated Macrophages in NSCLC

Tumor-associated macrophages (TAMs) frequently populates the myeloid cells in NSCLC tumor microenvironment. TAMs consist of classically-activated (M1) and alternatively activated (M2) phenotypes (215). M1 polarization is known to be promoted by IFN-γ, TNF-α and GM-CSF, whereas M2 macrophages were shown to be activated by IL-13, IL-4, and PGE2. While activation of M1 macrophages induces Th1 responses, impairs cell proliferation and promote tissue damage, M2 macrophages induce Th2 responses and promote immune suppression and tissue repair through production of IL-10 and TGF-β. M1 macrophages are characterized by iNOS, CD80, CD86, MHC II and TNF-α, whereas M2 macrophages predominantly express CD206, CD163, and Arg1. Additionally, M1 has superior ROS and NO production capability (Figure 2.7). Triggering receptors expressed on myeloid cells (TREM-1) expressing TAMs are frequently encountered in NSCLC patients and are associated with poor overall survival (Figure 2.7) (216, 217).

Some mouse studies demonstrated that there are angiogenic macrophages surrounding the tumor. Via secreting proangiogenic factors including vascular endothelial growth factor (VEGF) and platelet derived growth factor (PDGF), these TAMs were shown to be responsible in increased microvessel formation in the tumor microenvironment (Figure 2.7) (218). The inflammatory responses created by immune cells including macrophages were reported to be associated with tumor growth (219).

2.3.4. Other immune cells in NSCLC

As an innate immunity component, natural killer (NK) cells constitute the first line of defense against the tumor cells. In the tumor microenvironment, they exert multiple effector functions including perforin-, FasL-, and TRAIL- mediated killing

of tumor cells (Figure 2.7). NK cells induce the maturation of DCs and play a role in the activation of monocytes and CTLs (220). Cytokines including TNF-α, IFN-γ and GM-CSF produced by NK cells promote Th cell polarization. IFN-γ retains anti-tumor activity via inducing MHC I expression and CTL activity (221). NK cell activity and IFN-γ production are diminished in NSCLC patients. Depletion of NK cells was shown to result in tumor progression in NSCLC (222).

The efficacy of immune response to control tumor cells relies on the capacity of the antigen presentation through DCs. Immature dendritic cells in the periphery express diverse chemokine receptors including CCR1, CCR2, CCR4, CCR5, CCR6, CCR8, and CXCR4. Mature DCs are identified with lysosome associated membrane protein (LAMP) (223). $LAMP^+$ mature DC, together with B and T cells in Ti-BALT promotes effective anti-tumor function in NSCLC (Figure 2.7) (224). After encountered with the antigens including tumor derived antigens, dendritic cells take up the antigens and form MHC-antigen peptide complexes. They further migrate to the secondary lymphoid organs wherein they present this antigens to the T lymphocytes (225). Recent studies reported that high levels of immature DCs can be encountered in lung cancer. In order to inhibit DC maturation, tumor cells produce factors such as IL-6, IL-10, VEGF, PGE2 and TGF-β (226). DCs in the lung cancer were reported to express low levels of costimulatory molecules. The immaturity and low costimulatory molecule expression hamper antigen presentation and indirectly restricts adaptive immunity (Figure 2.7) (227).

Apart from its role in humoral immunity, B cells have also pro-and anti-tumorigenic functions (228). In NSCLC, tumor infiltrating follicular B cells and plasma cells are associated with better prognosis, indicating the anti-tumor role of antibodies and plasma cells. Immunoglobulins secreted by lung-tumor stimulated B cells can mediate tumor lysis through antibody-dependent cellular cytotoxicity (ADCC) or complement dependent cytotoxicity (CDC) (229). In addition to the production of antibodies, B cells can also support TIL's activation, expansion and memory formation (230). Colocalization of $CD20^+$ B cells with $CD8^+$ and $CD4^+$ T cells in the tumor microenvironment is found to be related with prolonged survival in NSCLC patients. On the other hand, the presence of tumor promoting regulatory B cells (Bregs) were shown in NSCLC. Bregs display their characteristic immune

suppression through suppressive cytokine secretion (IL-10 and TGF-β) and inhibitory molecules such as PD-L1, which impair T cell and NK cell responses (Figure 2.7) (231).

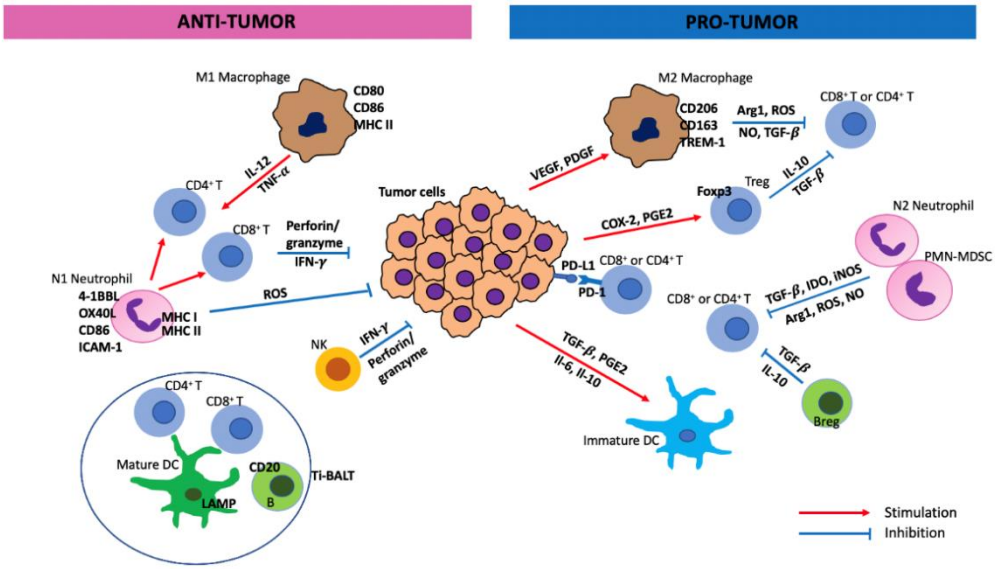

Figure 2.7. Schematic demonstration of anti-tumor and pro-tumor responses in **NSCLC**. N1 neutrophils, M1 macrophages, NK cells in the tumor microenvironment and the interaction between T cells, LAMP+ mature DCs, and B cells in tumor-induced bronchus-associated lymphoid tissue (Ti-BALT) are responsible for anti-tumor immune responses. In contrast, N2 neutrophils, PMN-MDSCs, M2 macrophages, Tregs, Bregs, and PD-L1 expressing tumor cells create suppressive environment.

Both pro-tumor and anti-tumor functions of mast cells were reported in NSCLC. A positive correlation has been found between mast cells and microvessel densities in the tumor microenvironment, supporting the involvement of mast cells in angiogenesis (232). On the other hand, tumor-infiltrating mast cells with high TNF-α production and degranulation capacity confer a survival advantage in NSCLC (233).

Natural killer T (NKT) cells exhibit characteristics of both innate and adaptive immune system. A single TCR from NKT cells can recognize numerous antigens and they can quickly initiate immune response. IFN-γ produced from the NKT cells act on NK and $CD8^+$ T cells (234). In the tumor microenvironment of NSCLC, NKT cells are not frequently found. Nevertheless, the presence of NKT cells in the tumor microenvironment is associated with extended survival in NSCLC patients (235).

A low number of eosinophils is generally found in tumor microenvironment of NSCLC (161). However, eosinophilia has been demonstrated in NSCLC patients with metastatic tumors (236).

3. MATERIALS AND METHODS

This study was performed in Hacettepe University Cancer Institute, Department of Basic Oncology Laboratories from January 2018 to May 2019. All experiments including human samples were conducted after the approval of the Hacettepe University Noninterventional Clinical Research Ethics Committee. (Approval No: GO 18/459-10)

3.1. Materials Used in This Study

RPMI-1640 (Capricorn Scientific, USA), high-glucose Dulbecco's modified Eagle's medium (DMEM) (Biological Industries, USA; Biowest, USA); phosphate buffered saline PBS powder (Advansta, USA); 10X trypsin-EDTA (Biological Industries, USA); heat-inactivated fetal bovine serum (FBS), L-glutamine, penicillin-Streptomycin (Biowest, France); histopaque 1.077 g/ml, ionomycin, trypan blue, histopaque 1.119 g/ml, 3-(4, 5-dimethylthiazolyl-2)-2, 5-diphenyltetrazolium bromide (MTT), propidium iodide, N-Formyl-Met-Leu-Phe (fMLP), N-Acetyl-L-cysteine (NAC), sodium dodecyl sulfate (SDS), N,N-Dimetilformamid (DMF), ethidium bromide solution (Sigma-Aldrich, USA); IgG isotype control, recombinant human IFN-γ, golgi stop (monensin), carboxyfluoresceinsuccinimidyl (CFSE) cell division tracker kit, LEGENDplex™ human CD8/NK Panel, DRAQ7™ (Biolegend, USA); recombinant human G-CSF (Amgen Inc, USA); 5mL round bottom tubes, RBC lysis buffer (Stem Cell Technologies, Canada); phorbol 12-myristate 13-acetate (PMA) (Cell Signaling, USA); purified anti-human CD3 mAb (Clone:Hit3a), cell proliferation dye eFluor670 (eBioscience, USA); 6X Loading dye, dimethyl sulfoxide (DMSO), 10X tris-borate-EDTA (TBE) buffer, 4',6-diamidino-2-phenylindole dihydrochloride (DAPI), 50 bp DNA size marker (Thermo Fisher Scientific, USA); isopropanol 98% , ethanol 96%, (AppliChem, Germany); 96-well plates cell, culture plates, T25 T75 flasks, serological pipettes and other plastic labware (Sarstedt, Germany; Nest, China; Orange Scientific, Belgium); Seakem® Le agarose (Lonza, USA), mounting medium (Abcam, UK), cellWash, accudrop beads (BD Biosciences, USA).

3.2. Buffers and Solutions

Complete RPMI-1640 and high glucose DMEM: Complete medium contains 10% heat-inactivated FBS, 1% penicillin and streptomycin and 1% L-glutamine. Prepared complete culture media were stored at 4°C.

Phosphate-buffered Saline (PBS): In order to obtain 1x PBS solution, commercial PBS powder was dissolved in 500 mL distilled water (dH_2O) and sterilized using by autoclaving. The solution was further kept at 4°C.

Fetal Bovine Serum (FBS): Heat-inactivated FBS was obtained commercially. Prior to use, it was brought to the room temperature and then aliquoted to 50 mL tubes. Aliquoted FBS was stored at -20°C.

Carboxyfluoresceinsuccinimidyl ester (CFSE) and eFluor670: Lyophilized CFSE (100 μg) and efluor670 (500 μg) was dissolved in 36 μl and 126 μl sterile DMSO, respectively to obtain 5 mM stock solution. Stock solutions were aliquoted and kept in -80°C.

Trypan blue: Trypan solution (4% w/v) was obtained by reconstituting 40 mg trypan blue with 1x PBS. The solution was then filtered through 0.22 μM filter to make it sterile.

MACS buffer: Buffer was obtained by 0.5% bovine serum albumin (BSA) and 2 mM EDTA in 50 μL PBS and stored at 4°C.

Tris-Borate EDTA (TBE) buffer: Prior to use, 10x buffer was diluted to 1x with distilled water.

Anti-human CD3 (α-CD3) monoclonal antibody (mAb): Anti-human CD3 (1 mg/mL) was diluted with serum-free RPMI-1640 to obtain 2 μg/mL working solution which was aliquoted and kept in -20°C.

Recombinant human (rh)IFN-γ: Lyophilized 500 μg IFN- γ protein was dissolved in serum-free RPMI-1640 and 10 μg/mL working solution was prepared and stored at -80°C.

Golgi stop (monensin): Working solution (40 μM) was prepared from monensin stock in serum-free RPMI, then it was aliquoted and stored at -20°C.

Recombinant human (rh)G-CSF: G-CSF (480 μg/0.5 mL) was obtained commercially from Neupogen (Filgrastim). Working solution (200 μg/mL) was prepared diluting with serum-free RPMI. The working solution was used immediately.

***N*-Acetyl-L-cysteine (NAC):** NAC powder was weighted and 100 mg powder was dissolved in 1mL distilled water. Stock solution (10 mg/mL) was diluted with serum-free RPMI to obtain 40 μM working solution. Then, the working solution was aliquoted and stored at -20°C.

N-Formylmethionine-leucyl-phenylalanine (fMLP): fMLP powder (5 mg) was dissolved in 1 mL DMSO. Then, the fMLP solution was diluted in serum-free RPMI to have 40 μM working solution which was aliquoted and kept in -20°C.

Propidium iodide (PI): Propidium iodide powder (5 mg) was dissolved in 1 mL distilled water. Then, it was aliquoted and stored at 4°C.

3-(4, 5-dimethylthiazolyl-2)-2, 5-diphenyltetrazolium bromide (MTT): MTT powder was weighted and 5 mg powder was dissolved in 1mL PBS, and it was stored at 4°C.

SDS/DMF solution: To obtain SDS/DMF solution, 25mL DMF were added into 25mL distilled water and then 10g SDS was added slowly. SDS was added dropwise and mixed thoroughly on a magnetic stirrer. After that, pH was adjusted to 4.7 by sodium hydroxide and hydrochloric acid when required. The solution was stored at room temperature.

Phorbol 12-myristate 13-acetate (PMA): PMA powder was dissolved in DMSO to obtain 200 μM stock solution. Then, it was diluted with serum-free RPMI 1640 to have 80 μM working solution. The working solution was then aliquoted and stored at -20°C.

RBC lysis buffer: RBC lysis buffer (10x) was diluted to 1x working solution. The working solution was aliquoted and then stored at 4°C.

3.3. Cell Culture and Purification

3.3.1. Cell Culture

When the confluency of the cells became around 80% in the flask, they were transferred into a T75 flask. Human lung epithelial adenocarcinoma cell lines used in

this study are NCI-H441, A549, NCI-H1299 (ATCC-LGC Promochem, USA). They are adherently growing cell lines. RPMI 1640 was used as a growth medium for NCI-H441 and NCI-H1299, whereas high-glucose DMEM was used for A549. Prior to use medium was supplemented with 10% FBS, 1% penicilin/streptomycin, and 1% L-glutamine (complete medium).

For the passaging of the cells, growth medium was discarded and the cells were washed with 1x PBS to get rid of remaining FBS. The cells were further treated with 10x trypsin/ EDTA (300 μL for T25 flask and 600 μL for T75 flask) for 3-4 minutes in a humidified incubator. Meanwhile, they were observed under microscope. As soon as the cell layer was detached, appropriate growth medium was gently added. Sub-cultivation ratio for NCI-H441, A549, NCI-H1299 are 1:5, 1:7, 1:10, respectively; thus at algorithmic growth phase, they needed 2 passages per week.

Isolated primer cells (Please see Section 3.3.4) were also maintained in complete RPMI. All cells were kept under appropriate conditions (37°C, 5% CO_2) in a humidified incubator (Thermo Fisher Scientific, Hera Cell 150i, USA).

3.3.2. Freezing and Thawing of Cell Lines

Before freezing, the cells were resuspended in a mixture containing complete RPMI medium (50%), FBS (%40) and DMSO (%10). The cells were further swiftly transferred into cryogenic vials. Then, they were put in “Mr. Frosty” Freezing Container (Thermo Fisher Scientific, USA) which was used to achieve a rate of cooling -1°C/ minute in -80°C. Then, the vials were placed at vapor phase in a liquid nitrogen tank.

For thawing of cryopreserved cell lines, cryogenic vials were rapidly transferred from liquid nitrogen into the 37°C water for 1-2 minutes. Afterwards, under laminar flow hood, the cell suspension was transferred into a 50 mL tube containing the pre-warmed complete growth medium appropriate for each cell line (high-glucose DMEM or RPMI 1640). They were centrifuged (1800 rpm, 5 min, 25°C) to remove the DMSO containing medium. The cells were further transferred into a T25 flask and resuspended in 20 mL complete medium.

3.3.3. Cell Counting

To count the cells accurately, cell suspension must be uniform and contain only single cells. Clump formation was avoided by gently pipetting the suspension obtained by trypsin-EDTA procedure (Section 3.3.1). A 10 μL volume from cell suspension was mixed with 10 μL 0.4 % trypan blue solution. Then the mix was transferred into the Fuchs-Rosenthal Counting Chamber (Hausser Scientific, USA). This chamber was covered with cover slip to provide capillary action. The distance between the chamber and coverslip is 0.1mm and the size of the chamber is 0.1 mm x 0.1 mm. Under a light microscope with 40x magnification, the chamber is seen with 16 small squares, the cells in the squares were counted (Figure 3.1).

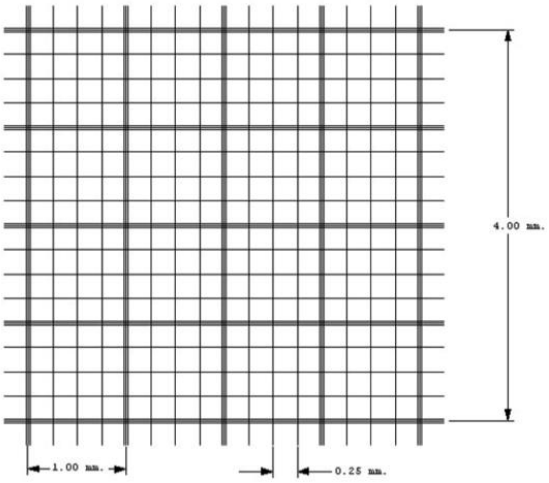

Figure 3.1. Schematic drawing of Fuchs-Rosenthal Counting Chamber (Hausser Scientific, USA) through microscope**.** One square, whose one side is 1 mm contains 16 small squares having the sides of 0.25 mm.

Cell density was calculated with the Formula 3.1. After the counting, the cover slide counting chamber were cleaned with 75% ethanol. (3.1)

$$\text{Area} = 1\ \text{mm} \times 1\ \text{mm} = 1\ \text{mm}^2$$

$$\text{Volume} = 1\ \text{mm}^2 \times 0.1\ \text{mm} = 0.1\ \text{mm}^3$$

$$\text{Cell concentration} = \frac{\text{Total cell count} \times 10^4}{\text{Number of counted squares}} \times \text{Dilution factor}$$

3.3.4. Isolation of the cells and Cell Sorting

Density gradient separation: Peripheral blood obtained from the healthy volunteers was collected in EDTA containing tubes (BD Biosciences, USA). One unit of blood was diluted with one unit of serum-free RPMI 1640 or 1x PBS. Meanwhile, 15 mL Histopaque 1.077 g/mL was gently layered over 15 mL Histopaque 1.119 g/mL in a 50 mL tube. Then, the blood was added slowly through the walls of the tube and centrifuged (400 x g, 25 min, 25°C) with no brake. After centrifugation, there were two layers containing PBMCs (upper layer) and PMNs (lower layer) (Figure 3.2). Upper layer and lower layer were carefully transferred into separate 50 mL tubes. These tubes were filled with 1x PBS solution and centrifuged (1800 rpm, 5 min, 25°C). After discarding the supernatant, the pellet was resuspended in complete RPMI medium.

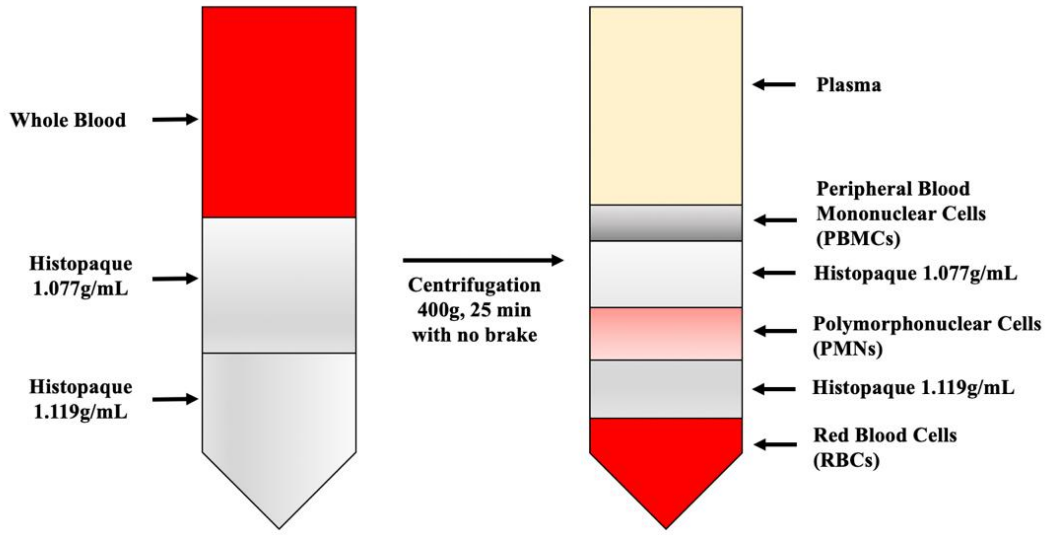

Figure 3.2. PBMC and PMN separation by biphasic density gradient centrifugation.

Lysis of Red Blood Cells : Residual red blood cells in PMN fraction were lysed by RBC lysis buffer (Stem Cell Technologies, Canada). Before use, 10x RBC lysis buffer was diluted to 1x with deionized water and brought to the room temperature. The buffer (2 mL) was added into the tube containing PMNs in 300-500 μL complete RPMI 1640. Buffer was gently mixed by pipetting up and down for 3-5

minutes. Then, the tube was filled with complete RPMI medium and centrifuged (1800 rpm, 5 min, 25°C) to wash away lysis buffer. The washing step was repeated twice. Supernatant was discarded and pellet was checked whether another lysing is necessary. PMNs were further resuspended in 2-3 mL complete RPMI medium.

Fluorescence-activated cell sorting (FACS): Fluorescence activated cell sorter (FACS) (FACSAria II, Biosciences, USA) and its software (FACS Diva V8.0.1, BD Biosciences, USA) were used to purify the cells of interest. Sorting must be performed on an optimized FACS device with a stable stream and drop delay value. Accudrop beads was used to set appropriate values for FACS.

Gating of singlet cells are the first step in flow cytometric analysis. Doublets were excluded by plotting the height (FSC-H) against area (FSC-A) on forward scatter. Singlet cells were gated and further distributed based on their size (FSC-A) and granularity (SSC-A). Then, the target population was identified based on the particular staining with fluorochrome labelled antibodies specific for the surface antigen of interest.

$CD4^+$ and $CD8^+$ T cells were sorted from freshly collected PBMCs. Firstly, PBMCs were resuspended in 1 mL serum-free RPMI medium. Then, they were incubated with anti-human CD4-APC and anti-human CD8-PE-Cy7 mAbs at room temperature for 25 minutes in dark. Then, the tube containing labelled PBMCs was filled with complete RPMI 1640 and the cells were filtered through 40 um sterile cell strainer (Stem Cell Technologies, Canada). After doublet discrimination and SSC-FSC gating, $CD4^+$ and $CD8^+$ T cells were sorted by FACS. Then, the purity of collected cell populations were determined by directly running them on the flow cytometer (Figure 3.3). Pure $CD4^+$ and $CD8^+$ T cells (with a purity of $\geq 95\%$) were resuspended in complete RPMI medium and used in further assays.

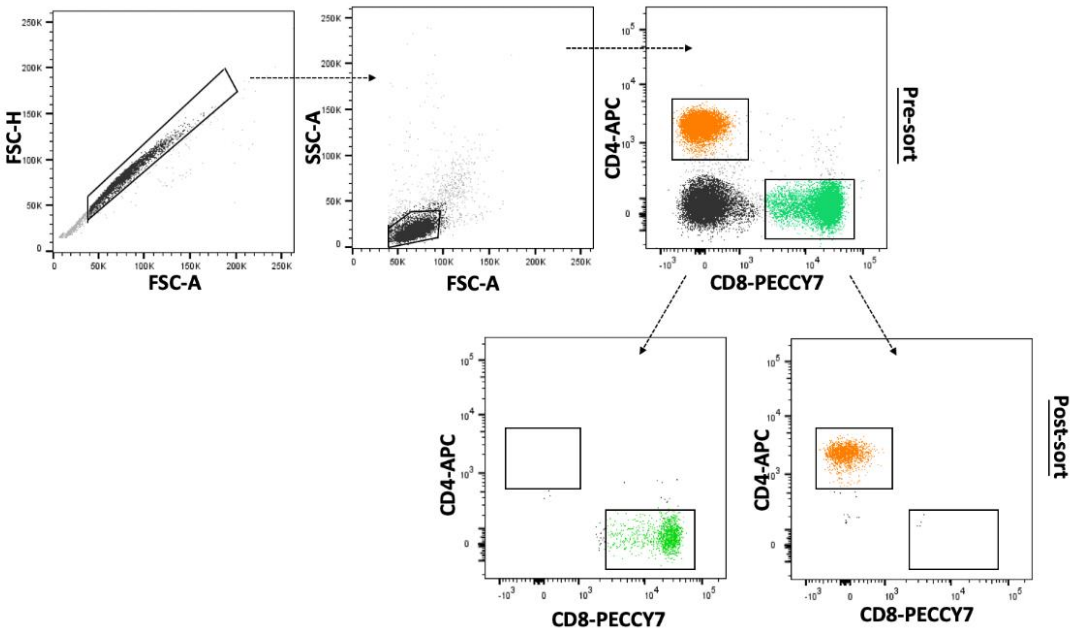

Figure 3.3. The gating strategies for the purification of $CD4^+$ and $CD8^+$ T cells from the isolated PBMCs of healthy volunteers by FACS. The cells before (pre-sort) and after (post-sort) sorting were also shown.

After 24h of incubation, $CD15^+$ PMNs were back-sorted from the co-cultures employing monocyte, lymphocyte and lung adenocarcinoma cells (Please see Section 3.3.5). Cells obtained from the co-cultures were stained with anti-human CD15-PE mAb. Then $CD15^+$ cells were gated and collected by FACS (Figure 3.4). In addition, from the co-cultures $CD8^+$ T cells were gated and $TIM3^{-/low}$ and $TIM\text{-}3^{mod/high}$ populations were separately back-sorted. The cell purity following FACS procedure (post-sort) was assessed in comparison to that of the initial mix population (pre-sort) (Figure 3.5).

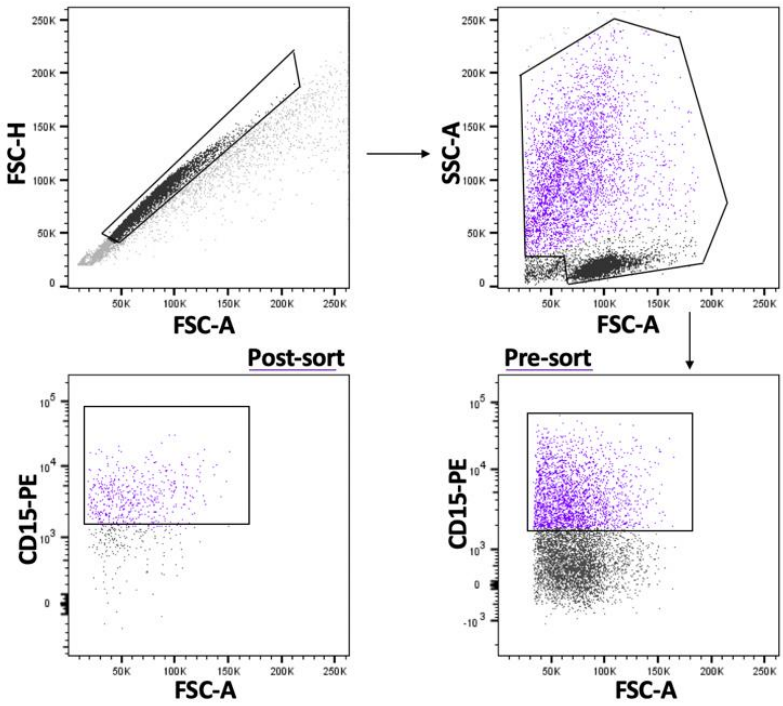

Figure 3.4. The gating strategies for the purification of $CD15^+$ PMNs from the co-cultures containing $CD8^+$ T cells, monocytes and lung adenocarcinoma cells by FACS. The cells before (pre-sort) and after (post-sort) sorting were also shown.

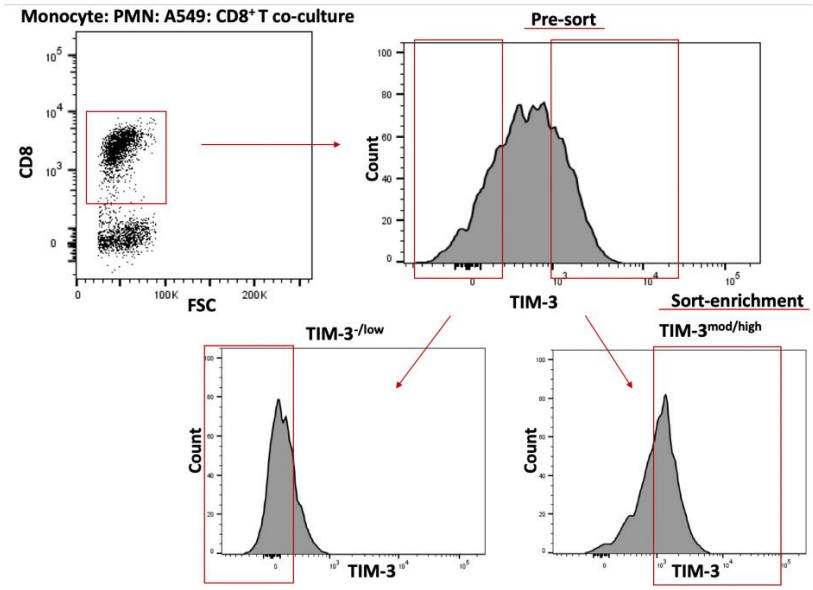

Figure 3.5. $CD8^+$ T cells were back-sorted from the co-cultures containing monocytes, PMNs and lung adenocarcinoma cells according to TIM-3 surface expression levels. TIM-3 expressing T cells were further enriched in $TIM3^{-/low}$ and $TIM\text{-}3^{mod/high}$ populations by FACS.

Magnetic-activated cell sorting (MACS): $CD14^+$ monocytes were purified from the PBMCs obtained from healthy volunteers based on the protocol given by CD14 MicroBeads, Magnetic Separation with LS columns (Miltenyi Biotech, USA). PBMCs (10^7) were resuspended in 80 µL of buffer (containing 0.5% bovine serum albumin (BSA), and 2 mM EDTA in phosphate- buffered saline (PBS)). CD14 Microbeads (20 µL) was further added into the cell suspension. Afterwards, this cell suspension was incubated at 4°C for 15 minutes. Then, the cells were washed with 1-2 mL buffer and centrifuged at 300 x g for 10 minutes. Supernatant was aspirated and cell pellet was resuspended in 500 µL buffer. Meanwhile, an LS column was placed in the magnetic field of MACS separator and cleaned with 3 mL buffer. Cell suspension was further applied onto the column. Column was washed with 3 mL buffer three times. After that, column was removed from the separator and placed on a 50 mL tube. By gently pushing the plunger into the column, magnetic labeled $CD14^+$ monocytes were flushed out. The cells were further centrifuged at 1800 rpm for 5 minutes and the cell pellet was resuspended in complete RPMI-1640. Efficiency of the MACS or the purity of the cells were assessed by labelling with a fluorochrome conjugated anti-human CD14 mAb and analyzed by flow cytometry. Purity of the cells after sort was 93-95%. (Figure 3.6)

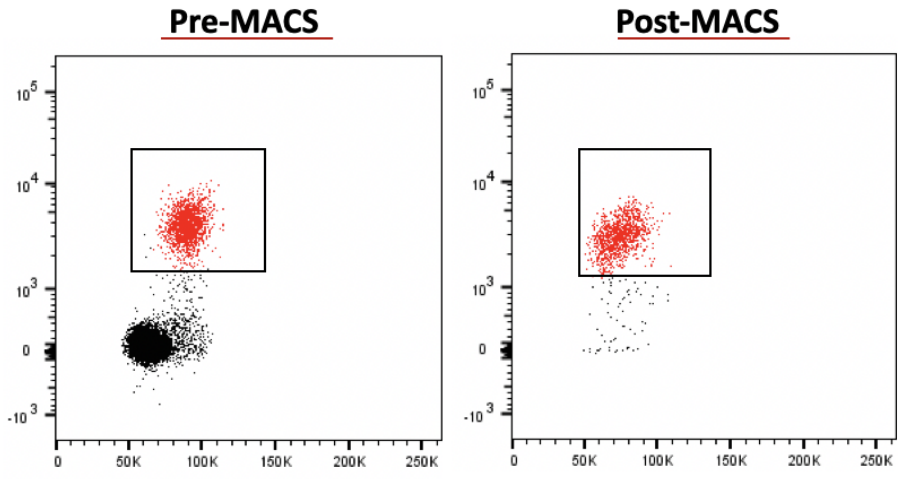

Figure 3.6. Confirmation of the purity of $CD14^+$ monocytes isolated by MACS. Before and after MACS, the cells were labelled with CD14-PE antibody and analyzed by flow cytometry.

3.3.5. Establishment of Co-cultures:

A549 and NCI-H1299 ($5x10^3$/well) and NCI-H441 ($30x10^3$/ well) were seeded in complete RPMI-1640 in 96-well round bottom and flat bottom plates. The number of cancer cells seeded in the beginning of co-cultures were empirically determined by the number of cells needed to reach 80-90% confluency by 72h of cultivation (Figure 3.7) or MTT proliferation assay (Please see Section 3.4.2).

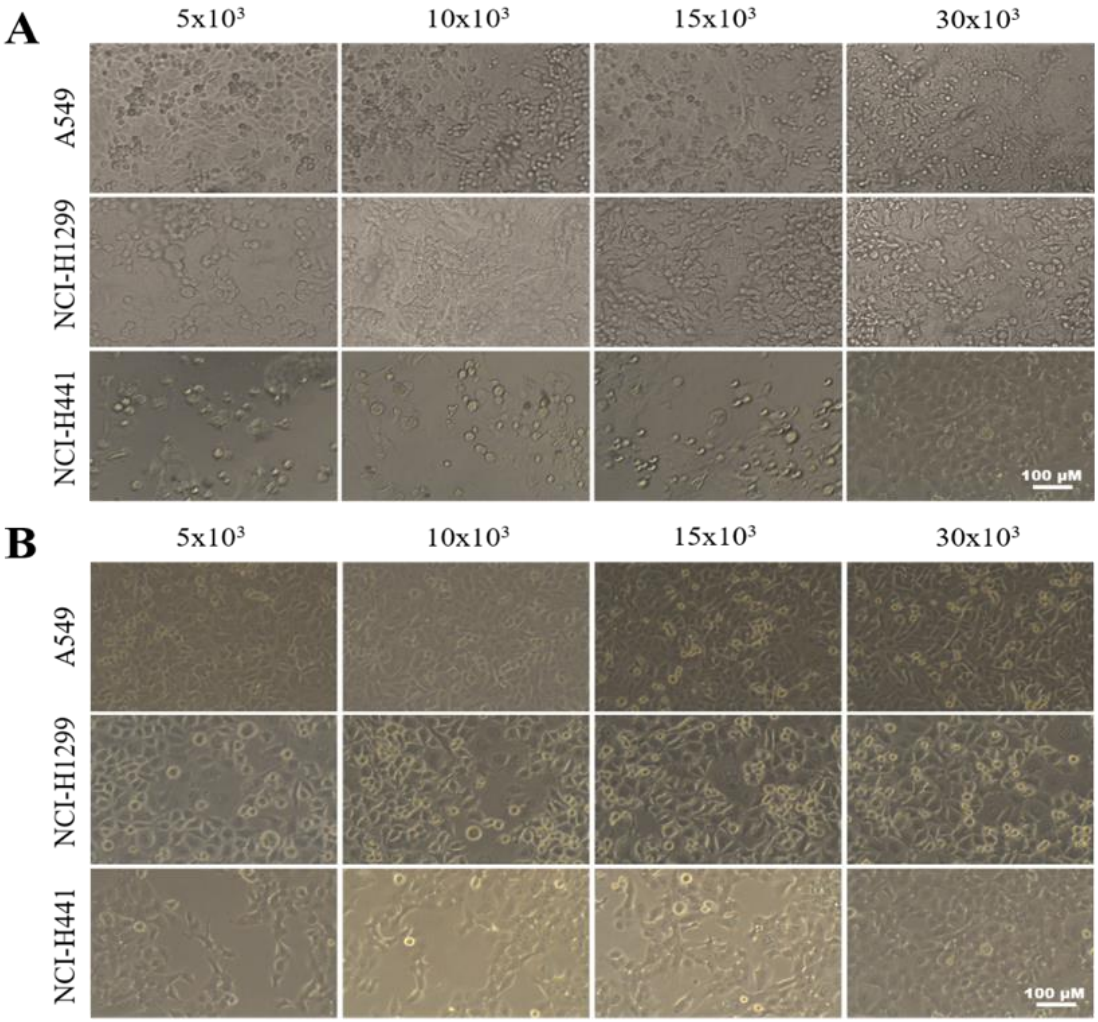

Figure 3.7. Confluency of the A549, NCI-H1299 and NCI-H441 after 72h of incubation. A) Pictures of A459, H1299 and H441 cells seeded in different numbers (5x103, 10x103, 15x103, and 30x103) in a round bottom 96-well plate and (B) in a flat bottom 96-well plate.

These cells were co-cultured with purified $CD8^+$ or $CD4^+$ T cells (labelled with eFluor670 for proliferation analysis), monocytes and PMNs in different ratios. Before

co-culture, stimulation of T cells with α-CD3 mAb (25 ng/mL) for 72hgives the first signal for T cell activation, whereas co-stimulatory signal for T cell activation was came from the myeloid cells in the co-cultures. The ratio of $CD8^+$ or $CD4^+$ T cells were used as the main variable (monocyte:PMN:$CD4^+$ T cell, 0:0:1, 0:0.5:1, 0.5:0:1, 0.5:0.5:1; monocyte:PMN:$CD8^+$ T cell, 0:0:1, 0:0.5:1, 0:1:1, 0.125:0:1, 0.25:0:1, 0.5:0:1, 0.125:0.5:1, 0.125:1:1, 0.25:0.5:1, 0.25:1:1, 0.5:0.5:1, 0.5:1:1) wherein "1" stands for $2x10^4$ cells/well in 96-well round-bottom plates. As controls, all conditions were performed in the absence of lung cancer cells as well. Instead of cells, conditioned media obtained from A549, NCI-H1299 and NCI-H441 cells were used for certain experiments. A549, NCI-H1299 and NCI-H44 cells were seeded ($2x10^6$) into a T25 flask in 6mL complete RPMI-1640. Following 24h, supernatants were collected into 15ml tube and centrifuged for 5 minutes at 1800 rpm. After centrifugation, supernatants were collected and defined as "conditioned media". NAC (1 μM) or G-CSF (50 ng/mL) were also used to modify ROS production and cell viability, respectively, added into the co-cultures.

PMNs were cultured ($5x10^5$) in complete RPMI medium in 5 mL tubes. Then, they were treated with G-CSF (50 ng/mL), NAC (1 μM), fMLP (1μM) or IFN-γ (50 ng/mL). After 24h, they were washed with complete medium and centrifuged (1800 rpm, 5 min, 25°C). Meanwhile, PBMCs (stimulated with 25 ng/mL α-CD3 mAb and labelled with eFluor670 proliferation dye) were put into the wells. PMNs were added onto the PBMCs at different ratios (PMN: PBMC, 0:1, 0.125:1; 0.25:1, 0.5:1, 1:1 wherein "1" indicates $1x10^5$ PBMCs).

3.3.6. 3-(4, 5-dimethylthiazolyl-2)-2, 5-diphenyltetrazolium bromide (MTT) cell viability assay:

Number of lung cancer cells used for the co-culture assays were also confirmed by MTT assay (Figure 3.8). A549, NCI-H1299 and NCI-H441 cells were seeded in 100 μL complete RPMI 1640 in a round bottom 96-well plate at different numbers ($5x10^3$, $10x10^3$, $15x10^3$, and $30x10^3$ per well) in triplicates. Following 72h of incubation, 25 μL from MTT (5 mg/mL) was added into each well and the plate was incubated for further 4 hours. After that, 80 μL SDS-DMF solution was added into each well containing cells. SDS-DMF was also added into an empty well (blank well).

Then, the plate was incubated for 24h. At the end of the incubation, the absorbance of each well was measured by at 570 nm Spectra Max Microplate Spectrophotometer (Molecular Devices, USA). Average OD values from triplicate readings were determined (OD_{sample}) and normalized to OD value from the blank by the following formula: $OD_{sample} - OD_{blank}$.

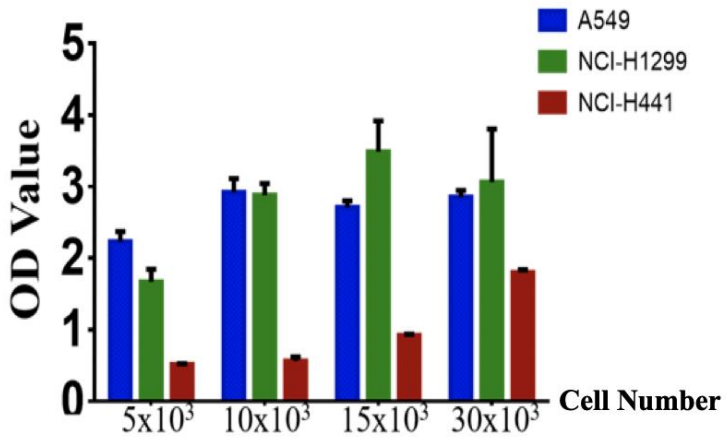

Figure 3.8. Optical densities (OD) of A459, NCI-H1299 and NCI-H441 cells seeded at different numbers. Cells were seeded in triplicate ($5x10^3$, $10x10^3$, $15x10^3$, and $30x10^3$ cells/well) and average OD at 570 nm was used.

3.4. Immunological Techniques

3.4.1. Flow Cytometry Analysis

Before staining**,** the cells were resuspended in 100 µL CellWash (BD Biosciences, USA) in 5 mL tubes. According to manufacturer's protocol, they were stained with roughly 100ng fluorophore conjugated antibodies (Table 3.1). The tubes were slightly vortexed and incubated for 40 minutes at 4°C in dark. After incubation, 1-2 mL CellWash was added into each tube and they were centrifuged (1800 rpm, 5 min, 25°C). The supernatant were discarded and the pellet was resuspended in 100-150 µL CellWash.

$CD8^+$ T cells obtained from the co-cultures was treated with 1 μM Monensin together with 100 ng CD107a-PE mAb in 100 µL CellWash. Cells were incubated for

5 hours. After incubation, the cells were washed with 1-2 mL CellWash and centrifuged (1800 rpm, 5 min, 25°C). The cells were further analyzed on a flow cytometer (FACSAria II, BD Biosciences, USA). Isotype-matched antibodies, as controls, were used to distinguish cell populations which were positive for specific markers.

Table 3.1. Antibodies used in flow cytometric analysis.

Antibodies (anti-human)	**Clone**	**Manufacturer**	**Fluorochrome**
CD4	RPA-T4	BD, USA	APC
CD8	RPA-T8	BD, USA	APC
CD8	SK1	Sony, USA	PE-Cy7
CD11b	M1/70	Biolegend, USA	APC
CD14	M5E2	Biolegend, USA	PERCP
CD15	HI98	Biolegend, USA	FITC
CD15	HI98	BD, USA	PE
CD25 (IL-2R)	BC96	Biolegend, USA	APC-Cy7
CD33	P67.6	Sony, USA	PE-Cy7
CD62L	DREG-56	Biolegend, USA	PE
CD66b	G10F5	Biolegend, USA	FITC
CD69	FN50	Biolegend, USA	FITC
CD86 (B7-2)	IT2.2	BD, USA	PE-Cy5
CD107a (LAMP-1)	H4A3	Biolegend, USA	PE
CD137	4B4-1	BD, USA	PE
CD152 (CTLA-4)	L3D10	Biolegend, USA	PE
CD223 (LAG3)	11C3C65	Biolegend, USA	FITC
CD279 (PD-1)	EH12-2H7	Biolegend, USA	APC-Cy7
CD366 (TIM-3)	F38-2E2	Biolegend, USA	PE
HLA-DR	L243	Biolegend, USA	APC-Cy7

Tracing the proliferation of $CD4^+$, $CD8^+$ and PBMCs in co-cultures with eFluor670: Isolated $CD4^+$, $CD8^+$ and PBMCs were resuspended in serum-free RPMI 1640 ($2x10^6$ cells/500 μL). They were stained with eFluor670 dye at a final concentration of 5 μM. The tubes containing cells were incubated for 10 minutes in dark. After incubation the tubes were filled with complete-RPMI medium and placed on ice for 5 minutes in dark. Then, they were centrifuged (1800 rpm, 5 min, 25°C), further refilled with complete-RPMI medium and centrifuged again. Having discarded the supernatants, the cells were resuspended in complete RPMI medium. Following

72h of incubation in the co-cultures, eFluor670 labelled immune cells were gated and percentage of proliferated cells were assessed by flow cytometry.

Assessment of TIM3$^{-/low}$ and TIM-3$^{mod/high}$ proliferation with CFSE: From the co-cultures employing PMNs, monocytes, and A549 cells, $CD8^+$ T cells were back-sorted based on TIM-3 expression levels after 72h of incubation. They were further enriched in TIM-3$^{-/low}$ and TIM-3$^{mod/\ high}$ by FACS. The two sub-populations were resuspended with serum-free RPMI 1640 ($1x10^6$ cells/ mL) in 15 mL tubes. Then, CFSE (5mM) was added into each tube at a final concentration of 5 μM. The cells were further incubated at 37˚C for 15 minutes. Afterwards, the tubes were filled with complete RPMI medium and placed on ice for 5 minutes. Then, they were centrifuged (1800 rpm, 5 min, 25°C), then refilled with complete-RPMI medium and centrifuged again. After discarding the supernatants, the cells were resuspended in appropriate amount of complete RPMI 1640 and stimulated with various agents. These two sub-populations were further incubated with rhIL-2 (5ng/mL) and/or plate bound α-CD3 (HIT3A) with or without soluble anti-CD28 (2ug/mL).Following 72h of incubation, the CFSE fluorescence was read by flow cytometry.

Flow cytometric viability assay: PMNs were co-cultured with A549 and NCI-H1299 lung adenocarcinoma cell lines (PMN: monocyte: cancer cell; 0.5:0.5:0.125). They were also cultured with conditioned media from the cell lines. Additionally, they were treated with G-CSF (50 ng/mL), NAC (1 μM), fMLP (1μM) or IFN-γ (50 ng/mL). Following 24h, 48h and 72h of incubation, PMNs recovered from the cultures were resuspended in 100 μL CellWash. They were either stained with propidium iodide (PI) or DRAQ7 to assess cell viability. PI was added into PMN containing tubes at a final concentration of 25 ng/mL, whereas DRAQ7 was applied to PMNs at a final concentration of 0,3 μM. PI-stained PMNs containing tubes were further placed in dark for 5 minutes, then filled with 1-2 mL of CellWash and centrifuged (1800 rpm, 5 min, 25°C). This washing step was not performed for PMNs stained with DRAQ7. After centrifugation, the cell pellet was resuspended in 100-150 μL CellWash and analyzed by flow cytometry.

Multiplex cytokine profiling by cytometric bead-based immunoassay: To identify cytokines derived from co-cultures, supernatants from co-cultures containing lung cancer cells, monocytes, PMNs and $CD8^+$ T cells were collected. Besides,

supernatants were also obtained from TIM-3^+ and TIM-3^- cells stimulated with PMA and ionomycin for 16h. Collected supernatants were stored at 80°C. Presence of IL-2, IL-4, IL-10, IL-6, IL-17A, TNF-α, sFas, sFasL, IFN-γ, granzyme A, granzyme B, perforin and granulysin was tested simultaneously in the supernatants with LEGENDplex™ Human CD8/NK Panel (Biolegend USA). This assay was performed according to manufacturer's protocol. Briefly, before the experiment, the supernatant samples were brought to the room temperature. In a 5 mL tube, 25 µL sample, 25 µL Assay buffer, 25 µL pre-mixed beads, and 25 µL detection antibodies were mixed thoroughly. Covered entirely with aluminum foil, tubes were incubated for 2 hour on a plate shaker. Without washing, 25 µL Streptavidin-PE (SA-PE) was added to each tube. The tubes were incubated for further 30 minutes on a plate shaker. Then, they were centrifuged (1000 x g, 5min, 25℃). Supernatant was removed and then 200 µL of Wash Buffer was added to each tube. Samples were read by flow cytometry and the data analysis were performed with LEGENDplex^{TM} data analysis software to quantify cytokine levels.

Flow cytometric measurement of ROS production: PMNs treated with G-CSF and/or fMLP in the presence or absence of NAC were analyzed for the capacity of ROS production. ROS production of PMNs obtained from the co-cultures containing lung cancer cells, monocytes in the presence and absence of $CD8^+$ T cells was also assessed. Moreover, ROS production of PMNs treated with conditioned media from lung cancer cells with or without monocytes was analyzed. Firstly, PMNs were resuspended in serum-free RPMI 1640 in 5 mL tubes and stained with 2',7' dichlorodihydrofluorescein diacetate (H_2DCFDA) at a final concentration of 10 µM. After gently vortexing, the tubes were incubated for 25 minutes at 37°C. Then, the tubes were swiftly placed on ice and 2 mL CellWash was added into each tube. The tubes were further centrifuged (1800 rpm, 5 min, 25°C). After the tubes were swiftly placed on ice, supernatants were discarded and cells were resuspended in 150 µL CellWash. Lastly, mean DCFDA fluorescence intensities (MFI) of the cells were analyzed by flow cytometry. For certain experiments, MFI of PMNs stimulated with NAC was normalized to MFI of unstimulated PMNs according to following formula: $MFI_{\text{NAC stimulated PMN}}$ / $MFI_{\text{unstimulated PMN}}$.

3.5. Molecular Techniques

3.5.1. Total RNA isolation and spectrophotometric analysis

RNA isolation was performed with RNA purification kit (Norgen Biotek, Canada) according to manufacturer's recommendations. PMNs collected from the co-cultures or freshly isolated PMNs or PMNs cultured for 24h were lysed with 100 μL RL buffer supplemented with %1 β-mercaptoethanol in 15 mL tubes. Ethanol (70%, 100 μL) was slowly added into each tube and the mixture was transferred into spin columns. Then, the spin columns were centrifuged (14.000 x g, 1 min, 25°C). Flow through was discarded and the columns were reassembled onto collection tubes. Wash buffer (400 μL) was applied to the columns and they were centrifuged (14.000 x g, 1 min, 25°C). Washing step was repeated for three times. Then, the columns were placed into elution tubes. Elution solution (25 μL) was added and centrifuged (200 x g, 2 min, 25°C, followed by 14.000 x g, 1 min, 25°C).

Quality and concentration of isolated RNAs were measured at UV Spectrophotometer at OD_{260}, OD_{280} and OD_{230} nm (NanoDrop ND-1000,USA). $OD_{260/280}$ and $OD_{260/230}$ ratios are used to determine the purity of nucleic acids.

3.5.2. cDNA synthesis

Complementary DNA (cDNA) was synthesized from the isolated RNA with Quantitect Reverse Transcription Kit (Qiagen, Netherlands), which enables both genomic DNA elimination and reverse transcription. Components and protocol of cDNA synthesis reaction are shown in Table 3.2. Briefly, a mix containing RNA sample, gDNA wipeout buffer and RNase-free water was prepared and incubated for 2 min at 42°C. Then, the mixture was rapidly placed on ice. Buffer, primer mix and reverse transcriptase were further added into the mixture and incubated for 2 min at 42°C, followed by 2 min at 95°C. All incubation steps were performed in a thermal cycler plate (Arktik Thermal Cycler, Thermo Fisher Scientific, USA).

Table 3.2. cDNA synthesis reaction set-up.

Component	Volume (µL)	Final Concentration
gDNA WipeOut (7x)	2	1x
Template RNA	11	2.5 ng/µL
RNase-free water	1	
Incubation		**42°C, 2 min**
RT Buffer (5x)	4	1x
RT Primer Mix	1	
Quantiscript Reverse Transcriptase	1	
Final Volume	20	
Incubation		**42°C, 30 min & 95°C, 3 min**

3.5.3. Polymerase chain reaction (PCR)

Primer sequences for B7-1, B7-2, B7-H2, 4-1BBL, OX-40L, LIGHT, and β-actin designed for gene expression analyses are listed below (Table 3.3).

Table 3.3. Forward and reverse primer sequences of the genes and related information.

	Forward Primer (5'-3')	Reverse Primer (5'-3')	Product Size	GeneBank No
B7-1	ccgagtacaagaaccggacc	ggtgtagggaagtcagctttga	181 bp	NM_005191.4
B7-2	atgggccgcacaagttttga	aggttgactgaagttagcaagca	171 bp	NM_175862.5
B7-H2	gccagacaggaaatgacatcg	ctgtgttggaggcatcggtc	166 bp	NM_001365759.1
4-1BBL	gcccaaaatgttctgctgatcg	agtgaaacggagcctgagc	200 bp	NM_003811.4
OX40L	aggtatcacatcggtatcctcg	acctttctccttcttatattcggt	71 bp	NM_003326.5
LIGHT	gcatctcacaggggccaact	gctgcaccttggagtagatgt	158 bp	NM_003807.4
***β*-actin**	ctggaacggtgaaggtgaca	aagggacttcctgtaacaatgca	139 bp	BC013835

Components and protocol for PCR reaction were indicated in Table 3.4. Prior to use, all reagents were brought to the room temperature and mixed well by vortexing, except for Taq DNA Polymerase (Thermo Fisher Scientific, USA).

Table 3.4. PCR components and reaction mixture.

Component	Volume (µL)	Final Concentration
Taq Buffer (10x)	2.5	1x
dNTP mix (2 mM)	2.5	0.2 mM
$MgCl_2$ (25 mM)	2.5	2.5 mM
Forward Primer	1	0.2 µM
Reverse Primer	1	0.2 µM
dH_2O	14.25	
Taq DNA Polymerase (5 U/µL)	0.25	0.05 U/µL
Template cDNA	1	
Final Volume	25	

All steps for the preparation of PCR mixture was performed on ice. For the reaction, a master mix was prepared in a 1.5 mL tube. Respectively, Taq Buffer, RNase/DNase free water, (dH_20), dNTP mix, forward and reverse primers, and $MgCl_2$ were added into the mix. The master mix was further mixed thoroughly by vortexing. Then, Taq DNA polymerase enzyme was added and the mix was distributed equally into 200 μL PCR tube. Lastly, corresponding cDNA was pipetted into each tube which was then placed into the thermal cycler's plate (Arktik Thermal Cycler, Thermo Fisher Scientific, USA). Gradient PCR program indicated in Table 3.5 was performed for all genes of interest including β-actin to determine the optimal annealing temperatures. The annealing temperatures assessed after gradient PCR were described in Table 3.6.

Table 3.5. Gradient PCR program for B7-1, B7-2, B7-H2, TNSFS9, TNFSF4 and TNFSF14.

Initial Denaturation	95°C	30 sec	
Denaturation	95°C	30 sec	35 cycles
Annealing	58-63°C	30 sec	
Extension	72°C	20 sec	
Final Extension	72°C	10 min	

Table 3.6. Specific annealing temperatures assessed after gradient PCR.

Genes	T_a(°C)
B7-1	**59**
B7-2	**60**
B7-H2	**62**
4-1BBL	**62**
OX40L	**60**
LIGHT	**63**
***β*-actin**	**60**

3.5.4. Real-time PCR (RT-PCR)

Following the determination of the optimal annealing temperatures specific for each gene, real-time PCR was performed quantitative analysis of gene expression. RT-PCR components and protocol are given in Table 3.7.

Table 3.7. Real-time PCR components and related information.

Component	Volume (μL)	Final Concentration
SsoAdvanced universal SYBR Green supermix (10x)	5	1x
Forward Primer	1	0.5 μM
Reverse Primer	1	0.5 μM
dH_2O	2	
cDNA template	1	
Final Volume	10	

The ingredients were brought to the room temperature prior to use and mixed-well by vortexing. To obtain a master mix, ssoAdvanced SYBR green supermix (Biorad, USA), nuclease free dH_2O, forward and reverse primers were mixed thoroughly on ice. The master mix was equally distributed into each PCR tubes (Biorad, USA). Lastly, template DNA was added into the tubes which then were placed into the RT-PCR instrument (BIO-RAD Real-time PCR Detection System, USA). According to these annealing temperatures, thermal cycler protocol for RT-PCR was designed (Table 3.8) Overall, the results for different genes were analyzed according to the formula given by Formula 3.2. Target gene expression in PMNs from different co-cultures were normalized to the target gene expression in freshly isolated PMNs. β-actin was used as a reference gene.

Table 3.8. Real-time PCR Thermal Cycling Protocol.

Polymerase activation and DNA denaturation	95°C	3 min	
Denaturation	95°C	15 sec	40 cycles
Annealing	58-63°C (Please see Table 3.7)	30 sec	
Extension	72°C	20 sec	
Melt-curve analysis	55-95°C, 0.5°C increment	5 sec/step	

(3.2)

$$2^{-\Delta\Delta Ct} = 2^{-(\Delta\text{Ct target gene} - \Delta\text{Ct target gene normalizer})}$$
$$= 2^{-[(\text{Ct target gene} - \text{Ct reference gene}) - (\text{Ct target gene normalizer} - \text{Ct reference gene})]}$$

3.5.5. Agarose gel electrophoresis

Agarose gel (2%) was prepared by mixing 1.5 g agarose with 75 mL 1x TBE buffer and this mixture was melted in microwave oven. After cooling to 60°C, ethidium bromide was added to a final concentration 10 mg/mL and mixed well. The agarose gel was poured into the gel casting tray and the combs were placed. After the gel was solidified, the combs were removed and the gel was placed into the electrophoresis tank. The PCR samples (5 µL) sample mixed with 1 µL 6x DNA loading dye was loaded into the wells. In addition, 0.5 µg DNA size marker was also loaded (Figure 3.9). The electrophoresis was run at 100V with constant current and for 30-40 minutes. Then, PCR products (bands) were observed and documented under UV light (Kodak gel Logic 1500 digital imaging system (Carestream Health, USA).

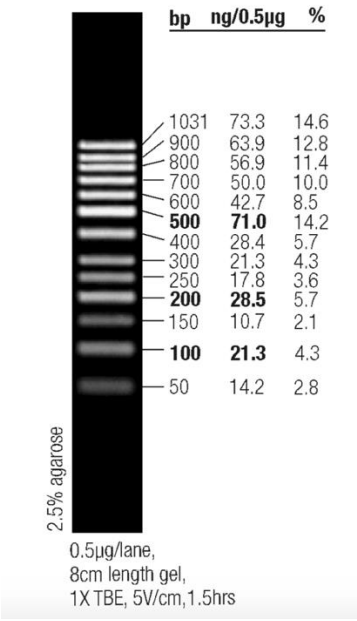

Figure 3.9. 50 bp DNA ladder (Thermo Fisher Scientific, USA).

3.6. Statistical analysis

Data collected from at least 3 independent experiments were statistically tested. Statistical tests including ANOVA, Student's paired or unpaired t-test and Chi-square were performed to indicate the statistical differences between the groups. The difference was accepted as statistically significant when $P \leq 0.05$ and statistically highly significant when $P \leq 0.001$. Mean values were presented with standard error. Data analysis were also performed with RStudio (Version 1.2.1335). Data values were transformed to color scale and heatmaps were designed by using gplots and RColorBrewer packages.

4. RESULTS

4.1. Preliminary analyses on PMN for the establishment of co-culture conditions

4.1.1. Assessment of the PMN viability

PMNs, which are found in a resting state in the blood circulation, become easily activated by signals derived from the stressed tissues (98). Even though, priming of PMNs promotes survival, the growth factor G-CSF, which is the major driver of granulopoiesis, can also delay PMN apoptosis in the peripheral tissues (237). The inflammatory factors such as IFN-γ or antigenic molecules such as fMLP represent two types of molecules that are of adaptive and innate immunity-related stimuli, respectively (237, 238) .

The activation of PMNs commonly results in the production of ROS, which may serve as an immunomodulatory factor both with anti-microbial, pro-inflammatory and immune suppressive actions, especially on T cells (239). Therefore, in this context, we stimulated PMNs ex-vivo with IFN-γ and fMLP in the presence of G-CSF to support their viability and/or NAC to reduce the effects of ROS. Then, the cell death was monitored at 24h, 48h, and 72h.

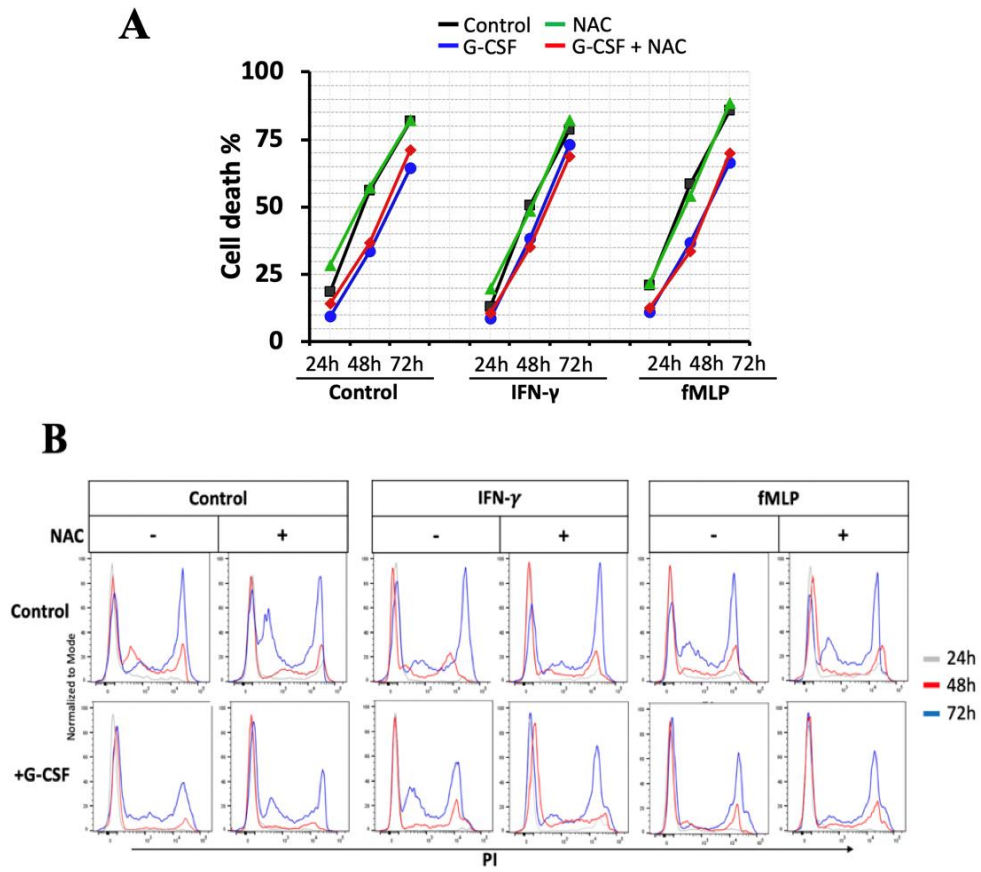

Figure 4.1. 24, 48, and 72h PMN viability upon exposure to G-CSF, NAC, fMLP and IFN-γ. A) The percentage of propidium iodide (PI)-positive (dead cells) after 24, 48 and 72h stimulation of PMNs with G-CSF (50 ng/mL), NAC (1μM) or their combinations in the presence of fMLP (1μM) and IFN-γ (50 ng/mL). Unstimulated PMNs were used as control (n$\geq$3). B) Representative flow cytometry histograms for PI staining after 24, 48 and 72h of stimulated PMNs.

As the culture period was extended, the viability of PMNs were drastically reduced. This effect was slightly ameliorated with IFN-γ, especially at 24h, whereas the viability of PMNs did not alter significantly with fMLP compared to control PMNs at all time points. Following 24h of stimulation, percentage of cell death was retarded in G-CSF and IFN-γ stimulated PMNs (control, 18$\pm$2.1%; G-CSF-stimulated, 7.2$\pm$2.4%; IFN-γ-stimulated, 10.2 $\pm$ 1.7%, $P<0.05$) (Figure 4.1 A and B). The effect of G-CSF on PMN viability was most prominent at 48h (control, 56.9$\pm$3.2%; G-CSF-stimulated, 28.8$\pm$2.1%) wherein fMLP and IFN-γ stimulation did not have a significant effect. Addition of G-CSF remarkably delayed the cell death, but NAC did

not show considerable influence either alone or in combination with G-CSF (Figure 4.1 and Figure 4.2). At 72h, the viability deteriorated under all stimuli. However, only G-CSF stimulated PMNs could survive up to a percentage of 57.5±2.2% dead cells. No significant difference between the viability of NAC and fMLP stimulated and control PMNs was detected. Moreover, the viability of IFN-γ stimulated PMNs displayed same profile with control PMNs (Figure 4.1 A and B).

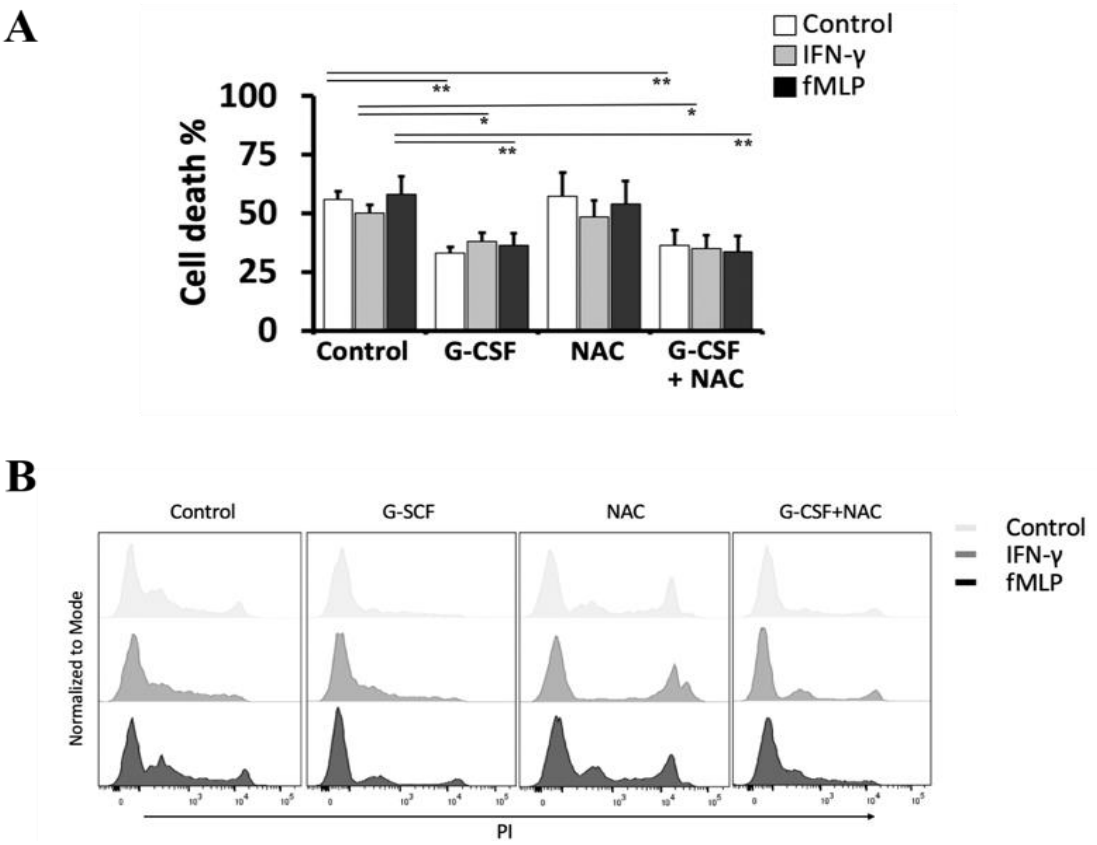

Figure 4.2. At 48h, PMN viability upon exposure to G-CSF, NAC, fMLP and IFN-γ. A) The percentage of propidium iodide (PI)-positive (dead cells) after 48h stimulation of PMNs with G-CSF (50 ng/mL) and NAC (1μM) or their combinations in the presence of fMLP (1μM) and IFN-γ (50 ng/mL). Unstimulated PMNs were used as control. B) Representative flow cytometry histograms for PI staining on PMNs stimulated for 48h (*P<0.05, **P<0.001, n≥3)

Since the final goal for this study is to test the influence of PMNs on immune reactions, co-cultures with PBMCs were performed. Before co-culturing them with PBMCs, 24h stimulated PMNs were washed to remove the factors including G-CSF,

NAC, fMLP and/or IFN-γ. The washing step (removal of stimulants) were included since the PMNs were going to be cultured with PBMCs and PBMCs should not have been stimulated with the factors carry-over from the initial priming of PMNs.

24h incubation led to a significant number of cell death in control PMNs, whereas this number was remarkably reduced with G-CSF stimulation (control, 18.6$\pm$1.8%; G-CSF-stimulated, 6.7$\pm$0.9%). In Addition, NAC did not show a considerable influence on PMN viability. At 48h, washing did not affect the viability mediated by G-CSF; however, it can cause a significant number of cell death in control and NAC stimulated PMNs. Moreover, washing did not alter the viability in both control and G-CSF stimulated PMNs in the presence of IFN-γ, whereas removed the positive effect of G-CSF on PMN survival in fMLP-stimulated PMNs (Figure 4.3 A). It also escalated the number of cell death in G-CSF and NAC stimulated PMNs (Figure 4.3 A and B), and the number of cell death did not significantly change in the presence of fMLP or IFN-γ (Figure 4.3 A).

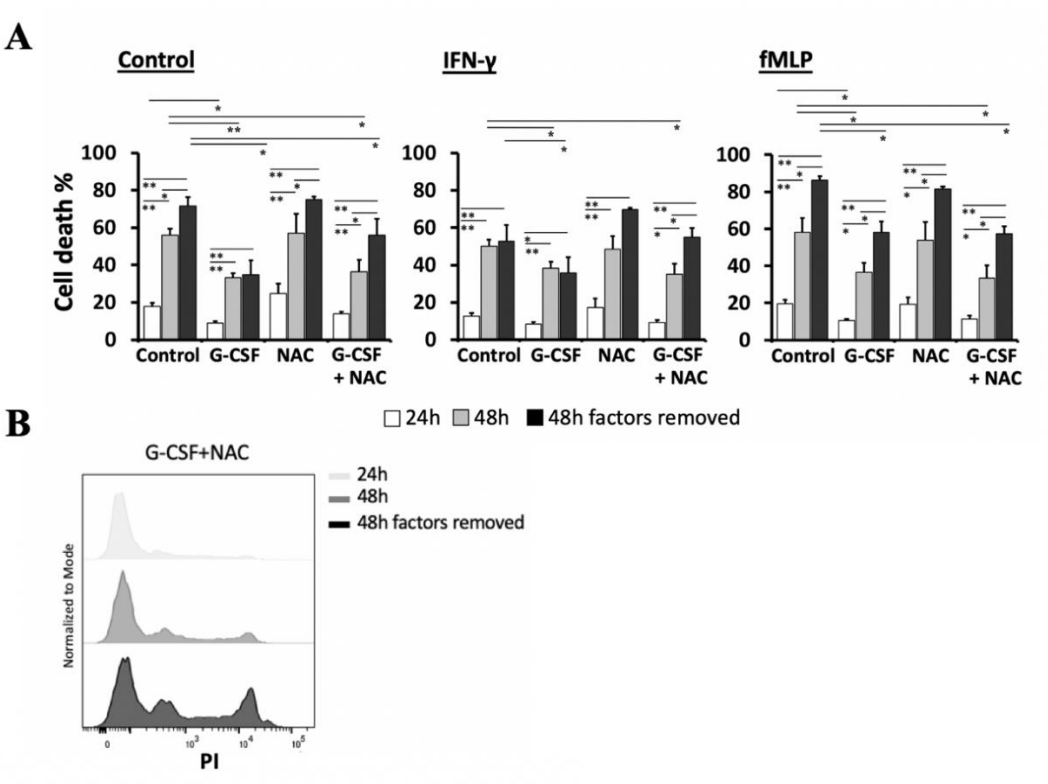

Figure 4.3. The effect of the removal of stimulants on PMN viability after PMNs were exposed to these stimulants for 24h. A) Percentage of propidium iodide (PI) positive (dead cells) in 24 and 48h of exposure to stimuli. PMNs were stimulated with G-CSF (50 ng/mL) and NAC (1μM) or their combinations in the presence of fMLP (1μM) and IFN-γ (50 ng/mL) for 24h and 48h. In some groups, the stimulants were washed away after 24h of exposure and following 24h, cell viability was assessed (48h factors removed). B) Representative flow cytometry histograms for PI staining on PMNs stimulated with G-CSF and NAC for 48h (*P<0.05, **P<0.001, n≥3)

Next, the viability of PMNs upon co-culturing with PBMCs were tested. Co-culturing did not significantly alter the viability of PMNs. Nevertheless, the PMNs' fitness was already hampered at 48h with or without co-culturing. Co-culturing did not have a remarkable influence on the viability of G-CSF stimulated PMNs (control, 56.9 $\pm$ 3.2%; G-CSF-stimulated, 28.8$\pm$2.1%; G-CSF-stimulated in PBMC co-culture, 37.9$\pm$4.1). Moreover, in IFN-γ stimulated PMNs, co-culturing with PBMCs did not affect the viability. Nevertheless, in the presence of fMLP, G-CSF stimulation did not significantly enhance the survival of PMNs in PBMC co-culture. Moreover, with or without PBMCs, NAC stimulation alone or in combination with IFN-γ or fMLP did

not prominently alter the viability (Figure 4.4 A). In the presence of PBMCs, NAC stimulation alone or in combination with IFN-γ hampered the positive effect of G-CSF on PMN survival, whereas in combination with fMLP, it did not (Figure 4.4 A and B).

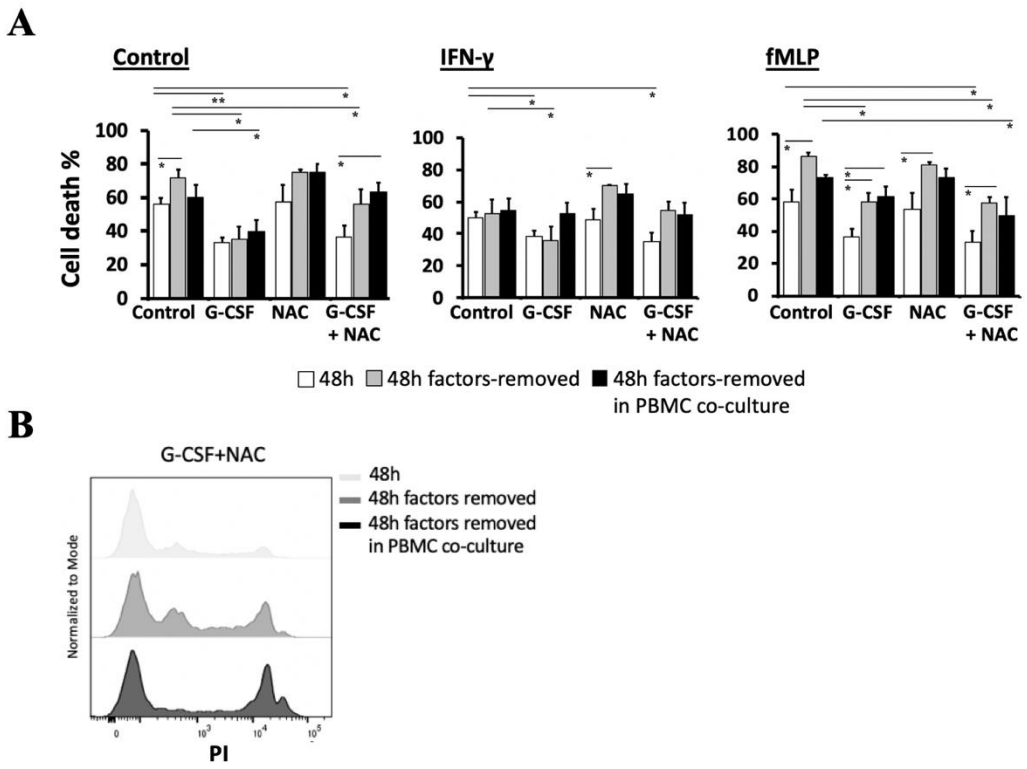

Figure 4.4. PMN viability in PBMC co-cultures. A) The percentage of propidium iodide (PI) positive (dead cells) in PMNs. PMNs were stimulated with G-CSF (50 ng/mL) and NAC (1μM) or their combinations in the presence of fMLP (1μM) and IFN-γ (50 ng/mL). After 24h, these stimulants were either washed away (48h factors removed) or not (48h). Then, they were co-cultured with PBMCs from healthy volunteers (48h factors removed in PBMC co-culture) for 24h. Following 24h stimulation, cell viability was determined in each group. B) Representative flow cytometry histograms for PI staining on PMNs stimulated with G-CSF and NAC and co-cultured with PBMCs (PMN:PBMC 1:1; *P<0.05, **P<0.001, n≥3).

In order to test the influence of lung cancer cells on PMN viability, which was planned as a component of co-cultures in the scope of this study, PMNs were co-cultured with two lung cancer cell lines with (A549 and NCI-H1299) with or without the presence of monocytes as an additional component.

A significant number of cell death was detected following 24h of incubation; however, being with lung cancer cells slightly reduced the number of cell death. Besides, the effect of lung cancer cells on the viability of PMNs was more pronounced at 48h. The percentage of viable cells was significantly higher in the PMNs co-cultured with lung cancer cells in comparison to that of obtained with unstimulated PMNs (control, 52.1±3.2%; A549-co-cultured, 75±1.3%; H1299-co-cultured, 78.2±1.6%) (Figure 4.5 A and Figure 4.6). In addition, conditioned media prolonged the PMN survival as well (control, 52.1±3.2%; A549 CM-cultured, 78.2±1.5%; H1299 CM-cultured, 76.4±1.8%) (Figure 4.5 B and Figure 4.6). On the other hand, the presence of monocytes did not remarkably affect the viability of PMNs (Figure 4.5 and Figure 4.6). Moreover, the effect of soluble factors derived from lung cancer cells on PMN survival was compared with the effect of G-CSF. At 48h, the number of viable cells was slightly higher in the PMNs stimulated with conditioned media than PMNs stimulated with G-CSF (A549 CM-cultured, 78.2±1.5%; H1299 CM-cultured, 76.4±1.8%, G-CSF-stimulated 65.4±2.8) (Figure 4.5 B and Figure 4.6).

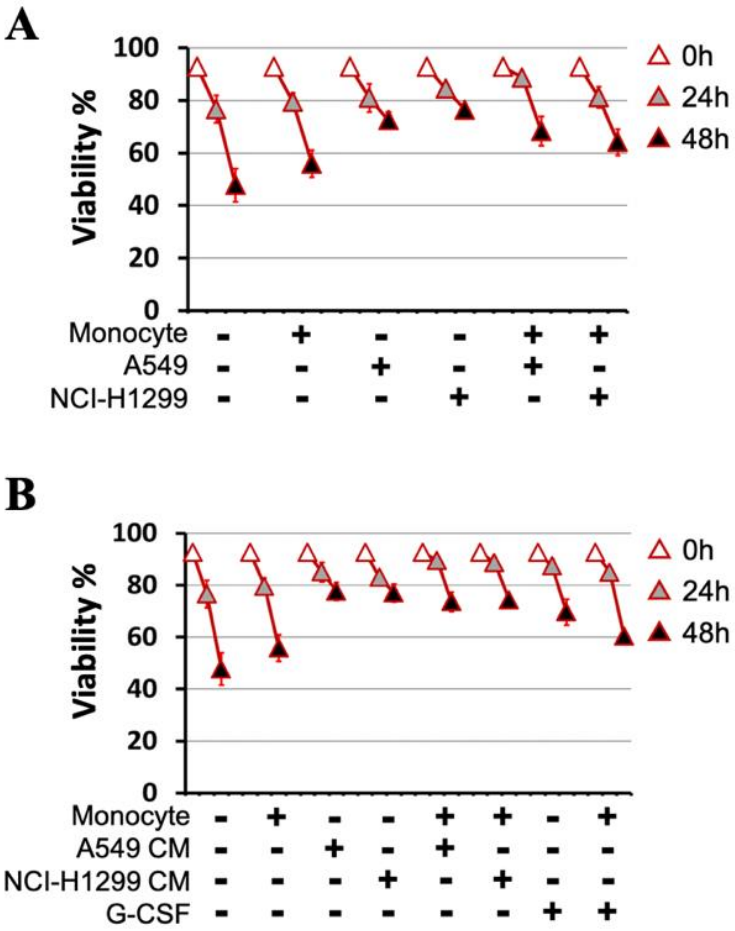

Figure 4.5. PMN viability in the presence of lung cancer cells. The percentage of PI negative cells (viable cells) were determined in PMNs (A) co-cultured with either A549 and NCI-H1299 cells (Co-culture) or (B) with their conditioned media (CM) or with G-CSF (50 ng/mL). PMNs were co-cultured in the presence or absence of monocytes. After 24 and 48h, cell viability was assessed. (PMN:Monocyte:lung cancer cells 0.5:0.5:0.25; n ≥ 3).

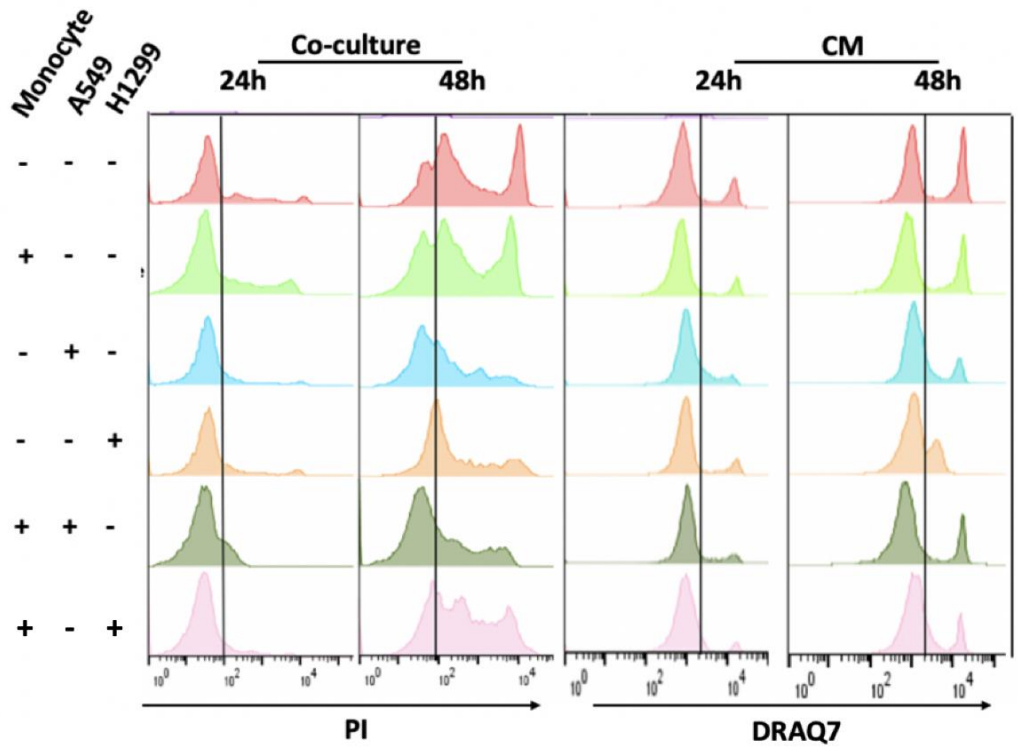

Figure 4.6. Representative flow cytometry histograms showing the PI and DRAQ7 staining of PMNs cultured with monocytes and lung cancer cells. PMNs were co-cultured either with A549 or NCI-H1299 cells (Co-culture) or their conditioned media (CM) in the presence or absence of monocytes for 24h and 48h. (PMN:Monocyte:A549 or NCI-H1299 cells 0.5:0.5:0.25).

Overall, G-CSF enhanced the survival of PMNs. Washing or being with PBMC could not remarkably alter this. Lung cancer cells or their conditioned media prolonged the PMN survival as well.

4.1.2. Assessment of PMN activation

PMN can become easily activated upon exposure to various stresses. In activation, ROS production and changes in certain surface molecules' expression such as CD66b, CD62L, and CD11b are observed (239, 240). To assess the change in activation status of PMNs, they were stimulated with G-CSF, NAC, fMLP and IFN-γ and ROS production was assessed. After 24h, in the absence of any stimuli, PMNs could spontaneously produce high amount of ROS, and stimulation with fMLP could

not make a difference. PMNs stimulated with G-CSF has lowest ROS production capacity (Figure 4.7 A). Moreover, as expected, NAC stimulation led to significant decreased in ROS production (Figure 4.7 A and B).

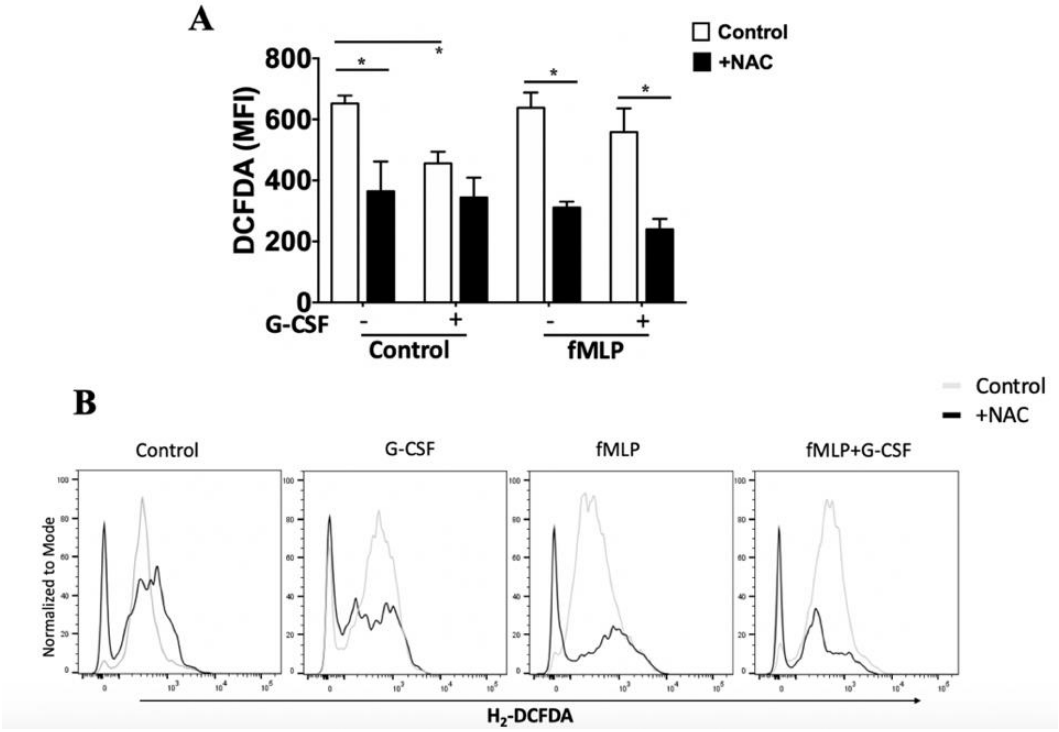

Figure 4.7. ROS levels in PMNs treated with G-CSF and fMLP in the presence or absence of NAC. A) Median fluorescence intensities (MFI) of H2-DCFDA on PMNs treated with G-CSF (50ng/mL) and fMLP (1μM) with or without NAC (1μM) for 24h. Control represents unstimulated PMNs. B) Histograms showing representative fluorescence intensities of H2-DCFDA in PMNs stimulated with the G-CSF and fMLP with or without NAC (*P<0.05, **P<0.001, n≥3).

Given that the viability of PMNs were prolonged in the presence of the lung cancer cells or the factors secreted thereof, the activation status of these PMNs was further investigated. ROS production capacity of PMNs and surface marker expression on PMNs were determined.

Being with lung cancer cells or their conditioned media significantly diminished the ROS production in PMNs (Figure 4.8 A). The presence of monocytes in the cultures also reduced the ROS levels in PMNs; however, either in the presence

or absence of monocytes, ROS levels were unequivocally reduced when exposed to cancer cells (Figure 4.8 A and B).

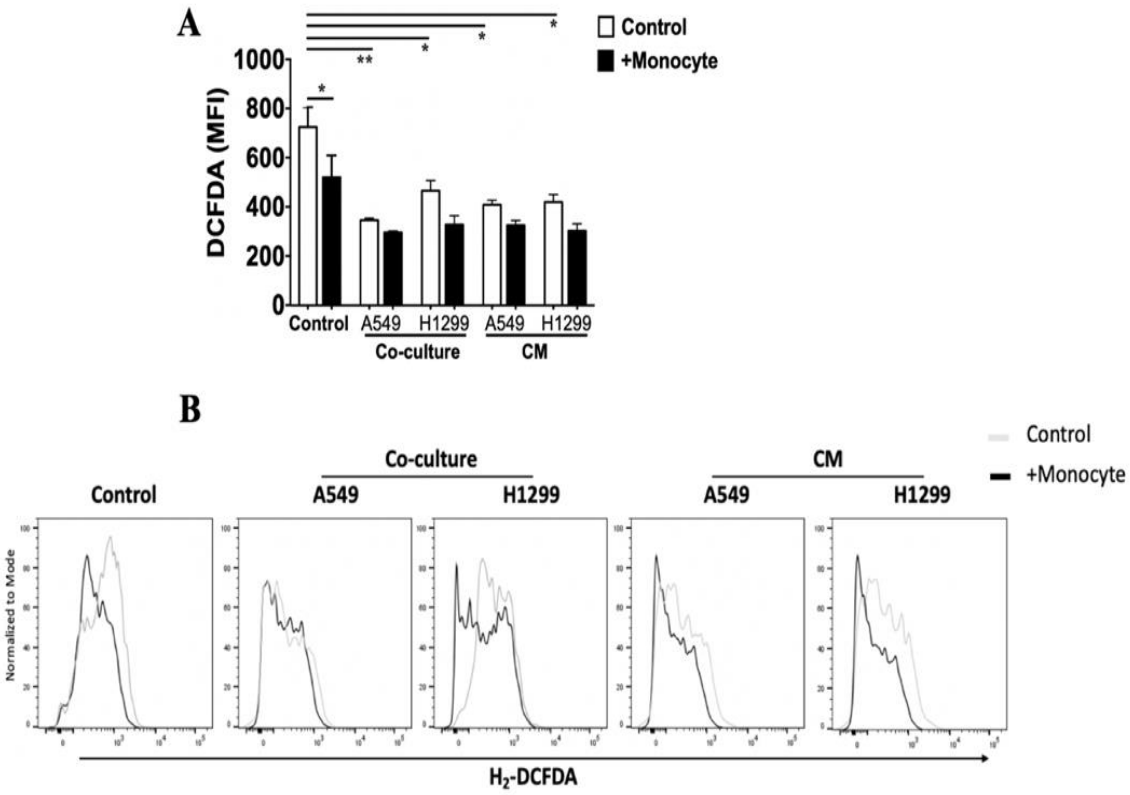

Figure 4.8. ROS production of PMNs in response to monocytes and lung cancer cells. A) Median fluorescence intensities (MFI) of H2-DCFDA on PMNs. PMNs were co-cultured with A549 or NCI-H1299 or cultured with their conditioned media (CM) in the presence or absence of monocytes for 24h (PMN:Monocyte:A549 or NCI-H1299 cells 0.5:0.5:0.25). After 24h, ROS production in PMNs were detected. Control represents unstimulated PMNs. B) Histograms showing representative fluorescence intensities of H2-DCFDA in PMNs co-cultured with A549 or NCI-H1299 in the presence or absence of monocytes (*P<0.05, **P<0.001, n≥3).

In freshly isolated PMNs, CD62L was expressed at high levels (99.8±0.3%). Following 24h and 48h of incubation, CD62L expression on PMNs was downregulated (24h, 25±4.2%; 48h, 10.2±1.5%). In lung cancer cells-containing co-cultures, expression of CD62L on PMNs was also diminished over time but not as prominently in the control PMNs (A549-co-cultured PMN: Oh, 99.8±0.3%; 24h,

43±4.6%; 48h, 28±1.8%, H1299-co-cultured PMN: Oh, 99.8±0.3%; 24h, 65±4.2 %; 48h, 22±2.5%; control PMN: Oh, 99.8±0.3%; 24h,25±4.2%; 48h,10.2±1.5%) (Figure 4.9 A and Figure 4.10). Similarly, in the presence of conditioned media from lung cancer cells, CD62L expression on PMNs were decreased over time but not as drastically as in control PMNs (A549 CM-cultured: Oh, 99.8±0.3%; 24h, 42±5.1 %; 48h, 18.2±2.8%, H1299 CM-cultured PMN: Oh, 99.8±0.3%; 24h, 40.1±1.2%; 48h, 21.1±1.5%; control PMN: Oh, 99.8±0.3%; 24h,25±4.2%; 48h,10.2±1.5%) (Figure 4.9 B). In other words, presence of lung cancer cells slightly restrained the downregulation of CD62L on PMNs, whereas the effect of conditioned media was not so potent.

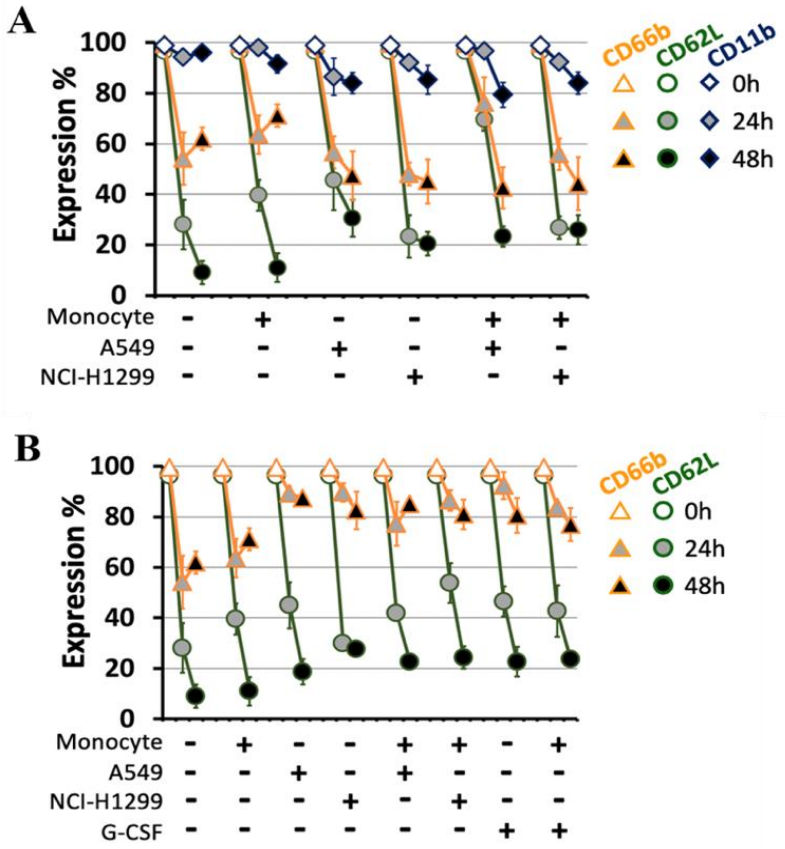

Figure 4.9. CD66b, CD62L and CD11b expression on PMNs in the co-cultures with lung cancer cells. PMNs were co-cultured with (A) A549 or NCI-H1299 cells or (B) their conditioned media in the presence or absence of monocytes for 24h and 48h (PMN:Monocytes: A549 or NCI-H1299 0.5:0.5:0.25). PMNs were gated as CD33+ HLA-DR- and viable PMNs were gated (n≥3).

As expected, CD66b was highly expressed on freshly isolated PMNs (99.7± 0.2). Within 48h, it decreases to 60.1± 3.3%. In the presence of lung cancer cells, the downregulation of CD66b expression was more drastic (A549-co-cultured PMN: Oh, 99.7±0.2%; 24h, 58.6±3.9%; 48h, 44.2±5.6%, H1299-co-cultured PMN: Oh, 99.7±0.2%; 24h, 46.5±2.1%; 48h, 42.1±4.9%) (Figure 4.9 A and Figure 4.10). On the other hand, in the presence of conditioned media, CD66b expression on PMNs remained high throughout the culture period. At 48h, the percentage of cells positive for CD66b was 80-85% in the conditioned media-stimulated PMNs, whereas 60-70% in control PMNs (Figure 4.9 B). G-CSF treated PMNs had a similar expression pattern for CD62L, CD66b, and CD11b with PMNs in conditioned media (Figure 4.9 B).

As the culture period extended, CD11b expression remained high in control PMN, whereas it was slightly diminished in the presence of lung cancer cells. Following 48h of incubation, PMNs co-cultured with lung cancer cells and monocytes had the lowest CD11b expression (Figure 4.9 A and 4.10). Addition of monocytes to the co-cultures did not remarkably affect the level of CD66b, CD62L and CD11b on PMNs (Figure 4.9 and 4.10).

All in all, the presence of lung cancer cells or their conditioned media delayed, but not inhibited the activation of PMNs.

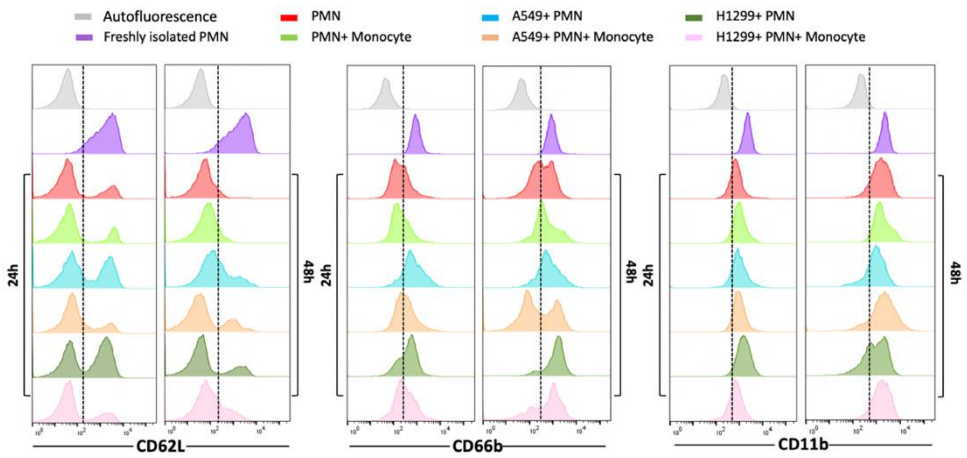

Figure 4.10. Representative histograms showing the expression of CD66b, CD62L, and CD11b on PMNs. PMNs were co-cultured with A549 or NCI-H1299 in the presence or absence of monocytes for 24h and 48h (PMN:A549 or NCI-H1299:Monocytes 0.5:0.5:0.25). PMNs were gated as $CD33^{+}$ HLA-DR- and viable PMNs were gated.

4.1.3. The influence of PMNs on T cell proliferation

To determine the effect of PMNs on T cell proliferation, freshly isolated PMNs were pre-treated with G-CSF, NAC, fMLP and IFN-γ and then, co-cultured with PBMCs at different ratios for 72h. The co-cultures were established in the presence of αCD3 mAb used to recapitulate the first signal, whereas monocytes in PBMCs was employed to give the co-stimulatory second signal required for T cell activation.

In the co-cultures established with control PMNs (that were cultured in complete medium without any stimulants for 24h), only a slight increment was observed in the proliferation of αCD3-induced T cells amongst PBMCs (range 110-125%) and no trendline was obtained as the ratio of PMNs was increased. Similarly, co-cultures with PMNs pre-treated with either IFN-γ or fMLP had minute influence on T cell proliferation. On the other hand, G-CSF pre-treatment restored the proliferation in combination with IFN-γ and fMLP or alone (range 150-175%). Moreover, NAC was another factor that promoted positive influence of PMNs on T cell proliferation in PBMC co-cultures. The combination of NAC and G-CSF, which reduced the levels of ROS and increased the viability of PMNs, resulted in the highest proliferation (range 150-225%) and displayed an increasing trend as the ratio of PMNs was augmented in the co-cultures (Figure 4.11 A and B).

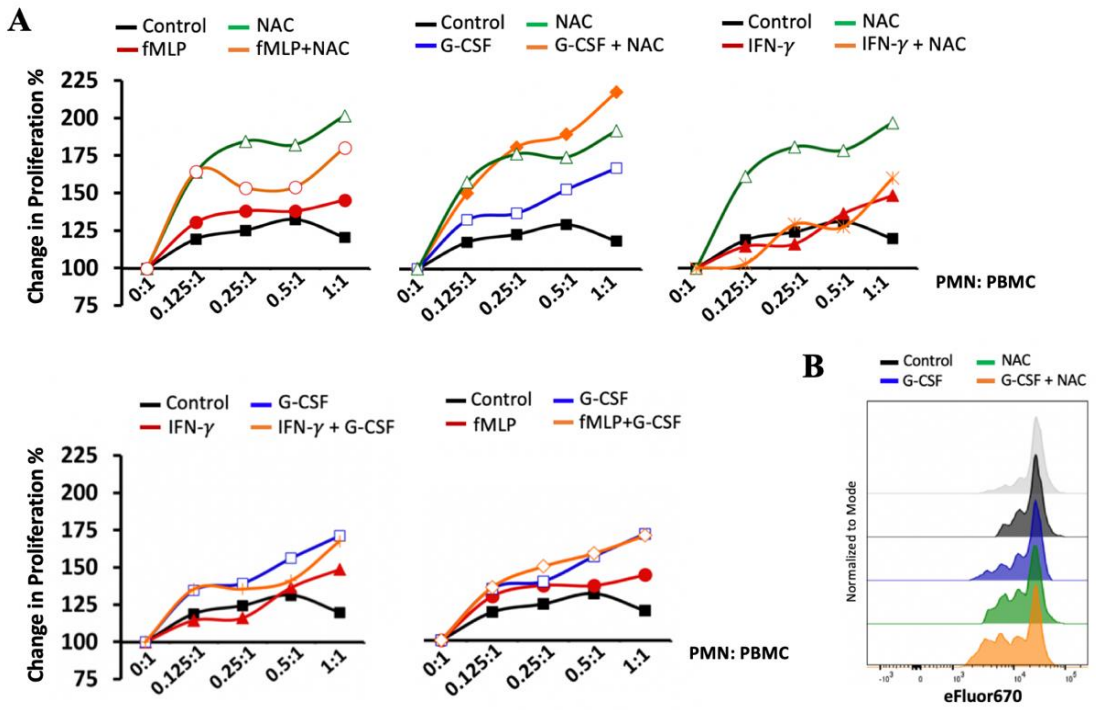

Figure 4.11. Proliferation of T cells amongst PBMCs co-cultured with PMNs. A) The changes in the proliferation PMN co-cultured of PBMCs to that of PBMC alone. PMNs were pre-treated with different combinations of G-CSF (50ng/mL), fMLP (1μM), IFN-γ (50ng/mL) and NAC (1μM) for 24h. Then these agents were washed away and PMNs were co-cultured with PBMCs at different ratios in the presence of 25ng/mL αCD3 mAb for 72h (n≥3). B) Representative proliferation histograms of eFluor670-labeled PBMCs co-cultured with PMNs at 1:1 ratio. Gray histogram represents cultures containing only PBMCs.

Accordingly, when the co-cultures were established with freshly isolated PMNs and the proliferation of T cells was compared with that of obtained with 24h cultured PMNs, a clear upregulation in the T cells duplication rate was seen (at 1:1 co-cultures with fresh PMNs, ~230%; with 24h cultured PMNs, ~120% change in proliferation) (Figure 4.12 A and B).

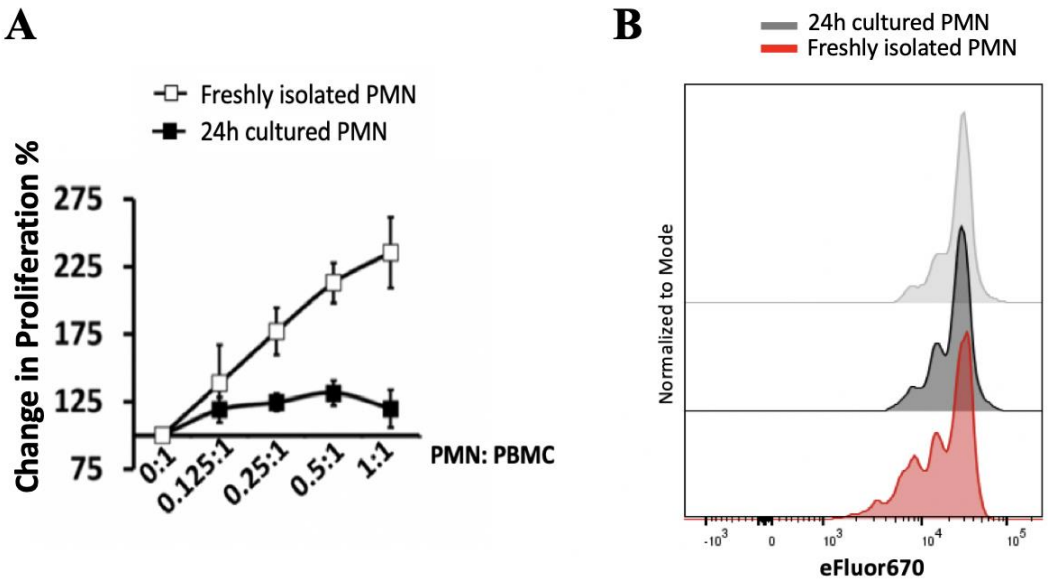

Figure 4.12. Proliferation of αCD3-stimulated PBMCs in the presence of freshly isolated and 24h cultured PMN. A) The changes in the proliferation of PBMCs. PMNs were either incubated for 24h or freshly isolated and co-cultured with PBMCs at different ratios under 25ng/mL αCD3 mAb for 72h (n≥3). B) Representative proliferation histograms of eFluor670 labeled PBMCs co-cultured with PMNs in 1:1 ratio. Gray histogram represents cultures containing only PBMCs.

Next, to determine the influence of PMNs in the proliferation of $CD8^+$ or $CD4^+$ T cells in the presence of NSCLC cells, a co-culture setup was established to partially model the tumor microenvironment, employing primarily freshly isolated PMNs, monocytes and $CD4^+$ or $CD8^+$ T cells together with two prototype lung cancer cell lines, A549 and NCI-H1299.

In monocyte, PMN, and lung cancer cell containing co-cultures, $CD4^+$ T cell proliferation was enhanced compared to the control cultures which did not include cancer cell lines (A549 co-cultures, 70.2±3.2%; H1299 co-cultures, 61.2±5.5%; control group, 44.2±5.4%) (Figure 4.13 A and D). In order to figure out whether direct contact with lung cancer cells was required for PMNs to stimulate T cell responses, conditioned media derived from lung cancer cells was used instead of A549 and NCI-H1299 cell lines themselves. Conditioned media from lung cancer cells could not alter the proliferative capacity of $CD4^+$ or $CD8^+$ T cells (Figure 4.13 A and B).

$CD8^+$ T cells' proliferation were also positively influenced when all three cell types were included in the co-cultures (A549 co-cultures, 62.4±5.1%; H1299 co-cultures, 70.3±3.5%; control group, 42.1±5.4%). Importantly, T cell and PMN co-cultures were also positively influenced T cell responses and this effect was pronounced with $CD8^+$ T cells, albeit not reaching to the level of monocyte stimulated T cells. Intriguingly, the presence of lung cancer cell lines together with PMNs (but with or without monocytes) promoted $CD8^+$ T cell proliferation (A549 co-cultures, 23.4±5.3%; H1299 co-cultures, 18.2±3.5%; control group, 2.1±1.4%) (Figure 4.13 B and D). Moreover, in the absence of myeloid cells, T cells removed quiescent (Figure 4.13 A, B and D).

Since our previous findings underlined the importance of PMNs viability in the co-cultures and positive influence of tumor cell-derived factors on PMN longevity, we asked whether this might be the reason for that the lung cancer cell co-cultured PMNs could better support the T cell proliferation. When, G-CSF was added to the co-cultures of PMNs, monocytes, and $CD4^+$ or $CD8^+$ T cells, no change was obtained in T cell proliferation (Figure 4.13 C and D). Therefore, not underscoring the positive influence of cancer cells on PMN viability, direct cell-to-cell contact with the lung cancer cells was necessary for PMNs to co-stimulate T cell proliferation. There may be a cross-talk between PMNs and especially $CD8^+$ T cells.

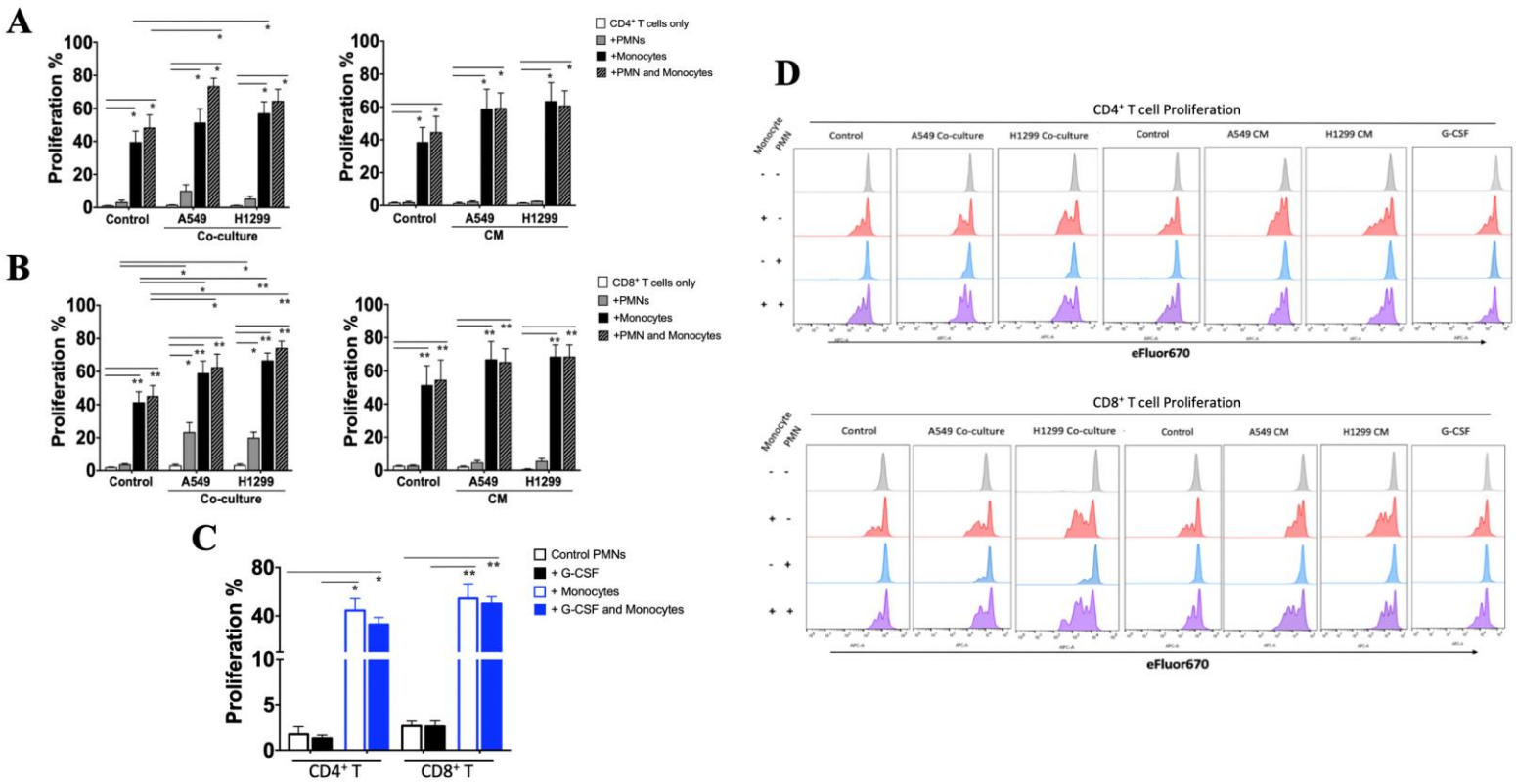

Figure 4.13. Proliferation of $CD4^+$ and $CD8^+$ T cells in the co-cultures established with lung cancer cells or their conditioned media with or without PMNs and monocytes. A) Proliferation percentages of CD4+ T cells and (B) $CD8^+$ T cells co-cultured with PMN, monocyte, and A549 or NCI-H1299 cells in the presence of αCD3 mAb (25ng/mL). C) Proliferation percentages of $CD4^+$ T cells and $CD8^+$ T cells co-cultured with PMN and/or monocyte in the presence of αCD3 mAb and/or G-CSF (50ng/mL). D) Representative proliferation histograms of eFluor670-labeled $CD4^+$ and $CD8^+$ T cells in the co-cultures are shown. (PMN: monocyte: lung cancer cell: T cell 0.5:0.5:0.25:1; CM: Conditioned media; *P<0.05, **P<0.001, n≥3).

To find out the optimal ratio for PMNs and monocytes to especially promote and reveal the importance of PMNs on $CD8^+$ T cell proliferation, these cells were titrated into the co-cultures.

In the absence of monocytes and with cancer cell lines, as the amount of PMNs increased in the co-cultures, the capacity of PMNs to stimulate $CD8^+$ T cell proliferation in the presence of lung cancer cells was augmented. The 1:0.125:1 PMN:Monocyte:$CD8^+$ T co-culture ratio, in the presence of cancer cells, that reached to the confluence (A549, NCI-H1299, and NCI-H441), the less amount of monocytes could reveal the contribution of PMNs to $CD8^+$ T cell proliferation (Figure 4.14). Therefore, this monocyte ratio (0.125) was selected to be used for the co-culture setups throughout this study. NCI-H441 cells co-cultured PMNs also positively influenced the T cell proliferation as other two NSCLC cell lines. At 1:1 PMN:$CD8^+$ T cell ratio, PMNs significantly contributed to the $CD8^+$ T cell proliferation in the presence of lung cancer cells (A549 co-cultures, 30.1±5.2%; H1299 co-cultures, 27.6±4.9%; H441 co-culture, 29.5± 6.1 %; control group 5.6±2.9%). (Figure 4.14 A and B).

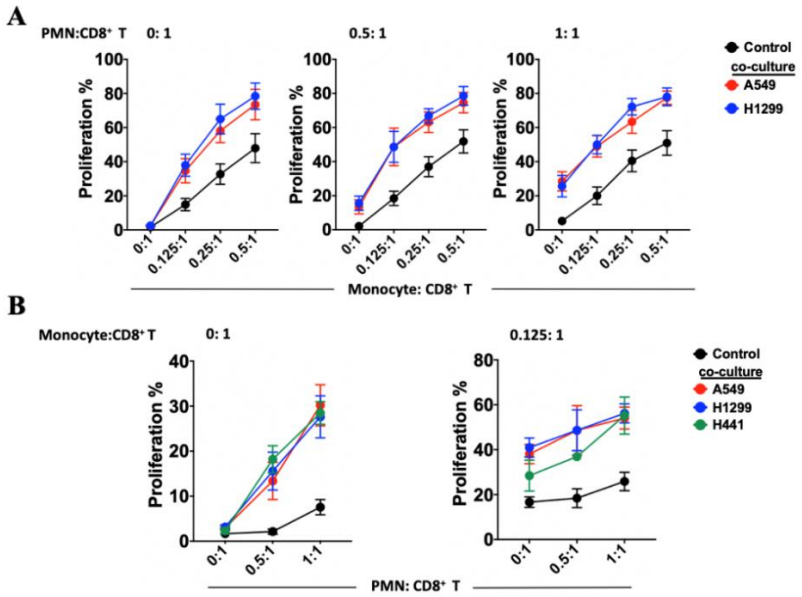

Figure 4.14. Proliferation of $CD8^+$ cells in the co-cultures established with different ratios of PMNs and monocytes. A) Proliferation percentages of $CD8^+$ T cells co-cultured with A549 or NCI-H1299 cells in the presence of αCD3 mAb (25ng/mL) at different ratios of PMNs and monocytes. B) Proliferation percentages of $CD8^+$ T cells co-cultured with A549, NCI-H1299 or NCI-H441 cells in the presence of αCD3 mAb at different ratios of PMNs and monocytes ($n \geq 3$).

4.2. Assessment of $CD8^+$ T cell responses in the co-cultures of PMNs, monocytes and NSCLC cells

Following the optimization of co-culture conditions that would be useful for revealing the influence of PMNs on $CD8^+$ T cell responses in the presence of NSCLC cells and monocytes, T cells' proliferation, activation states and functional differentiation were assessed.

4.2.1. $CD8^+$ T cell proliferation in the co-cultures

In accordance with preliminary experiments, $CD8^+$ T cell proliferation was especially supported in the presence of PMNs when co-cultured with the lung cancer cell lines. In addition, the presence lung cancer cells enhanced the T cell stimulatory capacity of monocytes. PMNs together with monocytes had an additive effect on $CD8^+$ T cell proliferation and this was enhanced in the presence of NSCLC cells (A549 co-cultures, 56.4±4.9%; H1299 co-cultures, 57.8±3.9%; H441 co-culture, 58.2± 5.9 %; control group 25.8±3.4%) (Figure 4.15 A and B).

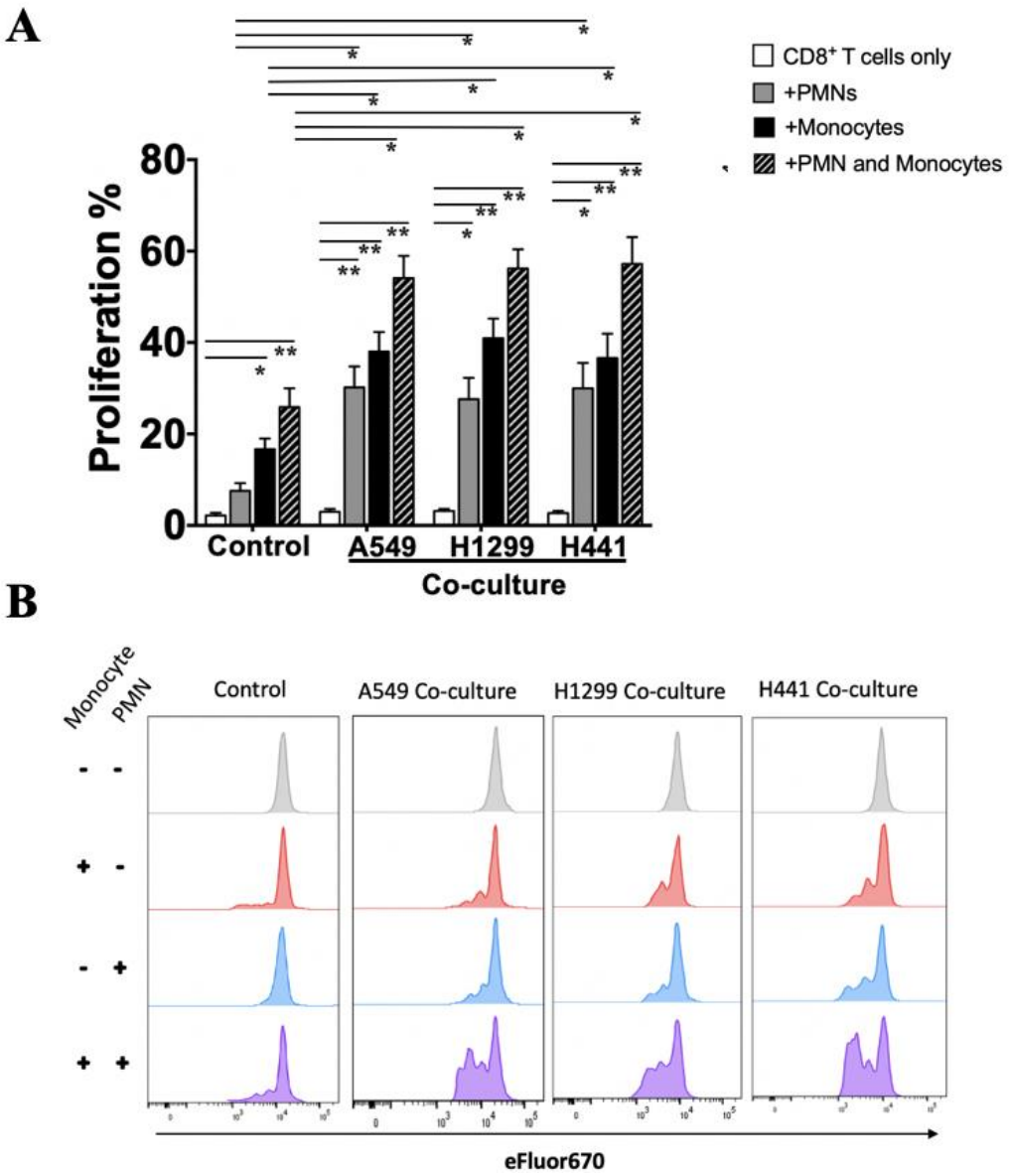

Figure 4.15. Proliferation of $CD8^+$ T cells co-cultured with pre-confluent lung cancer cells, PMN and monocytes at PMN:monocyte:T cell 1:0.125:1 ratio. A) Proliferation percentages and (B) representative eFluor670 assay proliferation histograms of $CD8^+$ T cells in the co-cultures with 25ng/mL αCD3 mAb (*P<0.05, **P<0.001, n≥3).

4.2.2. $CD8^+$ T cell activation in the co-cultures

The initial and effector phases of T cell responses can be followed by the upregulation of certain markers which are informative on the strength of stimuli and functional character to be gained by T cells (241).

Co-cultures containing PMNs could stimulate CD137 and CD69 expression on $CD8^+$ T cells. Upon co-culturing with monocytes and PMNs in the presence of stimulatory αCD3 mAb, $CD8^+$ T cells up-regulated CD137, CD69 and CD25 as early indicators of activation. The levels of CD69 and CD137 was relatively high and compatible in the presence of PMNs or monocytes (range 20-54%). The percentage of T cells expressing CD69 or CD137 was augmented when all the cell types was included in the co-cultures. Although its expression was slightly upregulated in the co-cultures containing all the cell types, CD25 was only detected on a small percentage of $CD8^+$ T cells (range 2-23%). No significant differences were observed in the expression level of CD137, CD69, and CD25 on between $CD8^+$ T cells recovered from the co-cultures with or without lung cancer cells (Figure 4.16, Figure 4.18, and 4.19). Therefore, the activation status of $CD8^+$ T cells did not alter in the lung cancer cells containing co-cultures.

As another activation marker, CD107a on $CD8^+$ T cells was augmented in the co-cultures containing, especially monocytes. However, the percentages of T cells positive for CD107a in the co-cultures which did not contain any lung cancer cells was similar to that obtained from the co-cultures with lung cancer cells (range 19-24%) (Figure 4.16, Figure 4.18, and 4.19).

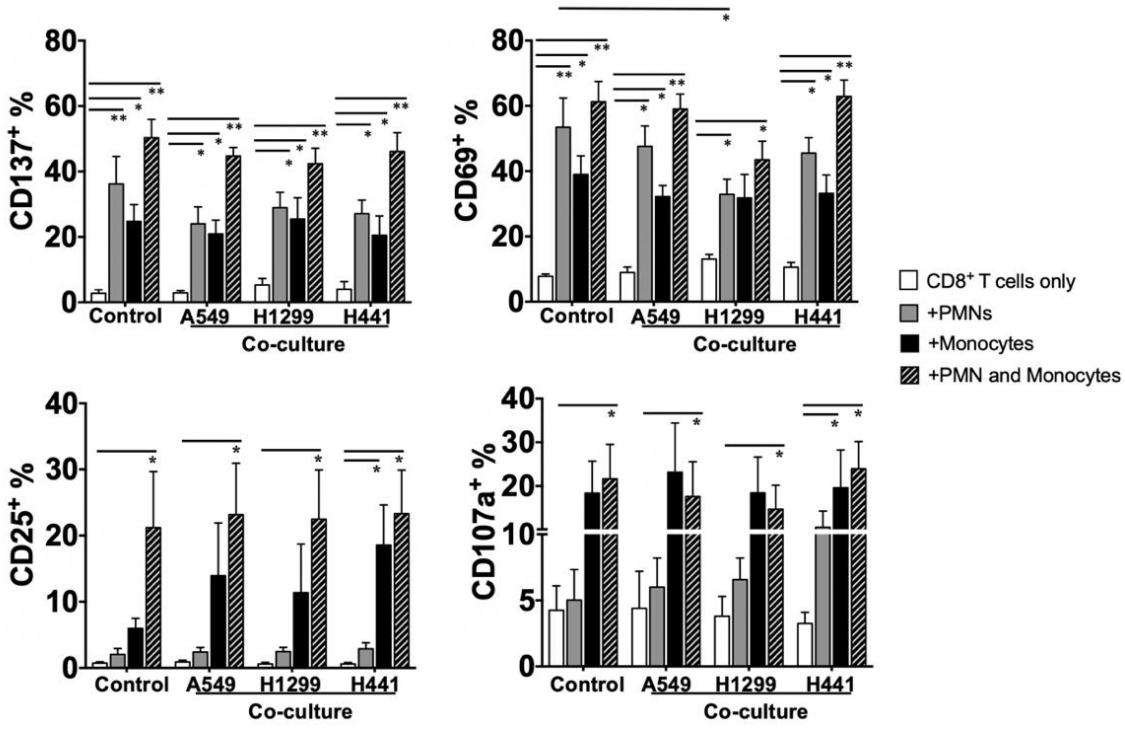

Figure 4.16. Expression of CD137, CD69, CD25 and CD107a on $CD8^+$ T cells co-cultured with PMN, monocytes and lung cancer cells. CD137 and CD69 expression were assessed at 24h, CD25 at 48h and CD107a at 72h of co-culturing (*P<0.05, **P<0.001, n≥3).

On the other hand, the expression of inhibitory receptors on $CD8^+$ T cells was enhanced in the presence of lung cancer cells. Especially, in the co-cultures of PMNs, monocyte and lung cancer cells, the expression of TIM-3 on $CD8^+$ T cells was significantly augmented compared to the controls, which did not contain lung cancer cells (A549 co-culture, 40.1±3.4%; H1299 co-culture, 32.1±3.2%; H441 co-culture 28±3.8%; Control group, 19.2±2.2%). Similarly, the presence of lung cancer cells induced significantly higher LAG3 expression on T cells. Even though, the presence of NSCLC cells led to a tendency to express higher levels of CTLA-4 and PD-1 on T cells; only A549 containing co-cultures stimulated higher CTLA-4 expression on $CD8^+$ T cells compared to the control groups. Similarly, only H1299 containing co-cultures could stimulate significantly higher PD-1 expression on $CD8^+$ T cells than the control groups. However, the percentage of PD-1^+ cells was quite low compared to other co-inhibitory receptors (range 1-10%) (Figure 4.17 and Figure 4.18).

Collectively, both activation- and inhibition-related surface molecules were augmented on $CD8^+$ T cells in the co-cultures, especially when the cancer cells were included (Figure 4.19).

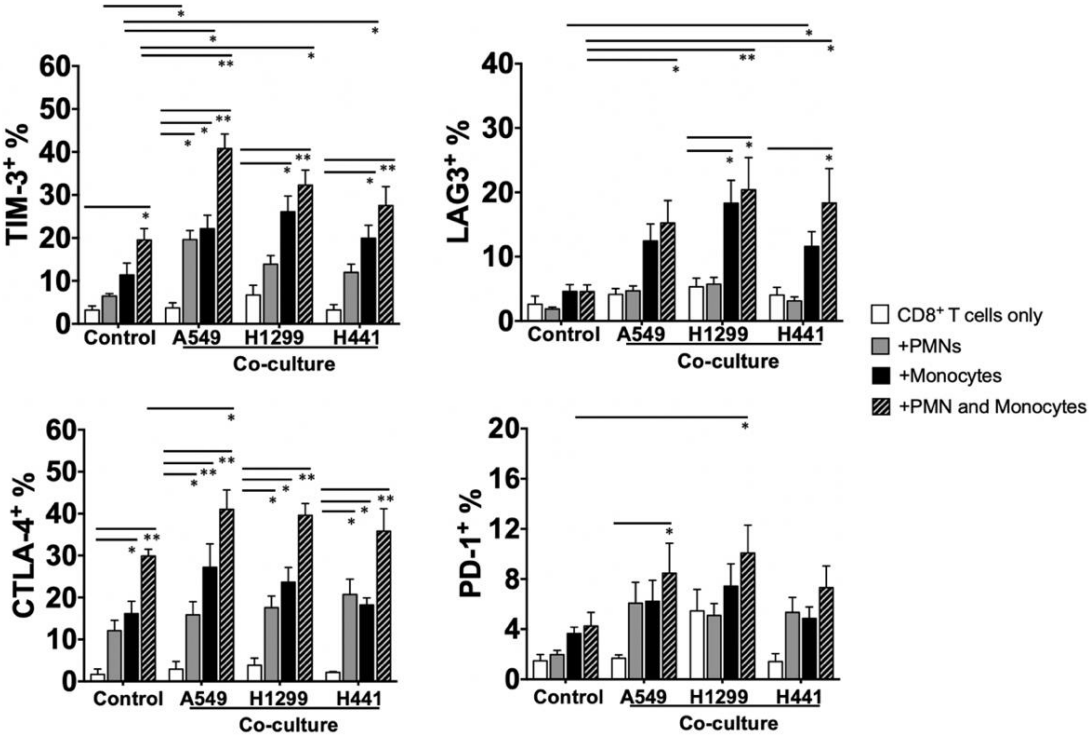

Figure 4.17. Expression of inhibitory receptors on $CD8^+$ T cells from 72h of co-cultures with PMNs, monocytes and lung cancer cells. TIM-3, LAG3, CTLA-4 and PD-1 expression on $CD8^+$ T cells were assessed (*P<0.05, **P<0.001, $n \geq 3$).

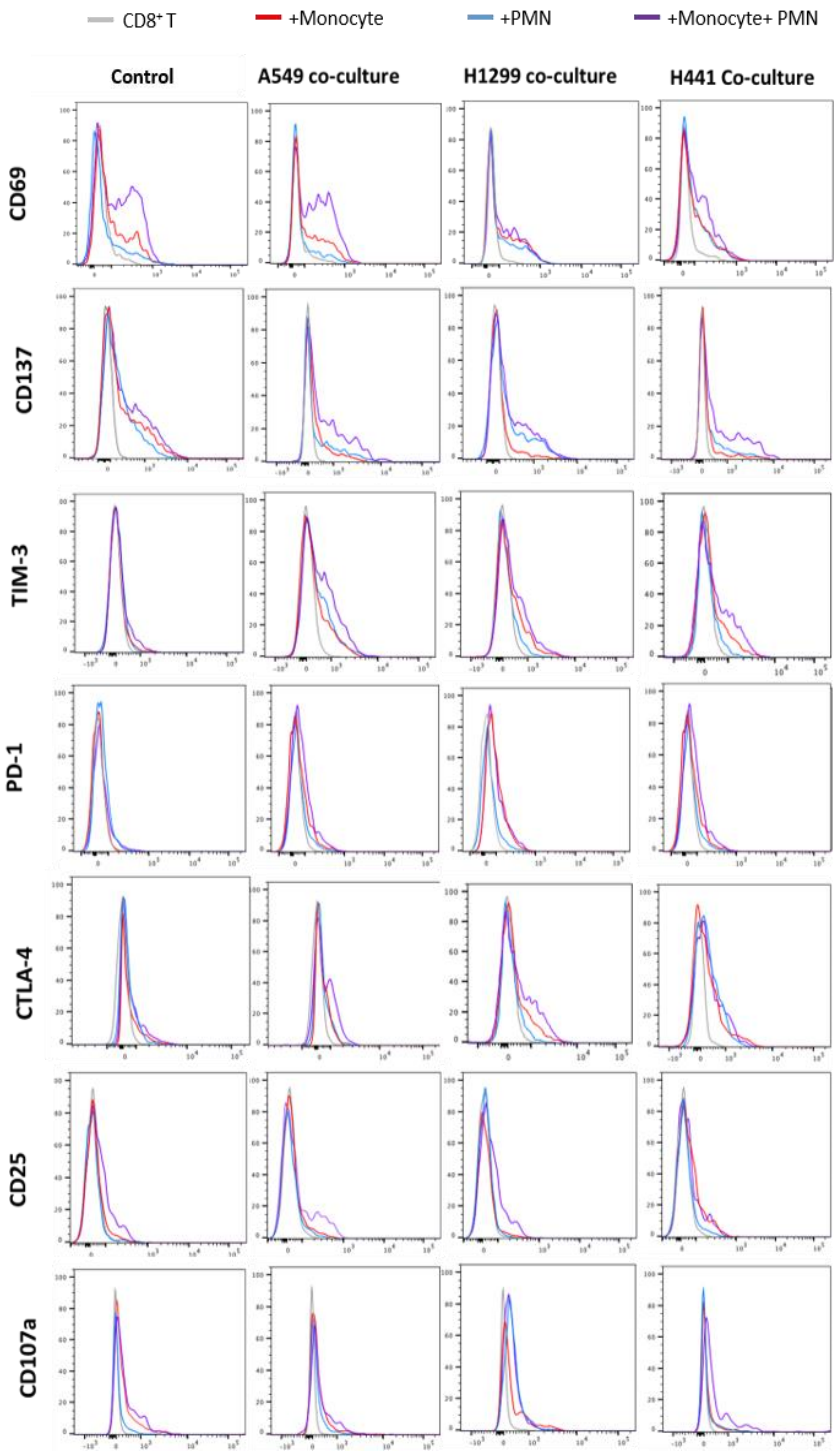

Figure 4.18. Representative histograms showing the expression of CD137, CD69, CD25, CD107a, TIM-3, CTLA-4 and PD-1 expression on $CD8^+$ T cells from different co-culture settings. CD137 and CD69 expression were assessed at 24h, CD25 at 48h and CD107a, CTLA-4, PD-1, and TIM-3 at 72h of co-culturing.

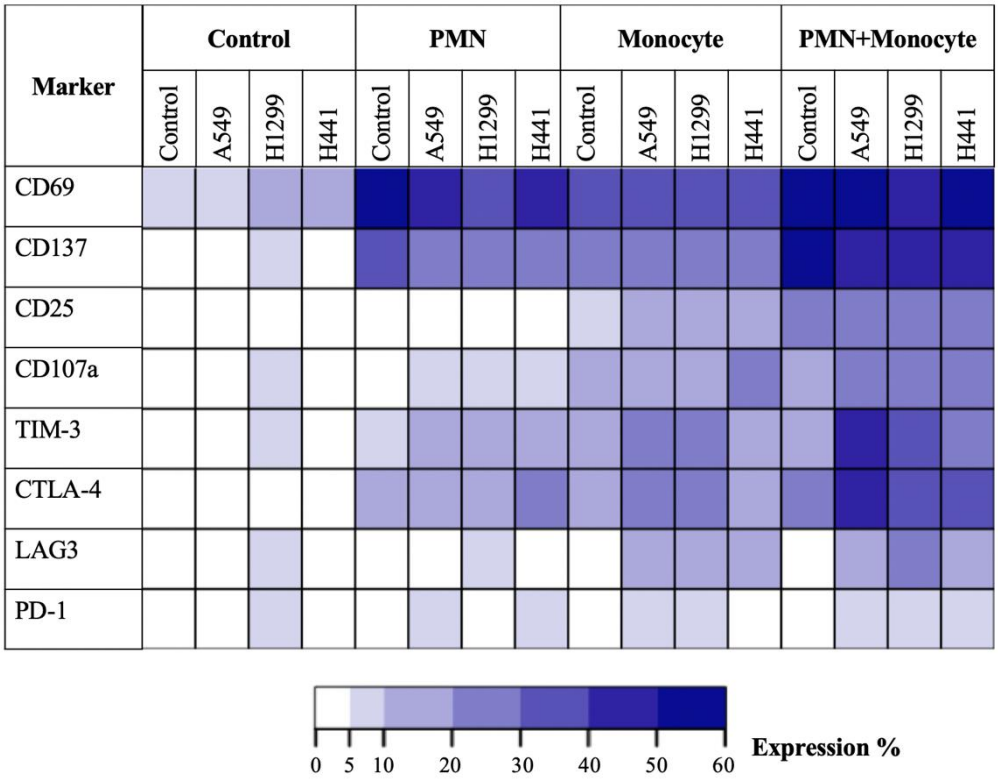

Figure 4.19. Schematic demonstration of CD137, CD69, CD25, CD107a, TIM-3, LAG3, CTLA-4, and PD-1 expression on $CD8^+$ T cells from different co-culture settings. The presence of markers was heat-mapped on the basis of the expression percentages, as depicted above.

4.2.3. $CD8^+$ T cell-related cytokine production in the co-cultures

Not only cell-to-cell contact but also the soluble factors found in the co-cultures determine the fate of $CD8^+$ T cell responses. Therefore, the inflammatory cytokines which are associated with T cells were assayed on the supernatants directly collected from the co-cultures at 72h.

In NCI-H1299 or NCI-H441 containing co-cultures, IFN-γ levels were remarkably high compared to the control group which did not contain lung cancer cells. IL-4 production was also significantly elevated in these co-cultures. Moreover, Il-4 production was not stimulated in the absence of PMNs and monocytes. On the other hand, with the presence of A549 cells, monocytes and PMNs, IL-6 production in the co-cultures was significantly augmented. Additionally, in the absence of

monocytes and PMNs, IL-6 production was below the detection level in the A549 co-cultures (Figure 4.20). Even though, IL-6, IL-4, and IFN-γ were the most abundantly produced cytokines in the co-cultures, production of granzyme A, granzyme B, TNF-α, IL-10, IL-2, sFas, sFasL, and granulysin was also analyzed; the levels of all cytokines; albeit not reaching to the significant level were given as a schematically drawn graph (Figure 4.21). The levels of TNF-α, IL-2, sFas, sFasL, and granulysin was not depicted, since they were below the detection level in all co-cultures.

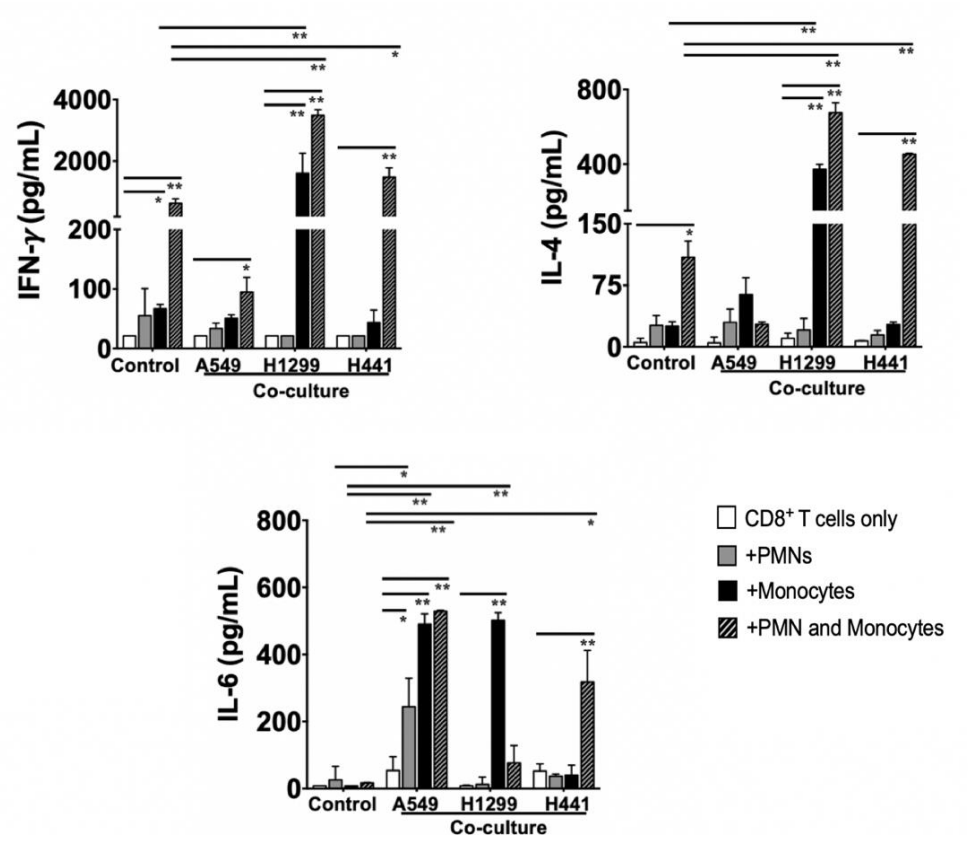

Figure 4.20. IFN-γ, IL-4, and IL-6 cytokine levels in the supernatants collected from the 72h co-cultures of PMN, monocytes and lung cancer cells under 25ng/mL αCD3 stimulation (PMN:monocyte:$CD8^+$ T cell 1:0.125:1 with pre-confluent NSCLC cell lines; *P<0.05, **P<0.001, n≥3).

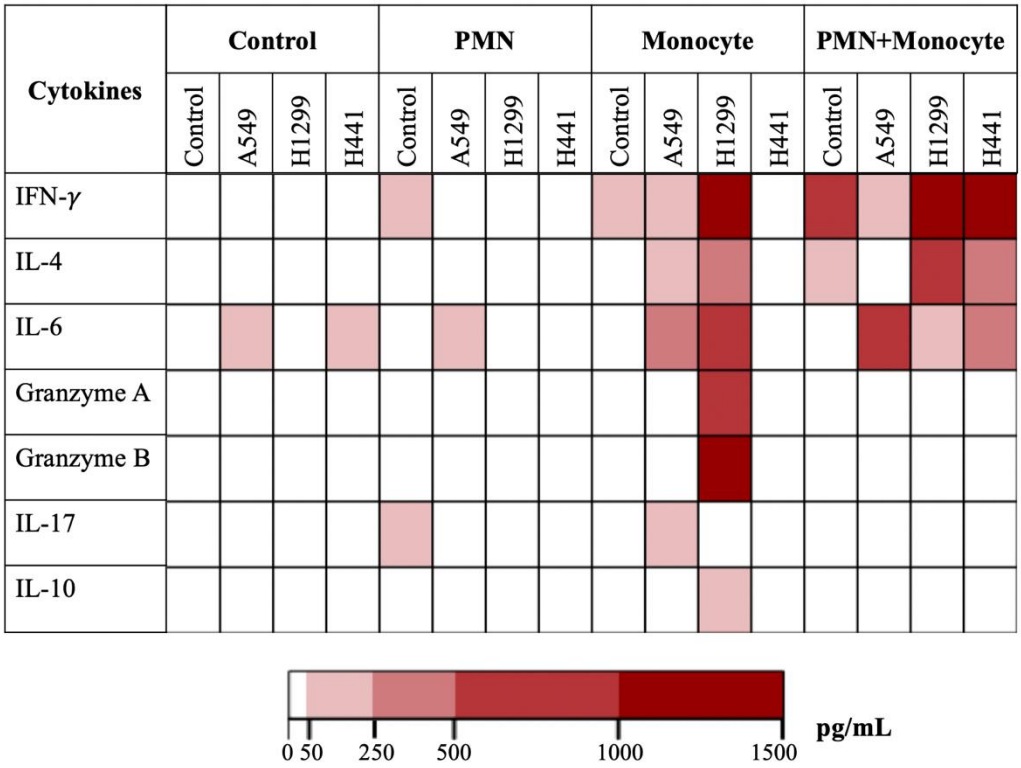

Figure 4.21. Schematic demonstration of IFN-γ, IL-4, IL-6, Granzyme A, Granzyme B, IL-17, and IL-10 production from different co-culture settings. The presence of each cytokine was heat-mapped on the basis of the concentration, as depicted above.

4.2.4. CD8$^+$ T cell exhaustion in the co-cultures

To confirm the effect of PMNs on TIM-3 expression, which was the most consistent and significant inhibitory receptor upregulated on CD8$^+$ T cells in the presence of lung cancer cells, PMNs were titrated into the co-cultures. Increasing the ratio of PMNs in the co-cultures with lung cancer cells resulted in increased percentage of CD8$^+$ T cells expressing TIM-3 (range 10-20% without monocytes; 20-55% with monocytes) (Figure 4.22).

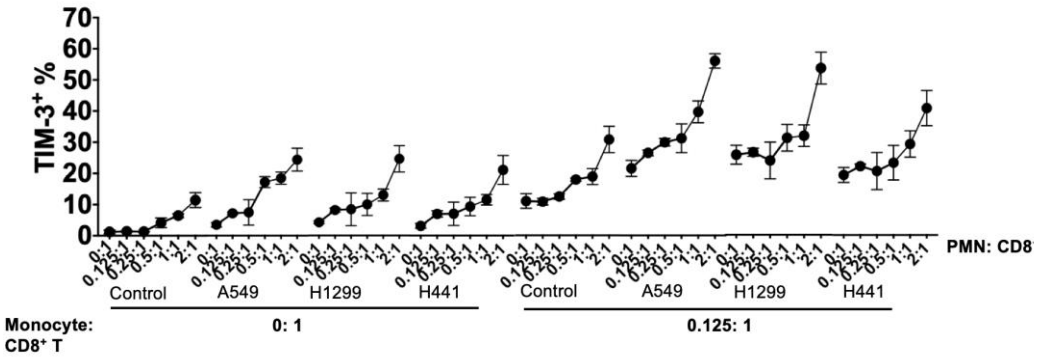

Figure 4.22. The change in the TIM-3 expression on $CD8^+$ T cells in the lung cancer cells containing co-cultures at 72h in the presence of different PMN ratio under αCD3 mAb (25 ng/ml) stimulation **(n≥3).**

Since the exhaustion related inhibitory receptors (i.e. TIM-3) were upregulated on $CD8^+$ T cells in the co-cultures, especially in the presence of PMNs and NSCLC cells, TIM-$3^{-/low}$ and TIM-$3^{mo/high}$ $CD8^+$ T cells were back-sorted from the co-cultures following 96h of co-culturing. In the co-cultures, A549 cells were used as the representative NSCLC line. Following the purification of TIM-$3^{-/lo}$ and TIM-$3^{mo/hi}$ $CD8^+$ T cells, they were labelled with CFSE and re-stimulated with rhIL-2, αCD28, and αCD3 mAb or their combinations for an additional 72h. Proliferative capacity of TIM-$3^{-/low}$ and TIM-$3^{mo/high}$ sub-populations was evaluated by CFSE proliferation assay. Under all conditions, the proliferation of TIM-$3^{mo/high}$ subpopulation was remarkably higher than that of TIM-$3^{-/low}$. The proliferation of TIM-$3^{mo/high}$ was maximized under αCD3/αCD28 stimulation or αCD3/rhIL-2, which also enhanced the proliferation of TIM-$3^{-/low}$ (Figure 4.23 A and B).

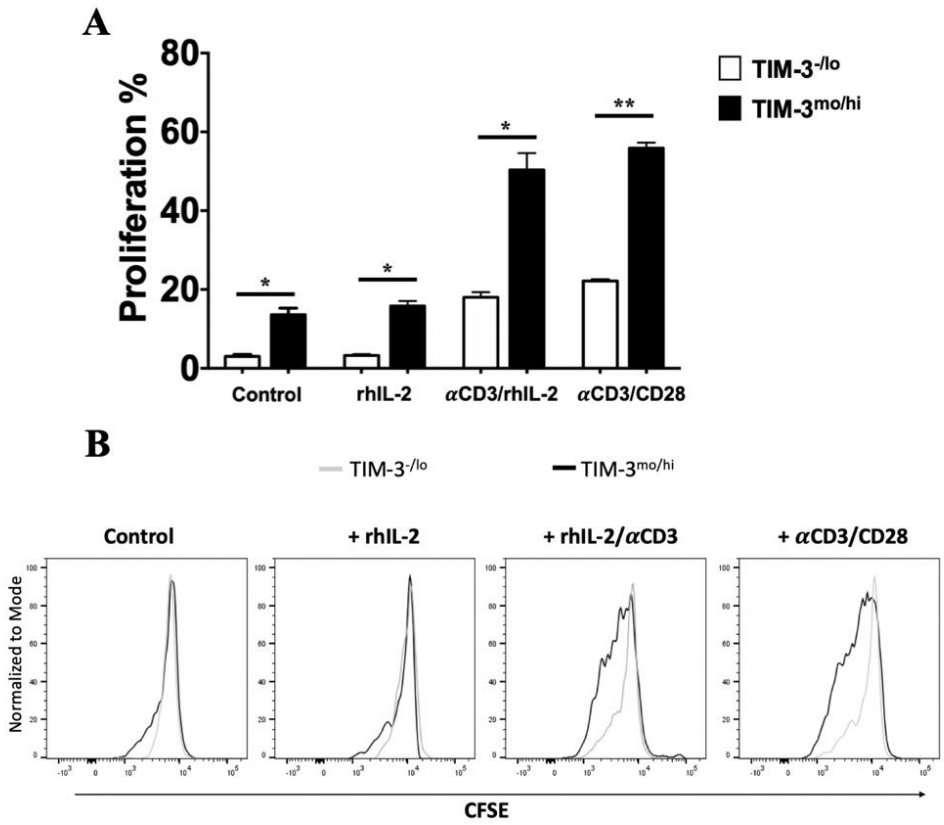

Figure 4.23. Re-stimulation capacity of $CD8^+$ T cells recovered from the co-cultures. According to the TIM-3 expression level, $CD8^+$ T cells were back-sorted from the co-cultures established with PMNs, monocytes, and A549 cells in the presence of 25ng/mL $\boldsymbol{\alpha}$CD3 mAb for 96h. (PMN:Monocyte:A549:$CD8^+$ T cell 1:0.125:0.25:1). TIM-$3^{-/lo}$ and TIM-$3^{mo/hi}$ sub-populations were back-sorted and labelled with CFSE and re-stimulated with various factors. A) Bar graphs and (B) overlay flow cytometric histograms show the proliferation of TIM-$3^{-/lo}$ and TIM-$3^{mo/hi}$ subpopulations stimulated with different combinations of rhIL-2 (5 ng/mL), plate-bound $\boldsymbol{\alpha}$CD3 and soluble CD28 (2 $\boldsymbol{\mu}$g/mL) (*P<0.05, **P<0.001, n=3)

Next, cytokine production by TIM-$3^{mo/hi}$ and TIM-$3^{-/lo}$ subpopulations was evaluated. Upon stimulation with PMA and ionomycin for 16 hours, in order to induce exocytosis of intracellular cytokine contents of $CD8^+$ T cells, supernatants were harvested and IL-2, IL-4, IL-10, IL-6 TNF-α, IFN-γ, and granzyme B levels were evaluated. Granzyme A, perforin, sFas, sFasL, and granulysin levels, which were also assessed, were below detection limit. Other cytokines were produced at high amounts in TIM-$3^{mo/hi}$ subpopulation. Especially IL-4 and IFN-γ production was significantly

higher in the TIM-3$^{mo/hi}$ subpopulation (Figure 4.24). Overall, these finding indicated that increased TIM-3 expression on CD8$^+$ T cells co-cultured with PMNs, monocytes and lung cancer cells was not related to exhaustion. These CD8$^+$ T cells were functional and due to their pre-activated state, vigorously responded to re-stimulation.

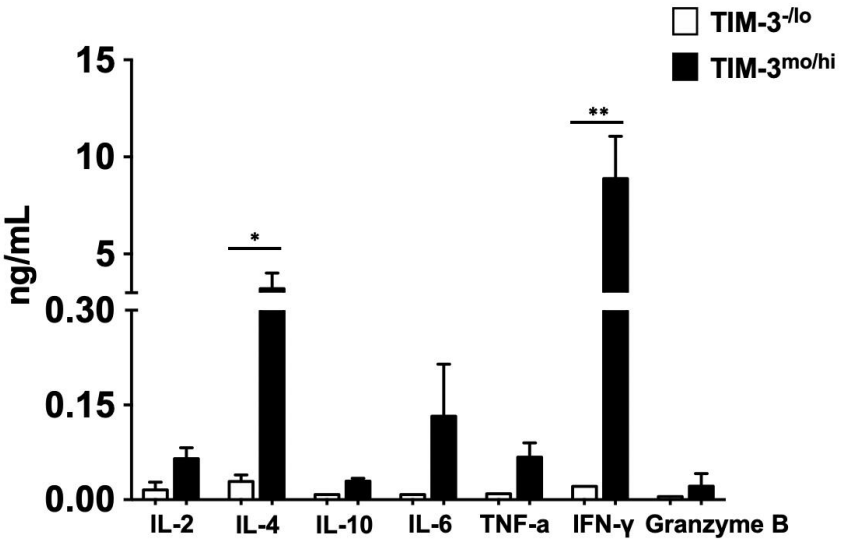

Figure 4.24. Cytokine levels secreted by TIM-3$^{-/lo}$ and TIM-3$^{mo/hi}$ CD8$^+$ T cells induced by PMA (5ng/mL) and ionomycin (2 μg/mL) for 16h were assessed by Multiplex bead-based flow cytometric array **(*P<0.05, **P<0.001, n=3).**

4.3. Potential influence of PMN in the co-cultures

4.3.1. ROS production and CD8$^+$ T cell responses

ROS production is one of the major mechanisms through which myeloid cells that regulate T cell responses (242). In order to observe the influence of ROS production on CD8$^+$ T cell proliferation and activation in the co-cultures, NAC was included as a ROS scavenger molecule. Following 24h of co-culturing, PMNs were gated and the ROS levels were measured by H_2-DCFDA reduction assay on flow cytometry.

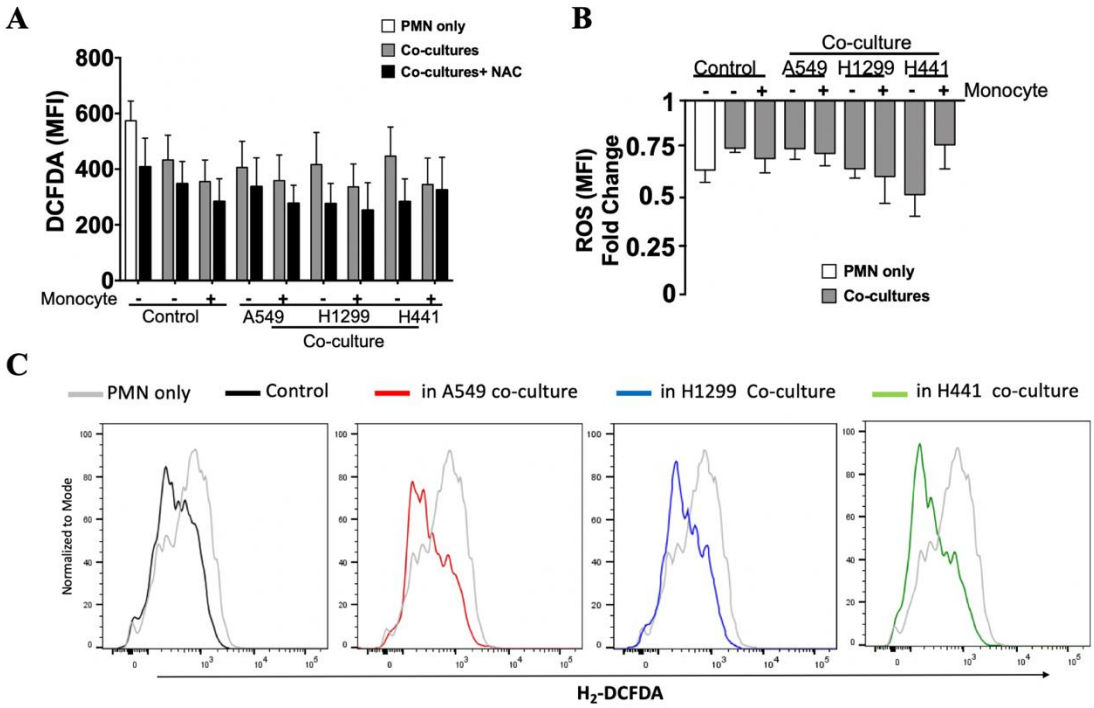

Figure 4.25. ROS levels of PMNs co-cultured with monocytes, $CD8^+$ T cells and lung cancer cells under 25ng/mL αCD3 stimulation. By the end of 24h, the PMNs were labelled with anti-CD15 and gated. A) Median fluorescence intensities (MFI) of H2-DCFDA on PMNs, and B) fold change decrement of ROS with NAC is given. C) Overlay histograms show the difference in ROS levels of PMNs only and PMNs in the co-cultures (*P<0.05, **P<0.001, n≥3).

As expected, NAC reduced the ROS levels both in the control PMNs and in the PMNs co-cultured with T cells, lung cancer cells and/or monocytes (Figure 4.25). Nevertheless, reduction of ROS activity by NAC did not lead to a significant change in $CD8^+$ T cell proliferation at 72h in the presence of PMNs (Figure 4.26 A and B).

Moreover, the exhaustion/activation of T cells which were followed by TIM-3 and LAG3 expression were comparable in the co-cultures established with or without NAC (Figure 4.26 C).

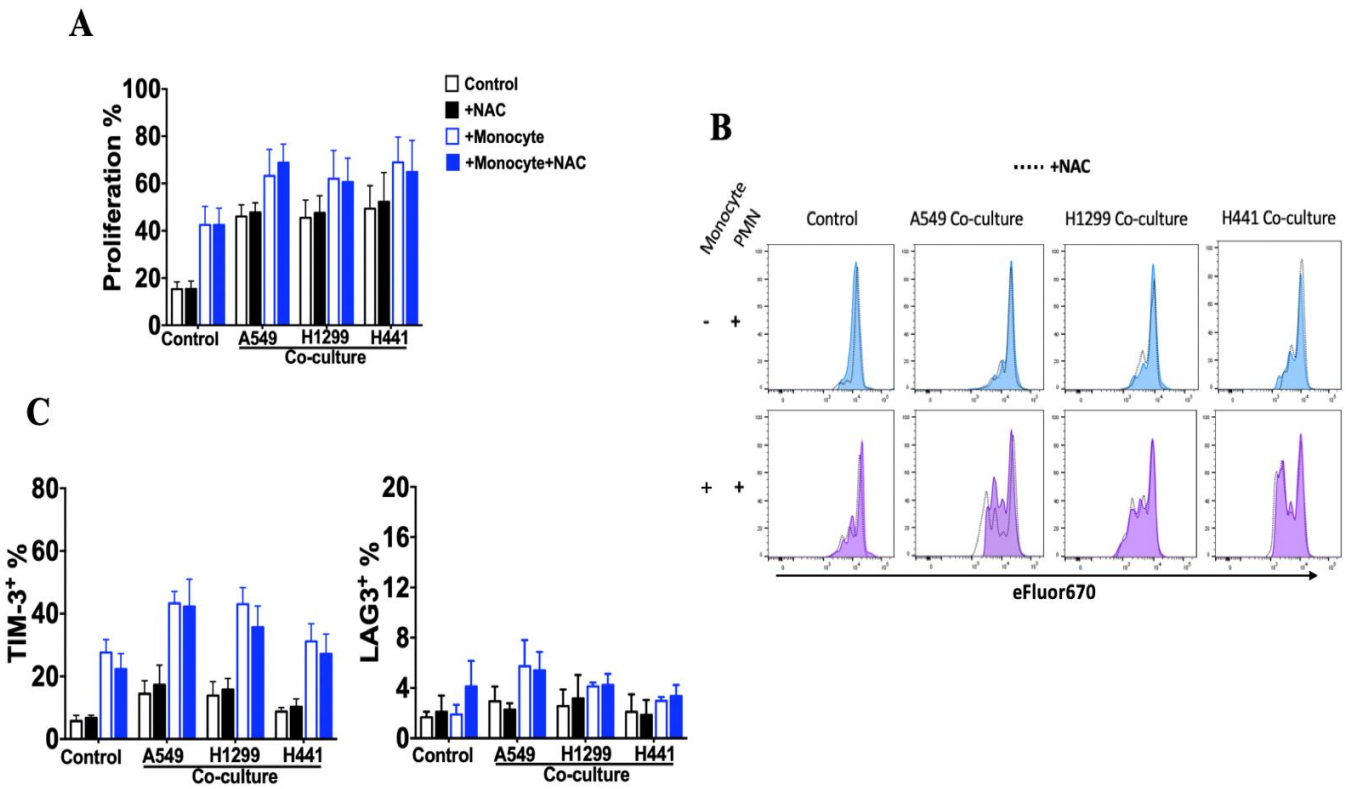

Figure 4.26. Effect of NAC on $CD8^+$ T cell proliferation and TIM-3/LAG3 expression in PMN containing co-cultures. A) Proliferation percentages $CD8^+$ T cells co-cultured with PMNs, monocytes and lung cancer cells in the presence of 25ng/mL αCD3 with or without NAC (1uM). B) Representative eFluor670 assay proliferation histograms of $CD8^+$ T cells. Co-cultures stimulated with NAC represents as empty histograms. C) Expression of TIM-3 and LAG3 on $CD8^+$ T cells in the co-cultures with or without NAC (*$P<0.05$, **$P<0.001$, $n\geq3$).

4.3.2. The costimulatory gene expression in PMNs

Costimulatory molecule expression in co-cultured PMNs was tested at mRNA level. PMNs were purified from the co-cultures established with monocytes, lung cancer cells and $CD8^+$ T cells under the stimulation of αCD3 mAb. Then, they were analyzed for co-stimulatory molecule expression by RT-PCR.

The data obtained from the experiments were normalized to that of obtained from the freshly isolated PMNs. Resting (24h cultured) PMNs had minimal expression of 4-1BBL, B7-2, 0X40L, LIGHT, B7-H2, and B7-1. On the other hand, 4-1BBL, B7-2 and 0X40L expression in PMNs purified from the co-cultures was elevated. Particularly, in NCI-H441 containing co-cultures, 4-1BBL, B7-2 and 0X40L expression in PMNs was significantly augmented, especially in the presence of monocytes and $CD8^+$ T cells, compared to the PMNs purified from the co-cultures of $CD8^+$ T cells and monocytes. No significant upregulation of LIGHT, B7-2, and B7-1 mRNA in PMNs purified from the co-cultures of lung cancer cells compared to that of purified from the $CD8^+$ T cells and monocyte co-cultures was detected (Figure 4.27).

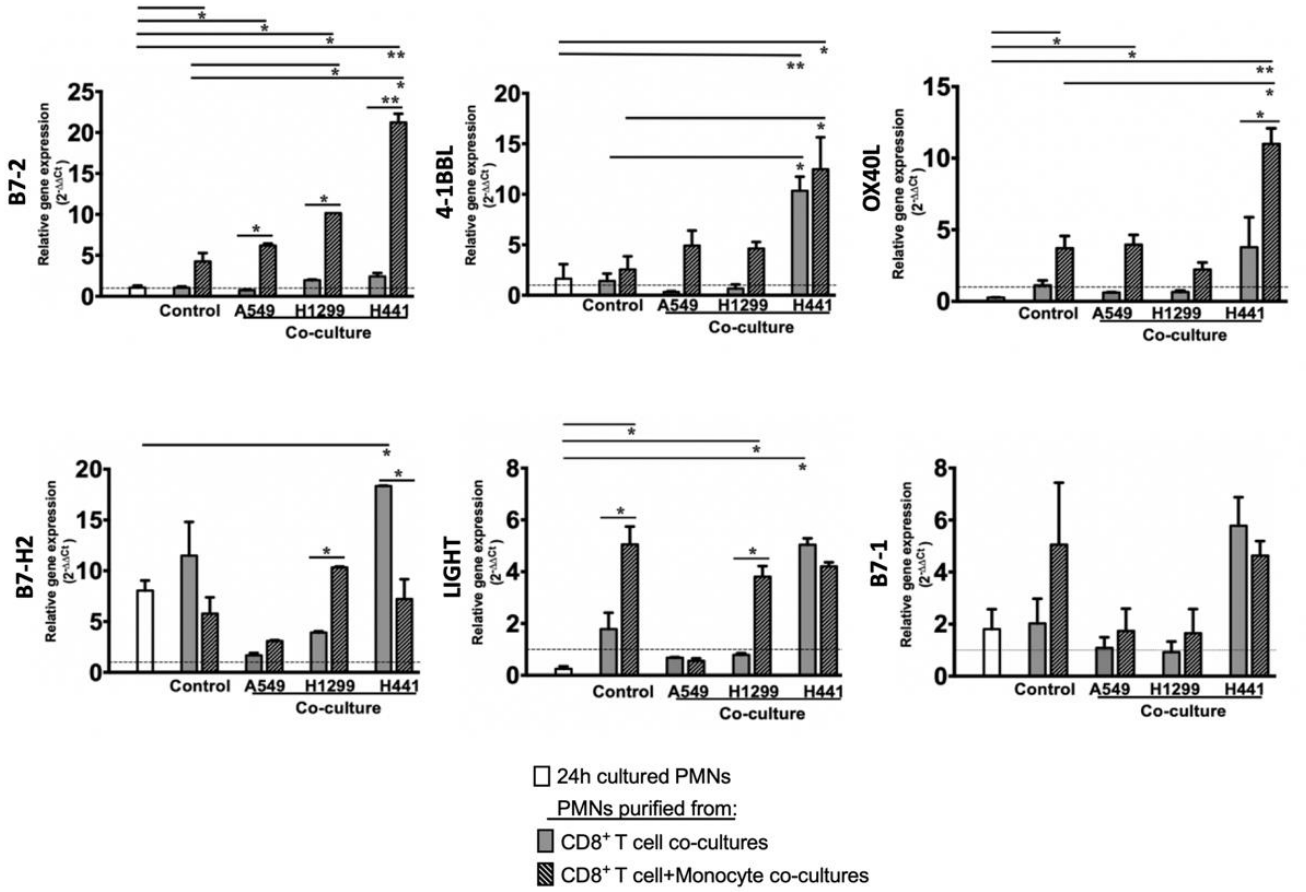

Figure 4.27. Expression of the co-stimulatory molecules in PMNs purified from co-cultures with monocytes, $CD8^+$ T cells and lung cancer cells under 25 ng/mL αCD3 stimulation was studied with RT-PCR. Dashed line (2-ΔΔCt value = 1) represents equal amount of gene expression between freshly isolated PMNs and 24h cultured PMNs (*P<0.05, **P<0.001, n=3).

5. DISCUSSION

The outcome of the immune responses in cancer rely on the interplay between the tumor cells and their local environment (160). In NSCLC, both tumor-promoting and tumor-suppressive immune cells have been found in the tumor microenvironment wherein myeloid cells and T lymphocytes prevail (243). Since the complexity of the interaction between immune cells and tumor cells have been increasingly reported, the reason of the limited potential of targeting a single molecule or pathway in the treatment of cancer became more apparent (244-246). Understanding the complexity and diversity of the immune composition in the tumor microenvironment and their influence on anti-tumor immune responses is critical for improving the outcomes of immunotherapy (247, 248). Neutrophils are acknowledged emerging as central players in inflammatory responses. In chronic cancer-related inflammation, they seem to promote tumor growth through key processes taking place during tumor initiation and progression. In therapeutic settings and if appropriately activated, neutrophils may also serve as potent anti-tumor effector cells (249, 250). Thus, investigating the interaction between neutrophils and other components found in the tumor microenvironment will contribute to understanding of the mechanisms of tumor progression and would have implications for the development of cancer therapies. Hence, this study aimed to evaluate T cell responses in the co-cultures, which was established to partially model the tumor microenvironment, employing PMNs, monocytes, T cells, and NSCLC cells.

Preliminary analyses were performed on PMNs for the establishment of co-culture conditions. An important limitation in studies on PMNs is represented by their short lifespan and spontaneous activation, ex vivo, even to minute stimuli; thus, preventing the routine performance of functional studies (251, 252). In this scope, G-CSF was used to enhance the survival of PMNs (253). To give adaptive and innate immunity-related stimuli, respectively, PMNs were treated with IFN-γ as a factor devoted to adaptive immune responses and fMLP which directly stimulates innate immunity via pattern recognition receptors (237, 238). Activated PMNs' viability depend on the strength and duration of the stimuli. Both ROS production, which is a major microbicidal mechanism, and netosis interfere with the survival of the PMNs upon receipt of the activating factors (254). Therefore, together with G-CSF, reactive

species were sequestered by the addition of NAC. Not only autocrine but also paracrine fashion (cell-to-cell proximity) is critical in ROS-related influence of PMNs (242). ROS could be responsible of reducing surface molecules and even penetrating into the target cells and in interfering with their function; for instance T cell responses and proliferation (255, 256). Accordingly, inhibition of ROS and promotion of PMN viability positively supported the co-stimulation on T cell proliferation. Intriguingly, the PMNs that were cultured for 24h were stimulated as fMLP- or IFN-γ-treated counterparts in terms of ROS production. Thus, control PMNs displayed similar influence that of observed with fMLP- or IFN-γ-treated counterparts on T cells found amongst PBMC co-cultures. The importance of using PMNs as soon as possible before they spontaneously become activated and lose viability was the first parameter set. Activated PMNs can exert suppressive actions on T cells (102, 257). Especially, Kleijn et al demonstrated that IFN-γ-stimulated neutrophils suppress T cell proliferation through the expression of PD-L1 (258). Nevertheless, our initial experiment showed no negative impact of either freshly isolated or 24h cultured (with or without fMLP or IFN-γ stimulation) PMNs on PBMC proliferation sustained by αCD3-modulated first signal. In contrast, PMNs supplied co-stimulatory signals for the T cells.

A549, NCI-H1299, and NCI-H441 cell lines used in this study as served representative of NSCLC cells. NCI-H1299 was established from a lymph node metastasis of the lung. A549 cells were maintained from lung carcinomatous tissue (259, 260). NCI-H441 cells were isolated from the pericardial fluid of a patient with papillary lung adenocarcinoma (261). All of the them exhibit epithelial phenotype. Doubling times in the appropriate complete medium for A549, NCI-H1299, and NCI-H441 are 22, 28, 58 hours, respectively and the number of cells seeded in the plates to reach to a pre-confluent state during co-culture period was determined accordingly (262, 263). Even though, three NSCLC cell lines differ in many aspects, compatible results were obtained from the co-cultures thereof. In the presence of lung cancer cells or their conditioned media, PMNs developed a significant survival advantage compared with control PMNs. It has been acknowledged that tumor microenvironment prolongs the survival of PMNs. Since the tumor conditioned medium has been reported to be rich in proinflammatory cytokines, including IL-6, IL-8, GM-CSF, and G-CSF, enhancement of the survival of PMNs is likely due to the presence of proinflammatory

factors to prolong the lifespan of PMNs by delaying the apoptosis (264). Moreover, a high level of ROS production was reported in the tumor infiltrating neutrophils in the literature (265, 266). Conversely, we found that ROS production of PMNs was diminished in the presence of lung cancer cells. Eruslanov et al. showed that TANs derived from lung tumors have an activated phenotype in tumor microenvironment (107). Similarly, in this study, PMNs spontaneously become activated and the presence of lung cancer cells delayed but could not totally abrogate the activation. Therefore, tumor-derived factors could maintain viability but hamper activation of peripheral blood PMNs that become into contact with lung cancer cells. Simply, the tumor could induce a more undifferentiated state in the PMNs which may resemble to PMN-MDSCs (115).

After initial experiments wherein PBMCs were employed, next experimental setups were conducted with $CD4^+$ or $CD8^+$ T cells to more clearly investigate the direct interaction between T cells, PMNs, and monocytes in the scope of NSCLC. Carefully designed functional assays are required to elicit the interactions between immune cells. Accordingly, determination of the number of the cells used in the co-culture assays should depend on the immune cell composition in the tumor microenvironment. Since the most prevalent immune cells in the tumor microenvironment is T cells, T cells should constitute the highest percentage of the cells in the co-cultures (161). T cells need two signals to become full activated. In the co-cultures, as a first signal, CD3/TCR triggering was mediated by soluble αCD3. High amount of soluble αCD3 mAb (8-40 fold compared to our study) or plate bound αCD3 mAb were preferred in the literature. Since the αCD3/CD28–stimulated T cell response involves a robust polyclonal T cell proliferation, in this study we preferred to use a relatively low amount of first signal to better emulate events occurring within the tumor microenvironment and reveal the impact of co-stimulation provided by the myeloid cells used on T cell responses. Thus, the second signals were provided by the costimulatory molecules on the myeloid cells (267). When primary monocytes were allowed to adhere to culture plate in vitro, they undergo spontaneous maturation and differentiate into macrophages(268). Therefore, the main co-stimulatory signals were planned to be given by monocytes in the co-cultures. The third signal is provided by the cytokines produced from myeloid and T cells (269). In this respect, at 0.5:0.5:1

monocyte:PMN:T cell ratio, $CD4^+$ and $CD8^+$ proliferation was assessed in the presence of lung cancer cells or their conditioned media. We found that in the presence of lung cancer cells, PMNs reinforced the $CD8^+$ T cell proliferation, but not $CD4^+$ T cell proliferation. This is likely due to that $CD8^+$ T cell responses have faster kinetics in almost every aspect of the response and $CD8^+$ T cells are more eager to than $CD4^+$ T cells. For instance, engagement of co-stimulatory receptors on memory T cells has been shown in some cases to stimulate memory $CD8^+$ T cells in the absence of TCR stimulation (270). Moreover, Chacon et al. demonstrated that co-stimulation of $CD8^+$ memory T cells with a 4-1BB agonist antibody induces proliferation and cytokine production in the absence of TCR stimulation (271). Therefore, in the context of our experimental co-culture models, $CD8^+$ T cells could be better responders, which promotes the co-stimulatory signals, especially derived from PMNs.

We further investigated the optimal ratio for PMNs and monocytes, especially to promote and reveal the importance of PMNs on $CD8^+$ T cell proliferation. PMN and monocytes were titrated into the co-cultures. At 0.125:1:1 monocyte:PMN:T cell ratio, in the presence of lung cancer cells, that reached to the confluence, the additive effect of PMN and monocytes on T cell proliferation was impressive. The low amount of monocytes was preferred in order to reveal the contribution of PMNs on T cell proliferation. Thus, this ratio was determined to be used throughout this study.

High neutrophil infiltration has been reported to presage for poorer survival in NSCLC (272, 273). Therefore, we anticipated that neutrophils exert pro-tumor N2 phenotype in the tumor microenvironment of NSCLC and they inhibit T cell responses. Intriguingly, in the presence of lung cancer cells, PMNs did not hinder rather promoted the proliferation of $CD8^+$ T cells. Same effect was not observed with the tumor conditioned media. Inhibition of ROS production and enhanced survival in the presence of lung cancer-derived soluble factors indicated that this interaction primarily requires direct cell-to-cell contact. Shaul et al. reported the presence of higher expression levels of MHC class-I antigen presentation-related genes in N1 neutrophils derived from NSCLC tumors (266). Similar to our results, this supported the notion of a cooperation between innate and adaptive arm of the immunity.

Esendagli et al reported that malignant lung tissue sections with high neutrophil counts are infiltrated by relatively low numbers of T cells, implying that

neutrophils and T cells do not prefer to co-localize in the lung tumor microenvironment (192). Here when we forced the co-localization of, PMNs and $CD8^+$ T cells ex-vivo in the presence of lung cancer cells, monocytes, and certain T cell responses were enhanced. It can be speculated that tumor cells may employ certain mechanisms to avoid bringing PMNs and T cells together in the tumor microenvironment. In the absence of monocytes, PMNs also exerted stimulatory effect on $CD8^+$ T cell proliferation, indicating that PMNs can upregulate costimulatory molecules on their surface. Direct contact with lung cancer cells may improve the costimulatory molecules on monocytes and PMNs and facilitate enhanced T cell proliferation. In the absence of PMNs and monocytes, lung cancer cells alone did not stimulate the proliferation of $CD8^+$ T cells. It can be explained by the lack of costimulatory molecules on the lung cancer cells. In other words, lung cancer cells were not capable to provide second signals for $CD8^+$ T cell proliferation in the absence of PMNs or monocytes. Taken together, these results demonstrate that co-stimulation molecules on PMNs and monocytes were enhanced in the presence of lung cancer in a contact-dependent manner. Many studies indicated that the interaction with macrophages can enhance the matrix-degrading activity and invasiveness of cancer cells (274, 275). On the other, number of studies also demonstrated that macrophage subtypes (M1/M2) with reverse functions can arise from the interaction between cancer cells and macrophages (170, 186). Spicer et al. reported that neutrophils can promote liver metastasis of lung carcinoma cells through CD11b/CD18-mediated interaction with tumor cells (276). In consistence with our study, Eruslanov et al. reported that co-stimulatory molecules were enhanced in the TANs recovered from lung tumors (107).

$CD8^+$ T cells in the co-cultures of PMNs and monocytes were in an activated state with increased CD137 (4-1BBL), CD69, CD25 (IL-2R), and CD107a (LAMP-1) expression. Activation of $CD8^+$ T cells and degranulation of their cytotoxic granules were not altered in the presence of lung cancer cells. As these results indicated no direct immune suppression by NSCLC cells, next we hypothesized if the maintenance of T cell responses may lead to a hyporesponsive state (exhaustion) in $CD8^+$ T cells. The percentage of $CD8^+$ T cells expressing coinhibitory molecules was higher in the co-cultures containing lung cancer cells. Specifically, TIM-3 expression was significantly higher in the presence of lung cancer cells. As the number of PMNs and

monocytes increase in the co-cultures, the percentage of TIM-3 expressing $CD8^+$ T cells increases. Neutrophil to T cell ratio has been used as a prognostic marker for various types of cancers (273, 277). In NSCLC, high neutrophil-to-T cell ratio is frequently associated with poor clinical outcomes (272). Since the percentage of TIM-3 expressing $CD8^+$ T cells were augmented, as the number of PMNs was increased in the co-cultures. One may simply conclude that the presence of PMN might have rendered the T cells to become prone to inhibitory signals, especially through TIM-3. The increased expression of inhibitory receptors augmented may lead to T cell dysfunction, thereby suppressing the anti-tumor immune responses.

Since the expression of inhibitory receptors is often regarded as a hallmark of "exhaustion" (278), $CD8^+$ T cells in the lung cancer cells' co-cultures were functionally evaluated. The most drastic increase was observed in A549-co-cultures and the most consistent and significant inhibitory receptor upregulated was TIM-3, therefore analyses were performed according to TIM-3 expression on $CD8^+$ T cells in the co-cultures established with A549 cells, monocytes, and PMNs. Functionally exhausted T cells are characterized with less proliferative capability, diminished cytokine production, and loss of cytotoxic activity. They express inhibitory receptors, including PD-1, CTLA-4, TIM-3, and LAG3 (279, 280). Strikingly, in this study, TIM-3 expression was not related to exhaustion, but rather activation. As TIM-$3^{mod/high}$ $CD8^+$ T cells displayed higher proliferative capacity and IFN-γ secretion than TIM-$3^{-/low}$ counterparts. The proliferation of TIM-$3^{mod/high}$ subpopulation was maximal under αCD3/CD28 or αCD3/rhIL-2 which also slightly enhanced the proliferation of TIM-$3^{-/low}$ subpopulation. Expression of CD25 (IL-2R) was very limited on co-cultured $CD8^+$ T cells, implying that in the co-cultures IL-2 signaling was not effective; therefore, recombinant IL-2 supplementation could slightly promote the proliferation of TIM-$3^{mod/high}$ and TIM-$3^{-/low}$ subpopulations. In consistence with our study, Amandine et al reported that expression of TIM-3 molecules does not only mark dysfunctional cells, but also it is tightly associated with activation and differentiation (281). In addition, in a number of studies, high TIM-3 expression was reported to be strongly linked to effector memory phenotype (282). Furthermore, it has been acknowledged to be a marker that indicates Th1 cell differentiation (280, 283). In accordance with our study, Fuertes at al showed that TIM-3 expressing $CD8^+$ T cells

in breast cancer model express CD137 and produce IFN-γ (284). Thus, TIM-3 expression primarily participates in T cell activation and differentiation. Conversely, Zhou et al showed that PD-1 and TIM-3 co-expression on $CD8^+$ T cells are indicative of T cell dysfunction and immune suppression, less IFN-γ, perforin and granzyme production. In our study, PD-1 expression was very low in the co-cultures. With the low number of monocytes as a critical supplier of costimulatory molecules, stimulation may not be sufficient in the co-cultures for upregulation of PD-1 on $CD8^+$ T cells. Since the activation and differentiation are strong primary drivers of inhibitory molecule expression, TIM-3 positivity can be indicative of $CD8^+$ T cells' potential to become dysfunctional and undergo exhaustion. Even though they produce high amount of IFN-γ, $TIM3^{mod/high}$ $CD8^+$ T cells derived from co-cultures produce scarce amount of granzyme A and B. Perforin and sFas/FasL were also undetectable levels. In support of this, expression of the functional markers granzyme B and perforin were shown to be lower in $CD8^+$ T cells in tumor tissues of NSCLC (107).

As an escape mechanism from immune surveillance, the ligands for T cell inhibitory receptors are expressed in many solid tumors including lung tumors. The expression of inhibitory ligands can be a direct consequence of malignant transformation which redesigns gene expression gene expression patterns or can be related to exposure to bio reactive mediators, especially secreted upon inflammatory reactions (285). Immune responses against tumor cells leads to the production of many cytokines such as IFN-γ and TNF-α (286). Nevertheless, interaction with immunity can lead to the acquisition of a suppressive character which may facilitate the immune evasion by tumor cells. The concept of adaptive resistance has been used to describe a process in which T cells attempt to attack the tumor cells, but then tumor cells reacts and acquires immune regulatory properties to adapt and protect itself from this immune attack (287). For instance, Pardoll et al. described how the production of IFN-γ by T cells upon recognition of tumor antigens induces PD-L1 expression on tumor cells, thereby inhibiting PD-1^+ T cell responses (288). As an inhibitory receptor, PD-1 is upregulated on activated/effector T cells. A higher frequency of PD-L1 expressing lung tumor cells and PD-1 expressing TILs were detected in NSCLC and correlated with poor survival (289) . In our study, $CD8^+$ T cells in the co-cultures with lung cancer cells barely expressed PD-1. Nevertheless, we did not analyze PD-L1 expression on

the cell lines. While Anti-PD-1 therapy has been shown to significantly prolong the survival in patients with metastatic melanoma, only a small proportion of NSCLC patients responded to anti-PD-1/PD-L1 therapy (290). It may likely due to the lack of PD-1 expression on T cells in the tumor microenvironment.

Galectin-9 (Gal-9) expression in tumor cells has been frequently reported. A549 and NCI-H1299 cell lines were also reported to express Gal-9. Gal-9 is highly expressed in the cytoplasm of lung cancer cell lines and is released following tumor cell death (291, 292). Release of Gal-9 could negatively regulate the T cell functions or induce apoptosis (293). Although, the expression of Gal-9 on the lung cancer cells was not checked in this study, TIM-3 expressing $CD8^+$ T cells are elevated in the presence lung cancer cells containing co-cultures. When Gal-9 is available in the tumor microenvironment, TIM-3 and Gal-9 interact and this interaction frequently results in immune suppression (285). Therefore, TIM-3 expression makes $CD8^+$ T cells susceptible for inhibition. Eruslanov et al. reported that TANs derived from NSCLC tumor support T cell responses in the early stage of the tumor, as the tumor grows, T cell responses become impaired (107). In support of this, PMNs reinforced the $CD8^+$ T cell responses in our study; however, potentially due to promotion of T cell activation, PMNs also contributed to expression of the inhibitor receptors such as TIM-3 expression on $CD8^+$ T cell. With strong and consistent stimulation of $CD8^+$ T cell in the presence of PMNs and monocytes, T cells may eventually become more prone to inhibitory signals. Collectively, one may speculate that the co-culture system established, which employs freshly obtained immune cells that encounters with lung cancer cells can represent initial states of immune system-tumor cell interactions. Other ligands for TIM-3 are phosphatidylserine (PS), high mobility group protein B1 (HMGB1), and carcinoembryonic antigen cell adhesion molecule 1 (Ceacam-1) (294). Future studies may decipher the expression of these ligands on monocytes, neutrophils, and NSCLC cell lines in our co-culture settings.

Expression of LAG3 and CTLA-4 on $CD8^+$ T cells were also upregulated in the presence of NSCLC cells; albeit not reaching to the level of TIM-3. LAG3 interacts with its ligands such as MHC-II and Fibrinogen-like protein 1 (FGL1) inhibit T cell activation (295). The co-expression of LAG3 with other inhibitory receptors including TIM-3 and PD-1 often results in T cell exhaustion (296). Besides PD-1, anti-CTLA-4

therapy was recognized as a widely used immunotherapy checkpoint inhibitor in NSCLC (297). CTLA-4 binds to CD80 and CD86 with higher affinity than CD28 and inhibit T cell activation. Attempts to combine PD-1/PD-L1 inhibitors with CTLA-4 inhibitors showed encouraging tumor responses despite increased toxicity (298). In NSCLC, LAG3 expression has been found on TILs in the tumor tissues, its expression was correlated with PD-1/PD-L1 expression, and it is related to poor survival (296). Expression of inhibitory ligands cognate for CTLA-4 and LAG3 such as CD80, CD86, HLA-DR, and FGL1 may also be investigated on myeloid cells and NSCLC cell lines in the co-cultures.

In addition to the activation-related molecules on $CD8^+$ T cells, the cytokine secretion, especially molecules associated with anti-tumor immunity, critical to understand ongoing reactions (269). Therefore, a cytokine array was performed to evaluate $CD8^+$ T cell responses and subsets in the co-cultures. In the co-cultures, since the secreted factors were directly tested from 72h supernatants, the mediators detected may be derived from cancer cells, PMNs, T cells and, to a lower extend, monocytes which constitute the least number. On the other hand, the factors IFN-γ, granzymes, IL-2, and IL-17A could be strongly assumed to be derived from T cells. On the other hand, IL-10, IL-4, TNF-α, and IL-6 may be produced by lung cancer cells, PMNs or monocytes. Nevertheless, the amount of these molecules is descriptive for the immune-mediated responses in the co-cultures established. In the literature, a strong association between tumor cell proliferation and IL-6 production has been found in NSCLC. Elevated IL-6 in the tumor microenvironment is related to poor survival (299). Along with IL-21, IL-6 has been reported to have a role in the differentiation of Tc17 cells. Tc17 cells exert impaired cytotoxic function with reduced IFN-γ, granzyme B, and perforin production (300). In accordance with this, in our study, high IL-6 levels were found in the A549 containing co-cultures wherein very less amount of IFN-γ , granzyme B, and perforin was detected. In parallel with this, IL-4 producing $CD8^+$ T cells, known as Tc2, has been recognized with their low perforin and granzyme B expression (301). In the NCI-H1299 or NCI-H441 containing co-cultures, high amount of IL-4 and IFN-γ indicated that both Tc2 and Tc1 cells could be induced in the co-cultures. Normally, IFN-γ producing $CD8^+$ T cells exhibit high cytotoxic activity (302), production of perforin, granzyme A and B was tremendously low in

these co-cultures, indicating that inhibitory factors derived from Tc2 cells may be superior. Activation of peripheral $CD8^+$ T cells induce localization of CD107a on the cell surface. It is associated with the release of perforin and granzyme B which mediate cytolytic activity of $CD8^+$ T cells (303). Since the presence of lung cancer cells did not enhance the degranulation of $CD8^+$ T cells and in the co-cultures, low level of granzyme B and perforin were found, poor cytolytic activity of $CD8^+$ T cells may be anticipated. Collectively, in the co-cultures consisting of monocytes, $CD8^+$ T cell activation was maintained and resulted in upregulation of inhibitory receptors. The cells possessed capacity to proliferate and secrete function-associated cytokines such as IFN-γ, but could not go through the effector phase to exert efficient cytotoxicity.

Even though IFN-γ production by $CD8^+$ T cells act paracrine fashion, systemic, whereas cytotoxins such as perforin require direct contact with the target cells (304). IFN-γ may enhance the ability of CTL to kill via Fas/FasL in the absence of perforin (305). However, soluble Fas (sFas) was also not detected in the co-cultures. Since Fas/FasL mediated cell killing is required direct cell to cell contact, expression of membrane bound FasL should have been investigated. Investigating FasL expression on $CD8^+$ T cells and other cytotoxic mediators would have planned in the future.

In NSCLC, high number of immunosuppressive PMN-MDSCs have been found in the tumor microenvironment (115). In our co-culture setup, we used peripheral blood neutrophils from healthy volunteers, PMN-MDSCs derived from lung cancer patients may exert a distinct effect on $CD8^+$ T cell responses. The inhibition of T cell responses by human immunosuppressive neutrophils primarily occurs through overproduction of ROS (256). Eruslanov et al demonstrated that TANs derived from lung tumor exhibit high ROS production capability, *in vitro* (107). Conversely, in our study, ROS production was diminished in PMNs co-cultured with lung cancer cells. Even though, NAC treatment reduced the ROS further, it did not influence T cell stimulatory capacity of PMNs.

Direct cell to cell contacts with lung cancer cells was required for PMN-mediated T cell proliferation. Upon co-culturing with the lung cancer cells, PMNs upregulated costimulatory gene expression B7-2, OX40L, and 4-1BBL. These data are consistent with the previous studies showing the neutrophil mediated T cell

stimulation. For instance, Eruslanov et al. reported the consistent results and showed the expression of 4-1BBL, OX40L, B7-2, and ICAM-1 in TANs derived from early stage lung tumor; thus, revealing the costimulatory effects of neutrophils on $CD8^+$ T cells (107). Governa et al. also demonstrated the co-stimulatory effect of neutrophils on $CD8^+$ T cells in human colorectal cancer (306).

Costimulatory molecules of two major families; B7/CD28 and Tumor necrosis factor (TNF)/tumor necrosis factor receptor (TNFR are involved in the triggering of adaptive immune responses (241). The B7-1/B7-2:CD28/CTLA-4 pathway is the best characterized pathway of T-cell co-stimulation and co-inhibition and symbolizes the classical way where the ligand can bind two receptors for regulating both T-cell activation and tolerance (307). Through CD28 pathway, the strongest costimulatory signals are delivered by APCs to provide a full activation of T cells, promoting their proliferation and IL-2 secretion (308). The TNF/TNFR family members such as 4-1BBL/4-1BB, OX4OL/ OX40, and LIGHT/HVEM are involved in the later phases of T-cell activation and are induced from hours to days following the TCR engagement. TNFR molecules provide costimulatory signals to both $CD4^+$ and $CD8^+$ T cells, with a greater effect on the expansion of $CD8^+$ T cells (309). 4-1BBL/4-1BB pathway possess capacity to amplify the existing costimulatory signals (310). In the co-cultures, especially wherein the lung cancer cell lines were present, the contribution of PMNs to $CD8^+$ T cell responses was noteworthy. Nevertheless, the number of PMNs was 8 fold higher than that of monocytes (at the initiation of the co-cultures), but the co-stimulatory support given by PMNs could not reach to the level of monocytes. There could be several reasons, including (1) Monocytes can better communicate with T cells through adhesion, cytokine, and costimulatory molecule expression as they are professional APCs. (2) Monocytes can differentiate into macrophages ex-vivo and become better partners for T cells. (3) Monocytes last longer in the co-cultures than PMNs. On the other hand, PMNs significantly contributed to $CD8^+$ T cell responses and had an additive effect together with monocytes. The increase in the costimulatory molecule expression in PMNs upon co-culturing may indicate the enhanced capacity of these cells to support $CD8^+$ T cell responses, even in the presence of cancer cells. Co-presence of monocytes had also a positive influence of PMN's co-stimulatory gene

expression. Therefore, the NSCLC cell lines used may have provided a suitable niche for immune cells to interact and exert pro-inflammatory actions.

Collectively, the notion of potential neutrophil-T cell interaction on tumor sites was supported by this thesis. The contact-dependent mechanisms required for this interaction may be promoted by several receptor/ligand expressions. Soluble factors have been also reported to enhance this interaction. For instance; Fridlender et al. reported that the mechanisms by which T cells might attract and/or activate neutrophils are not known for certain, but include the ability of tumor-stimulated activated T-cells to produce granulocyte-macrophage colony stimulating factor (GM-CSF) and macrophage inflammatory protein 2 (MIP2), or cytokines such as TNF–α and IFN-γ. These cytokines may recruit neutrophils by stimulating tumor macrophages or endothelial cells to produce chemokines and cell adhesion molecules (103). It was also demonstrated that TANs promote non-activated $CD8^{+}CD69^{-}$ T cell apoptosis in NO and contact dependent mechanism in mouse lung cancer model (311). Governa et al. demonstrated that neutrophils implement co-stimulation on $CD8^{+}$ T cells through CD11a/ICAM-1 interaction and neutrophil mediated co-stimulation results in the expansion of memory $CD8^{+}$ T cells (306). In our study, the expression of adhesion molecules on PMNs and the viability of non-activated $CD8^{+}$ T cell in the co-cultures may be also investigated. Other possible interaction between tumor cells and PMNs may be promoted through CD47/SIRPα molecules. Upregulation of CD47, which is known as a “do not eat me” signal in tumor cells was reported in many cancers to avoid phagocytosis. The signal-regulatory protein α (SIRPα) is expressed on myeloid cells including neutrophils (312). Barrera et al. reported that CD47 overexpression is associated with decreased apoptosis in neutrophils and phagocytosis and poor survival in NSCLC (313). CD47/SIRPα can be another pathway to be analyzed in our study. Recruitment of myeloid cells to the damaged tissues in which they can resolve infections and stimulate wound healing is mediated by integrins, a family of adhesion receptors that includes CD11b (314). LFA-1 is an essential initiator of the immunological synapse between cytotoxic T or NK cells and tumor cells. It mediates both firm adhesion to the target cell and the orientation of the cytotoxic granules towards the target (315). Therefore, effective cytotoxic activity is mediated by a firm cell to cell contact. Importantly, Reina et al. reported that neutrophil-cancer cell

interactions mediated by LFA-1 facilitates breast cancer dissemination in a model of metastasis (316). According to another study, in ovarian cancer patients, the adhesive properties of blood neutrophils are increased, due to increase in CD11b levels, implying that the neutrophil-cancer cell contacts may modulate malignant behavior of the cancer cells (249).

Neutrophils were reported to suppress tumor growth via Fas/FasL pathway in a study performed with A549 cells and neutrophils (317). Within this scope, future studies may decipher neutrophil subpopulations in NSCLC microenvironment and the effect of PMNs in tumor cell proliferation, angiogenesis and metastasis using in vivo models. To better emulate events occurring within the tumor microenvironment, we may use a three-dimensional (3D) tumor spheroid model (318). For the full activation of T cells, third signal comes from the cytokines produced by immune cells. Cytokines produced specifically from PMNs co-cultured with lung cancer cells, monocytes, and $CD8^+$ T cells may also reveal additional mechanism that contribute to inflammatory environment in NSCLC.

In summary, our findings indicate the importance of PMNs as a considerable modulator in the regulation of $CD8^+$ T cell responses in NSCLC. In the presence of lung cancer cells, monocytes, and PMNs, $CD8^+$ T cells could be activated and exert effector responses; however, this process led them to express relatively higher levels of inhibitory receptors, in particular TIM-3. Nevertheless, in our setting these inhibitory receptors did not deteriorate proliferation capacity and IFN-γ production; albeit making them susceptible to inhibition. Cell-to-cell contact is likely to be critical mechanism by which PMNs exert stimulatory effects on $CD8^+$ T cell proliferation; however, the role of soluble factors derived from lung cancer cells on PMNs cannot be underscored. Ultimately, these findings may have important implications in the understanding of immunobiology in lung cancer and immunotherapy approaches.

6. RESULTS AND RECOMMENDATION

- PMNs pre-treated with G-CSF and NAC exhibited prolonged survival and diminished ROS production. Consequently, they enhanced T cell proliferation.
- IFN-γ and fMLP pre-treatment of PMNs did not alter the proliferation of T cells.
- The presence of lung cancer cells delayed the death and reduced ROS production of PMNs.
- PMNs became spontaneously activated after 24h culturing. Being with lung cancer cells or conditioned media delayed but not inhibit the activation of PMNs.
- In the co-cultures of PMNs, monocytes, and lung cancer cells, T cell responses were enhanced. In the absence of myeloid cells, lung cancer cells did not promote T cell proliferation. PMN co-cultures positively influenced T cell responses, albeit not reaching to the level of monocyte stimulated T cells. $CD8^+$ T cell proliferation was more significantly promoted than $CD4^+$ T cells by the presence of PMNs. Co-cultures established with cancer cell- derived conditioned media did not promote T cell proliferation, indicating that cell-to-cell contact is required. Increased expression of CD137, CD69, CD25, and CD107a was observed on $CD8^+$ T cells co-cultured with monocytes and PMNs. Expression of these receptors was not altered in the presence of lung cancer cells.
- IL-6 was the most prominently increased cytokine in the co-cultures with A549 cells, PMNs, and monocytes. High level of IFN-γ was detected in the co-cultures with H1299 or H441 cells, PMNs, and monocytes. IL-4 was also prominently found in the co-cultures of H1299 or H441 cells.
- Upregulation of inhibitory receptors PD-1, CTLA4, LAG3, and especially TIM-3 were detected on $CD8^+$ T cells co-cultured with lung cancer cells, PMNs, and monocytes.
- In response to re-stimulation, TIM-$3^{mod/high}$ $CD8^+$ T cells recovered from co-cultures with A549 cells, monocytes, and PMNs has higher proliferative capability and higher IFN-γ production compared to $TIM^{-/low}$ subpopulation.

- ROS production was diminished in lung cancer cells-co-cultured PMNs. NAC treatment diminished it further, but did not alter T cell stimulatory capacity of PMNs.
- Moderate but statistically significant upregulation of CD86, OX40L, and 4-1BBL mRNA were detected in PMNs purified from the co-cultures of monocytes, $CD8^+$ T cells, and lung cancer cells.
- Since inhibitory receptor expression was upregulated in the presence of lung cancer cells, the expression of inhibitory ligands, especially that are cognate for TIM-3 may be evaluated in the co-cultures and lung cancer cell lines.
- To reveal the contact dependent mechanism through which PMNs interacted with lung cancer cells and $CD8^+$ T cells, the expression of adhesion molecules on PMNs upon co-culturing may be investigated.
- Cytokines specifically derived from PMNs in the co-cultures to can be determined.
- Since this study is performed with healthy donor PMNs, similar co-cultures might be established with patient-derived PMN-MDSCs and normal density PMNs.
- To better mimic the tumor microenvironment, 3D cell cultures may be performed with the same co-culture settings.

7. REFERENCES

1. Ostroumov D, Fekete-Drimusz N, Saborowski M, Kuhnel F, Woller N. CD4 and CD8 T lymphocyte interplay in controlling tumor growth. Cell Mol Life Sci. 2018;75(4):689-713.
2. Bubenik J. Tumour MHC class I downregulation and immunotherapy (Review). Oncol Rep. 2003;10(6):2005-8.
3. Sers C, Emmenegger U, Husmann K, Bucher K, Andres AC, Schafer R. Growth-inhibitory activity and downregulation of the class II tumor-suppressor gene H-rev107 in tumor cell lines and experimental tumors. J Cell Biol. 1997;136(4):935-44.
4. Zou W, Chen L. Inhibitory B7-family molecules in the tumour microenvironment. Nat Rev Immunol. 2008;8(6):467-77.
5. Kim TJ, Hong SA, Kim O, Kim SJ, Yang JH, Joung EK, et al. Changes in PD-L1 expression according to tumor infiltrating lymphocytes of acquired EGFR-TKI resistant EGFR-mutant non-small-cell lung cancer. Oncotarget. 2017;8(64):107630-9.
6. Mandarano M, Bellezza G, Belladonna ML, Van den Eynde BJ, Chiari R, Vannucci J, et al. Assessment of TILs, IDO-1, and PD-L1 in resected non-small cell lung cancer: an immunohistochemical study with clinicopathological and prognostic implications. Virchows Arch. 2019;474(2):159-68.
7. Barclay J, Creswell J, Leon J. Cancer immunotherapy and the PD-1/PD-L1 checkpoint pathway. Arch Esp Urol. 2018;71(4):393-9.
8. Chae YK, Arya A, Iams W, Cruz MR, Chandra S, Choi J, et al. Current landscape and future of dual anti-CTLA4 and PD-1/PD-L1 blockade immunotherapy in cancer; lessons learned from clinical trials with melanoma and non-small cell lung cancer (NSCLC). J Immunother Cancer. 2018;6(1):39.
9. Tvinnereim AR, Hamilton SE, Harty JT. Neutrophil involvement in cross-priming CD8+ T cell responses to bacterial antigens. J Immunol. 2004;173(3):1994-2002.
10. Vono M, Lin A, Norrby-Teglund A, Koup RA, Liang F, Lore K. Neutrophils acquire the capacity for antigen presentation to memory CD4(+) T cells in vitro and ex vivo. Blood. 2017;129(14):1991-2001.
11. Xu F, Xu P, Cui W, Gong W, Wei Y, Liu B, et al. Neutrophil-to-lymphocyte and platelet-to-lymphocyte ratios may aid in identifying patients with non-small cell lung cancer and predicting Tumor-Node-Metastasis stages. Oncol Lett. 2018;16(1):483-90.
12. Singel KL, Emmons TR, Khan ANH, Mayor PC, Shen S, Wong JT, et al. Mature neutrophils suppress T cell immunity in ovarian cancer microenvironment. JCI Insight. 2019;4(5).
13. Aeed PA, Nakajima M, Welch DR. The role of polymorphonuclear leukocytes (PMN) on the growth and metastatic potential of 13762NF mammary adenocarcinoma cells. Int J Cancer. 1988;42(5):748-59.

14. Borregaard N, Cowland JB. Granules of the human neutrophilic polymorphonuclear leukocyte. Blood. 1997;89(10):3503-21.

15. Kuijpers TW, Tool AT, van der Schoot CE, Ginsel LA, Onderwater JJ, Roos D, et al. Membrane surface antigen expression on neutrophils: a reappraisal of the use of surface markers for neutrophil activation. Blood. 1991;78(4):1105-11.

16. Scapini P, Marini O, Tecchio C, Cassatella MA. Human neutrophils in the saga of cellular heterogeneity: insights and open questions. Immunol Rev. 2016;273(1):48-60.

17. Boyce JA, Friend D, Matsumoto R, Austen KF, Owen WF. Differentiation in vitro of hybrid eosinophil/basophil granulocytes: autocrine function of an eosinophil developmental intermediate. J Exp Med. 1995;182(1):49-57.

18. Nadif R, Zerimech F, Bouzigon E, Matran R. The role of eosinophils and basophils in allergic diseases considering genetic findings. Curr Opin Allergy Clin Immunol. 2013;13(5):507-13.

19. Borregaard N. Neutrophils, from marrow to microbes. Immunity. 2010;33(5):657-70.

20. Summers C, Rankin SM, Condliffe AM, Singh N, Peters AM, Chilvers ER. Neutrophil kinetics in health and disease. Trends Immunol. 2010;31(8):318-24.

21. Amulic B, Cazalet C, Hayes GL, Metzler KD, Zychlinsky A. Neutrophil function: from mechanisms to disease. Annu Rev Immunol. 2012;30:459-89.

22. Carmona-Rivera C, Kaplan MJ. Low-density granulocytes: a distinct class of neutrophils in systemic autoimmunity. Semin Immunopathol. 2013;35(4):455-63.

23. Dumitru CA, Moses K, Trellakis S, Lang S, Brandau S. Neutrophils and granulocytic myeloid-derived suppressor cells: immunophenotyping, cell biology and clinical relevance in human oncology. Cancer Immunol Immunother. 2012;61(8):1155-67.

24. Christensen RD. Hematopoiesis in the fetus and neonate. Pediatr Res. 1989;26(6):531-5.

25. Zhang P, Iwasaki-Arai J, Iwasaki H, Fenyus ML, Dayaram T, Owens BM, et al. Enhancement of hematopoietic stem cell repopulating capacity and self-renewal in the absence of the transcription factor C/EBP alpha. Immunity. 2004;21(6):853-63.

26. Lawrence SM, Corriden R, Nizet V. The Ontogeny of a Neutrophil: Mechanisms of Granulopoiesis and Homeostasis. Microbiol Mol Biol Rev. 2018;82(1).

27. da Silva FM, Massart-Leen AM, Burvenich C. Development and maturation of neutrophils. Vet Q. 1994;16(4):220-5.

28. Hirai H, Zhang P, Dayaram T, Hetherington CJ, Mizuno S, Imanishi J, et al. C/EBPbeta is required for 'emergency' granulopoiesis. Nat Immunol. 2006;7(7):732-9.

29. Gullberg U, Bengtsson N, Bulow E, Garwicz D, Lindmark A, Olsson I. Processing and targeting of granule proteins in human neutrophils. J Immunol Methods. 1999;232(1-2):201-10.

30. Valent P. The phenotype of human eosinophils, basophils, and mast cells. J Allergy Clin Immunol. 1994;94(6 Pt 2):1177-83.

31. Kulessa H, Frampton J, Graf T. GATA-1 reprograms avian myelomonocytic cell lines into eosinophils, thromboblasts, and erythroblasts. Genes Dev. 1995;9(10):1250-62.

32. Ward AC, Loeb DM, Soede-Bobok AA, Touw IP, Friedman AD. Regulation of granulopoiesis by transcription factors and cytokine signals. Leukemia. 2000;14(6):973-90.

33. Smith BR. Regulation of hematopoiesis. Yale J Biol Med. 1990;63(5):371-80.

34. Pitrak DL. Effects of granulocyte colony-stimulating factor and granulocyte-macrophage colony-stimulating factor on the bactericidal functions of neutrophils. Curr Opin Hematol. 1997;4(3):183-90.

35. Basu S, Hodgson G, Zhang HH, Katz M, Quilici C, Dunn AR. "Emergency" granulopoiesis in G-CSF-deficient mice in response to Candida albicans infection. Blood. 2000;95(12):3725-33.

36. Vacek A, Hofer M, Hola J, Weiterova L, Streitova D, Svoboda J. The role of G-CSF and IL-6 in the granulopoiesis-stimulating activity of murine blood serum induced by perorally administered ultrafiltered pig leukocyte extract, IMUNOR. Int Immunopharmacol. 2007;7(5):656-61.

37. Singh P, Hu P, Hoggatt J, Moh A, Pelus LM. Expansion of bone marrow neutrophils following G-CSF administration in mice results in osteolineage cell apoptosis and mobilization of hematopoietic stem and progenitor cells. Leukemia. 2012;26(11):2375-83.

38. Tsuji T, Sugimoto K, Yanai T, Takashita E, Mori KJ. Induction of granulocyte-macrophage colony-stimulating factor (GM-CSF) and granulocyte colony-stimulating factor (G-CSF) expression in bone marrow and fractionated marrow cell populations by interleukin 3 (IL-3): IL-3-mediated positive feedback mechanisms of granulopoiesis. Growth Factors. 1994;11(1):71-9.

39. Hohaus S, Petrovick MS, Voso MT, Sun Z, Zhang DE, Tenen DG. PU.1 (Spi-1) and C/EBP alpha regulate expression of the granulocyte-macrophage colony-stimulating factor receptor alpha gene. Mol Cell Biol. 1995;15(10):5830-45.

40. Halene S, Gaines P, Sun H, Zibello T, Lin S, Khanna-Gupta A, et al. C/EBPepsilon directs granulocytic-vs-monocytic lineage determination and confers chemotactic function via Hlx. Exp Hematol. 2010;38(2):90-103.

41. Oelgeschlager M, Nuchprayoon I, Luscher B, Friedman AD. C/EBP, c-Myb, and PU.1 cooperate to regulate the neutrophil elastase promoter. Mol Cell Biol. 1996;16(9):4717-25.

42. Lekstrom-Himes JA. The role of C/EBP(epsilon) in the terminal stages of granulocyte differentiation. Stem Cells. 2001;19(2):125-33.

43. Austin GE, Chan WC, Zhao W, Racine M. Myeloperoxidase gene expression in normal granulopoiesis and acute leukemias. Leuk Lymphoma. 1994;15(3-4):209-26.

44. Tian SS, Lamb P, Seidel HM, Stein RB, Rosen J. Rapid activation of the STAT3 transcription factor by granulocyte colony-stimulating factor. Blood. 1994;84(6):1760-4.

45. Litherland SA, Xie TX, Grebe KM, Davoodi-Semiromi A, Elf J, Belkin NS, et al. Signal transduction activator of transcription 5 (STAT5) dysfunction in autoimmune monocytes and macrophages. J Autoimmun. 2005;24(4):297-310.

46. Korkmaz B, Horwitz MS, Jenne DE, Gauthier F. Neutrophil elastase, proteinase 3, and cathepsin G as therapeutic targets in human diseases. Pharmacol Rev. 2010;62(4):726-59.

47. Nolte MA. SLPI is essential for granulopoiesis. Blood. 2014;123(8):1121-3.

48. Potera RM, Jensen MJ, Hilkin BM, South GK, Hook JS, Gross EA, et al. Neutrophil azurophilic granule exocytosis is primed by TNF-alpha and partially regulated by NADPH oxidase. Innate Immun. 2016;22(8):635-46.

49. Cieutat AM, Lobel P, August JT, Kjeldsen L, Sengelov H, Borregaard N, et al. Azurophilic granules of human neutrophilic leukocytes are deficient in lysosome-associated membrane proteins but retain the mannose 6-phosphate recognition marker. Blood. 1998;91(3):1044-58.

50. Ullyot JL, Bainton DF. Azurophil and specific granules of blood neutrophils in chronic myelogenous leukemia: an ultrastructural and cytochemical analysis. Blood. 1975;45(4):469-82.

51. Ambruso DR, Johnston RB, Jr. Lactoferrin enhances hydroxyl radical production by human neutrophils, neutrophil particulate fractions, and an enzymatic generating system. J Clin Invest. 1981;67(2):352-60.

52. Yamanaka R, Barlow C, Lekstrom-Himes J, Castilla LH, Liu PP, Eckhaus M, et al. Impaired granulopoiesis, myelodysplasia, and early lethality in CCAAT/enhancer binding protein epsilon-deficient mice. Proc Natl Acad Sci U S A. 1997;94(24):13187-92.

53. Jacobsen LC, Theilgaard-Monch K, Christensen EI, Borregaard N. Arginase 1 is expressed in myelocytes/metamyelocytes and localized in gelatinase granules of human neutrophils. Blood. 2007;109(7):3084-7.

54. Sengelov H, Kjeldsen L, Kroeze W, Berger M, Borregaard N. Secretory vesicles are the intracellular reservoir of complement receptor 1 in human neutrophils. J Immunol. 1994;153(2):804-10.

55. Faurschou M, Borregaard N. Neutrophil granules and secretory vesicles in inflammation. Microbes Infect. 2003;5(14):1317-27.

56. Bugl S, Wirths S, Radsak MP, Schild H, Stein P, Andre MC, et al. Steady-state neutrophil homeostasis is dependent on TLR4/TRIF signaling. Blood. 2013;121(5):723-33.

57. Cain DW, Snowden PB, Sempowski GD, Kelsoe G. Inflammation triggers emergency granulopoiesis through a density-dependent feedback mechanism. PLoS One. 2011;6(5):e19957.

58. Eash KJ, Greenbaum AM, Gopalan PK, Link DC. CXCR2 and CXCR4 antagonistically regulate neutrophil trafficking from murine bone marrow. J Clin Invest. 2010;120(7):2423-31.

59. Nguyen-Jackson H, Panopoulos AD, Zhang H, Li HS, Watowich SS. STAT3 controls the neutrophil migratory response to CXCR2 ligands by direct activation of G-CSF-induced CXCR2 expression and via modulation of CXCR2 signal transduction. Blood. 2010;115(16):3354-63.

60. de Oliveira S, Rosowski EE, Huttenlocher A. Neutrophil migration in infection and wound repair: going forward in reverse. Nat Rev Immunol. 2016;16(6):378-91.

61. Tavares N, Afonso L, Suarez M, Ampuero M, Prates DB, Araujo-Santos T, et al. Degranulating Neutrophils Promote Leukotriene B4 Production by Infected Macrophages To Kill Leishmania amazonensis Parasites. J Immunol. 2016;196(4):1865-73.

62. Lee PY, Kumagai Y, Xu Y, Li Y, Barker T, Liu C, et al. IL-1alpha modulates neutrophil recruitment in chronic inflammation induced by hydrocarbon oil. J Immunol. 2011;186(3):1747-54.

63. de Oliveira S, Reyes-Aldasoro CC, Candel S, Renshaw SA, Mulero V, Calado A. Cxcl8 (IL-8) mediates neutrophil recruitment and behavior in the zebrafish inflammatory response. J Immunol. 2013;190(8):4349-59.

64. Gane J, Stockley R. Mechanisms of neutrophil transmigration across the vascular endothelium in COPD. Thorax. 2012;67(6):553-61.

65. Lyck R, Enzmann G. The physiological roles of ICAM-1 and ICAM-2 in neutrophil migration into tissues. Curr Opin Hematol. 2015;22(1):53-9.

66. Yang L, Froio RM, Sciuto TE, Dvorak AM, Alon R, Luscinskas FW. ICAM-1 regulates neutrophil adhesion and transcellular migration of TNF-alpha-activated vascular endothelium under flow. Blood. 2005;106(2):584-92.

67. Walter UM, Issekutz AC. The role of E- and P-selectin in neutrophil and monocyte migration in adjuvant-induced arthritis in the rat. Eur J Immunol. 1997;27(6):1498-505.

68. von Andrian UH, Chambers JD, Berg EL, Michie SA, Brown DA, Karolak D, et al. L-selectin mediates neutrophil rolling in inflamed venules through sialyl LewisX-dependent and -independent recognition pathways. Blood. 1993;82(1):182-91.

69. Choi EY, Santoso S, Chavakis T. Mechanisms of neutrophil transendothelial migration. Front Biosci (Landmark Ed). 2009;14:1596-605.

70. Sullivan DP, Muller WA. Neutrophil and monocyte recruitment by PECAM, CD99, and other molecules via the LBRC. Semin Immunopathol. 2014;36(2):193-209.

71. Lenglet S, Mach F, Montecucco F. Role of matrix metalloproteinase-8 in atherosclerosis. Mediators Inflamm. 2013;2013:659282.

72. Ong CW, Pabisiak PJ, Brilha S, Singh P, Roncaroli F, Elkington PT, et al. Complex regulation of neutrophil-derived MMP-9 secretion in central nervous system tuberculosis. J Neuroinflammation. 2017;14(1):31.

73. Kolaczkowska E, Kubes P. Neutrophil recruitment and function in health and inflammation. Nat Rev Immunol. 2013;13(3):159-75.

74. Rozman S, Yousefi S, Oberson K, Kaufmann T, Benarafa C, Simon HU. The generation of neutrophils in the bone marrow is controlled by autophagy. Cell Death Differ. 2015;22(3):445-56.

75. Navarini AA, Lang KS, Verschoor A, Recher M, Zinkernagel AS, Nizet V, et al. Innate immune-induced depletion of bone marrow neutrophils aggravates systemic bacterial infections. Proc Natl Acad Sci U S A. 2009;106(17):7107-12.

76. Nomellini V, Brubaker AL, Mahbub S, Palmer JL, Gomez CR, Kovacs EJ. Dysregulation of neutrophil CXCR2 and pulmonary endothelial icam-1 promotes age-related pulmonary inflammation. Aging Dis. 2012;3(3):234-47.

77. Silva MT. Macrophage phagocytosis of neutrophils at inflammatory/infectious foci: a cooperative mechanism in the control of infection and infectious inflammation. J Leukoc Biol. 2011;89(5):675-83.

78. Azzouz D, Palaniyar N. ApoNETosis: discovery of a novel form of neutrophil death with concomitant apoptosis and NETosis. Cell Death Dis. 2018;9(8):839.

79. Spitznagel JK, Shafer WM. Neutrophil killing of bacteria by oxygen-independent mechanisms: a historical summary. Rev Infect Dis. 1985;7(3):398-403.

80. Lu T, Porter AR, Kennedy AD, Kobayashi SD, DeLeo FR. Phagocytosis and killing of Staphylococcus aureus by human neutrophils. J Innate Immun. 2014;6(5):639-49.

81. Sorensen OE, Borregaard N. Neutrophil extracellular traps - the dark side of neutrophils. J Clin Invest. 2016;126(5):1612-20.

82. Kaplan MJ, Radic M. Neutrophil extracellular traps: double-edged swords of innate immunity. J Immunol. 2012;189(6):2689-95.

83. Mocsai A. Diverse novel functions of neutrophils in immunity, inflammation, and beyond. J Exp Med. 2013;210(7):1283-99.

84. Moens E, Veldhoen M. Epithelial barrier biology: good fences make good neighbours. Immunology. 2012;135(1):1-8.

85. Ito T. PAMPs and DAMPs as triggers for DIC. J Intensive Care. 2014;2(1):67.

86. McDonald B, Pittman K, Menezes GB, Hirota SA, Slaba I, Waterhouse CC, et al. Intravascular danger signals guide neutrophils to sites of sterile inflammation. Science. 2010;330(6002):362-6.

87. van Kessel KP, Bestebroer J, van Strijp JA. Neutrophil-Mediated Phagocytosis of Staphylococcus aureus. Front Immunol. 2014;5:467.

88. Chen Y, Junger WG. Measurement of oxidative burst in neutrophils. Methods Mol Biol. 2012;844:115-24.

89. Jablonska E, Puzewska W, Marcinczyk M, Grabowska Z, Jablonski J. iNOS expression and NO production by neutrophils in cancer patients. Arch Immunol Ther Exp (Warsz). 2005;53(2):175-9.

90. Eash KJ, Means JM, White DW, Link DC. CXCR4 is a key regulator of neutrophil release from the bone marrow under basal and stress granulopoiesis conditions. Blood. 2009;113(19):4711-9.

91. Mayadas TN, Cullere X, Lowell CA. The multifaceted functions of neutrophils. Annu Rev Pathol. 2014;9:181-218.

92. Abi Abdallah DS, Egan CE, Butcher BA, Denkers EY. Mouse neutrophils are professional antigen-presenting cells programmed to instruct Th1 and Th17 T-cell differentiation. Int Immunol. 2011;23(5):317-26.

93. Sangaletti S, Tripodo C, Chiodoni C, Guarnotta C, Cappetti B, Casalini P, et al. Neutrophil extracellular traps mediate transfer of cytoplasmic neutrophil antigens to myeloid dendritic cells toward ANCA induction and associated autoimmunity. Blood. 2012;120(15):3007-18.

94. Ueda R, Narumi K, Hashimoto H, Miyakawa R, Okusaka T, Aoki K. Interaction of natural killer cells with neutrophils exerts a significant antitumor immunity in hematopoietic stem cell transplantation recipients. Cancer Med. 2016;5(1):49-60.

95. Yeramilli VA, Knight KL. Requirement for BAFF and APRIL during B cell development in GALT. J Immunol. 2010;184(10):5527-36.

96. Coquery CM, Wade NS, Loo WM, Kinchen JM, Cox KM, Jiang C, et al. Neutrophils contribute to excess serum BAFF levels and promote CD4+ T cell and B cell responses in lupus-prone mice. PLoS One. 2014;9(7):e102284.

97. Rosales C. Neutrophil: A Cell with Many Roles in Inflammation or Several Cell Types? Front Physiol. 2018;9:113.

98. Zhang D, Chen G, Manwani D, Mortha A, Xu C, Faith JJ, et al. Neutrophil ageing is regulated by the microbiome. Nature. 2015;525(7570):528-32.

99. Adrover JM, Nicolas-Avila JA, Hidalgo A. Aging: A Temporal Dimension for Neutrophils. Trends Immunol. 2016;37(5):334-45.

100. Gifford AM, Chalmers JD. The role of neutrophils in cystic fibrosis. Curr Opin Hematol. 2014;21(1):16-22.

101. Ingersoll SA, Laval J, Forrest OA, Preininger M, Brown MR, Arafat D, et al. Mature cystic fibrosis airway neutrophils suppress T cell function: evidence for a role of arginase 1 but not programmed death-ligand 1. J Immunol. 2015;194(11):5520-8.

102. Perobelli SM, Galvani RG, Goncalves-Silva T, Xavier CR, Nobrega A, Bonomo A. Plasticity of neutrophils reveals modulatory capacity. Braz J Med Biol Res. 2015;48(8):665-75.

103. Fridlender ZG, Sun J, Kim S, Kapoor V, Cheng G, Ling L, et al. Polarization of tumor-associated neutrophil phenotype by TGF-beta: "N1" versus "N2" TAN. Cancer Cell. 2009;16(3):183-94.

104. Andzinski L, Kasnitz N, Stahnke S, Wu CF, Gereke M, von Kockritz-Blickwede M, et al. Type I IFNs induce anti-tumor polarization of tumor associated neutrophils in mice and human. Int J Cancer. 2016;138(8):1982-93.

105. Andzinski L, Wu CF, Lienenklaus S, Kroger A, Weiss S, Jablonska J. Delayed apoptosis of tumor associated neutrophils in the absence of endogenous IFN-beta. Int J Cancer. 2015;136(3):572-83.

106. De Larco JE, Wuertz BR, Furcht LT. The potential role of neutrophils in promoting the metastatic phenotype of tumors releasing interleukin-8. Clin Cancer Res. 2004;10(15):4895-900.

107. Eruslanov EB, Bhojnagarwala PS, Quatromoni JG, Stephen TL, Ranganathan A, Deshpande C, et al. Tumor-associated neutrophils stimulate T cell responses in early-stage human lung cancer. J Clin Invest. 2014;124(12):5466-80.

108. Christoffersson G, Vagesjo E, Vandooren J, Liden M, Massena S, Reinert RB, et al. VEGF-A recruits a proangiogenic MMP-9-delivering neutrophil subset that induces angiogenesis in transplanted hypoxic tissue. Blood. 2012;120(23):4653-62.

109. Gabrilovich DI, Bronte V, Chen SH, Colombo MP, Ochoa A, Ostrand-Rosenberg S, et al. The terminology issue for myeloid-derived suppressor cells. Cancer Res. 2007;67(1):425; author reply 6.

110. Marini O, Costa S, Bevilacqua D, Calzetti F, Tamassia N, Spina C, et al. Mature CD10(+) and immature CD10(-) neutrophils present in G-CSF-treated donors display opposite effects on T cells. Blood. 2017;129(10):1343-56.

111. Kostlin N, Vogelmann M, Spring B, Schwarz J, Feucht J, Hartel C, et al. Granulocytic myeloid-derived suppressor cells from human cord blood modulate T-helper cell response towards an anti-inflammatory phenotype. Immunology. 2017;152(1):89-101.

112. Brandau S, Trellakis S, Bruderek K, Schmaltz D, Steller G, Elian M, et al. Myeloid-derived suppressor cells in the peripheral blood of cancer patients contain a subset of immature neutrophils with impaired migratory properties. J Leukoc Biol. 2011;89(2):311-7.

113. Condamine T, Dominguez GA, Youn JI, Kossenkov AV, Mony S, Alicea-Torres K, et al. Lectin-type oxidized LDL receptor-1 distinguishes population of human polymorphonuclear myeloid-derived suppressor cells in cancer patients. Sci Immunol. 2016;1(2).

114. Bruger AM, Dorhoi A, Esendagli G, Barczyk-Kahlert K, van der Bruggen P, Lipoldova M, et al. How to measure the immunosuppressive activity of MDSC: assays, problems and potential solutions. Cancer Immunol Immunother. 2019;68(4):631-44.

115. Veglia F, Perego M, Gabrilovich D. Myeloid-derived suppressor cells coming of age. Nat Immunol. 2018;19(2):108-19.

116. Bai M, Grieshaber-Bouyer R, Wang J, Schmider AB, Wilson ZS, Zeng L, et al. CD177 modulates human neutrophil migration through activation-mediated integrin and chemoreceptor regulation. Blood. 2017;130(19):2092-100.

117. Bauer S, Abdgawad M, Gunnarsson L, Segelmark M, Tapper H, Hellmark T. Proteinase 3 and CD177 are expressed on the plasma membrane of the same subset of neutrophils. J Leukoc Biol. 2007;81(2):458-64.

118. Hu N, Mora-Jensen H, Theilgaard-Monch K, Doornbos-van der Meer B, Huitema MG, Stegeman CA, et al. Differential expression of granulopoiesis related genes in neutrophil subsets distinguished by membrane expression of CD177. PLoS One. 2014;9(6):e99671.

119. Liu W, Yan M, Sugui JA, Li H, Xu C, Joo J, et al. Olfm4 deletion enhances defense against Staphylococcus aureus in chronic granulomatous disease. J Clin Invest. 2013;123(9):3751-5.

120. Clemmensen SN, Bohr CT, Rorvig S, Glenthoj A, Mora-Jensen H, Cramer EP, et al. Olfactomedin 4 defines a subset of human neutrophils. J Leukoc Biol. 2012;91(3):495-500.

121. Fuchs T, Puellmann K, Scharfenstein O, Eichner R, Stobe E, Becker A, et al. The neutrophil recombinatorial TCR-like immune receptor is expressed across the entire human life span but repertoire diversity declines in old age. Biochem Biophys Res Commun. 2012;419(2):309-15.

122. Pillay J, Kamp VM, van Hoffen E, Visser T, Tak T, Lammers JW, et al. A subset of neutrophils in human systemic inflammation inhibits T cell responses through Mac-1. J Clin Invest. 2012;122(1):327-36.

123. Chen F, Wu W, Millman A, Craft JF, Chen E, Patel N, et al. Neutrophils prime a long-lived effector macrophage phenotype that mediates accelerated helminth expulsion. Nat Immunol. 2014;15(10):938-46.

124. Taylor PR, Roy S, Leal SM, Jr., Sun Y, Howell SJ, Cobb BA, et al. Activation of neutrophils by autocrine IL-17A-IL-17RC interactions during fungal infection is regulated by IL-6, IL-23, RORgammat and dectin-2. Nat Immunol. 2014;15(2):143-51.

125. Scapini P, Cassatella MA. Social networking of human neutrophils within the immune system. Blood. 2014;124(5):710-9.

126. Lasky CE, Jamison KE, Sidelinger DR, Pratt CL, Zhang G, Brown CR. Infection of Interleukin 17 Receptor A-Deficient C3H Mice with Borrelia burgdorferi Does Not Affect Their Development of Lyme Arthritis and Carditis. Infect Immun. 2015;83(7):2882-8.

127. Stark MA, Huo Y, Burcin TL, Morris MA, Olson TS, Ley K. Phagocytosis of apoptotic neutrophils regulates granulopoiesis via IL-23 and IL-17. Immunity. 2005;22(3):285-94.

128. Sabbione F, Gabelloni ML, Ernst G, Gori MS, Salamone G, Oleastro M, et al. Neutrophils suppress gammadelta T-cell function. Eur J Immunol. 2014;44(3):819-30.

129. Zheng L, Hu Y, Wang Y, Huang X, Xu Y, Shen Y, et al. Recruitment of Neutrophils Mediated by Vgamma2 gammadelta T Cells Deteriorates Liver Fibrosis Induced by Schistosoma japonicum Infection in C57BL/6 Mice. Infect Immun. 2017;85(8).

130. Zhang X, Xu W. Neutrophils diminish T-cell immunity to foster gastric cancer progression: the role of GM-CSF/PD-L1/PD-1 signalling pathway. Gut. 2017;66(11):1878-80.

131. Nagaraj S, Gabrilovich DI. Regulation of suppressive function of myeloid-derived suppressor cells by CD4+ T cells. Semin Cancer Biol. 2012;22(4):282-8.

132. Munn DH, Shafizadeh E, Attwood JT, Bondarev I, Pashine A, Mellor AL. Inhibition of T cell proliferation by macrophage tryptophan catabolism. J Exp Med. 1999;189(9):1363-72.

133. Ohl K, Tenbrock K. Reactive Oxygen Species as Regulators of MDSC-Mediated Immune Suppression. Front Immunol. 2018;9:2499.

134. Wegner A, Verhagen J, Wraith DC. Myeloid-derived suppressor cells mediate tolerance induction in autoimmune disease. Immunology. 2017;151(1):26-42.

135. Dietlin TA, Hofman FM, Lund BT, Gilmore W, Stohlman SA, van der Veen RC. Mycobacteria-induced Gr-1+ subsets from distinct myeloid lineages have opposite effects on T cell expansion. J Leukoc Biol. 2007;81(5):1205-12.

136. Fleming V, Hu X, Weber R, Nagibin V, Groth C, Altevogt P, et al. Targeting Myeloid-Derived Suppressor Cells to Bypass Tumor-Induced Immunosuppression. Front Immunol. 2018;9:398.

137. Rodriguez PC, Ochoa AC, Al-Khami AA. Arginine Metabolism in Myeloid Cells Shapes Innate and Adaptive Immunity. Front Immunol. 2017;8:93.

138. Raber P, Ochoa AC, Rodriguez PC. Metabolism of L-arginine by myeloid-derived suppressor cells in cancer: mechanisms of T cell suppression and therapeutic perspectives. Immunol Invest. 2012;41(6-7):614-34.

139. Monu NR, Frey AB. Myeloid-derived suppressor cells and anti-tumor T cells: a complex relationship. Immunol Invest. 2012;41(6-7):595-613.

140. Siegel RL, Miller KD, Jemal A. Cancer statistics, 2019. CA Cancer J Clin. 2019;69(1):7-34.

141. Cakir Edis E, Karlikaya C. The cost of lung cancer in Turkey. Tuberk Toraks. 2007;55(1):51-8.

142. Yilmaz HH, Yazihan N, Tunca D, Sevinc A, Olcayto EO, Ozgul N, et al. Cancer trends and incidence and mortality patterns in Turkey. Jpn J Clin Oncol. 2011;41(1):10-6.

143. Inamura K. Lung Cancer: Understanding Its Molecular Pathology and the 2015 WHO Classification. Front Oncol. 2017;7:193.

144. Spella M, Lilis I, Stathopoulos GT. Shared epithelial pathways to lung repair and disease. Eur Respir Rev. 2017;26(144).

145. Sen M, Akeno N, Reece A, Miller AL, Simpson DS, Wikenheiser-Brokamp KA. p16 controls epithelial cell growth and suppresses carcinogenesis through mechanisms that do not require RB1 function. Oncogenesis. 2017;6(4):e320.

146. Gomperts BN, Spira A, Massion PP, Walser TC, Wistuba, II, Minna JD, et al. Evolving concepts in lung carcinogenesis. Semin Respir Crit Care Med. 2011;32(1):32-43.

147. Elizegi E, Pino I, Vicent S, Blanco D, Saffiotti U, Montuenga LM. Hyperplasia of alveolar neuroendocrine cells in rat lung carcinogenesis by silica with selective expression of proadrenomedullin-derived peptides and amidating enzymes. Lab Invest. 2001;81(12):1627-38.

148. Sutherland KD, Berns A. Cell of origin of lung cancer. Mol Oncol. 2010;4(5):397-403.

149. Li L, Li JC, Yang H, Zhang X, Liu LL, Li Y, et al. Expansion of cancer stem cell pool initiates lung cancer recurrence before angiogenesis. Proc Natl Acad Sci U S A. 2018;115(38):E8948-E57.

150. Xu X, Rock JR, Lu Y, Futtner C, Schwab B, Guinney J, et al. Evidence for type II cells as cells of origin of K-Ras-induced distal lung adenocarcinoma. Proc Natl Acad Sci U S A. 2012;109(13):4910-5.

151. Jeong C, Lee J, Ryu S, Lee HY, Shin AY, Kim JS, et al. A Case of Ectopic Adrenocorticotropic Hormone Syndrome in Small Cell Lung Cancer. Tuberc Respir Dis (Seoul). 2015;78(4):436-9.

152. Chen Z, Fillmore CM, Hammerman PS, Kim CF, Wong KK. Non-small-cell lung cancers: a heterogeneous set of diseases. Nat Rev Cancer. 2014;14(8):535-46.

153. Ho C, Tong KM, Ramsden K, Ionescu DN, Laskin J. Histologic classification of non-small-cell lung cancer over time: reducing the rates of not-otherwise-specified. Curr Oncol. 2015;22(3):e164-70.

154. Rigden HM, Alias A, Havelock T, O'Donnell R, Djukanovic R, Davies DE, et al. Squamous Metaplasia Is Increased in the Bronchial Epithelium of Smokers with Chronic Obstructive Pulmonary Disease. PLoS One. 2016;11(5):e0156009.

155. Yan W, Wistuba, II, Emmert-Buck MR, Erickson HS. Squamous Cell Carcinoma - Similarities and Differences among Anatomical Sites. Am J Cancer Res. 2011;1(3):275-300.

156. Pao W, Miller V, Zakowski M, Doherty J, Politi K, Sarkaria I, et al. EGF receptor gene mutations are common in lung cancers from "never smokers" and are associated with sensitivity of tumors to gefitinib and erlotinib. Proc Natl Acad Sci U S A. 2004;101(36):13306-11.

157. Turk M, Yildirim F, Yurdakul AS, Ozturk C. Hospitalization costs of lung cancer diagnosis in Turkey: Is there a difference between histological types and stages? Tuberk Toraks. 2016;64(4):263-8.

158. Knowles MR, Boucher RC. Mucus clearance as a primary innate defense mechanism for mammalian airways. J Clin Invest. 2002;109(5):571-7.

159. Chen L, Deng H, Cui H, Fang J, Zuo Z, Deng J, et al. Inflammatory responses and inflammation-associated diseases in organs. Oncotarget. 2018;9(6):7204-18.

160. Binnewies M, Roberts EW, Kersten K, Chan V, Fearon DF, Merad M, et al. Understanding the tumor immune microenvironment (TIME) for effective therapy. Nat Med. 2018;24(5):541-50.

161. Stankovic B, Bjorhovde HAK, Skarshaug R, Aamodt H, Frafjord A, Muller E, et al. Immune Cell Composition in Human Non-small Cell Lung Cancer. Front Immunol. 2018;9:3101.

162. Langer CJ, Besse B, Gualberto A, Brambilla E, Soria JC. The evolving role of histology in the management of advanced non-small-cell lung cancer. J Clin Oncol. 2010;28(36):5311-20.

163. Seo JS, Kim A, Shin JY, Kim YT. Comprehensive analysis of the tumor immune micro-environment in non-small cell lung cancer for efficacy of checkpoint inhibitor. Sci Rep. 2018;8(1):14576.

164. Romero Vielva L. Tumor lymphocytic infiltration in non-small cell lung cancer: the ultimate prognostic marker? Transl Lung Cancer Res. 2016;5(4):370-2.

165. Mittal D, Gubin MM, Schreiber RD, Smyth MJ. New insights into cancer immunoediting and its three component phases--elimination, equilibrium and escape. Curr Opin Immunol. 2014;27:16-25.

166. Kim R, Emi M, Tanabe K. Cancer immunoediting from immune surveillance to immune escape. Immunology. 2007;121(1):1-14.

167. Hernandez-Martinez JM, Vergara E, Montes-Servin E, Arrieta O. Interplay between immune cells in lung cancer: beyond T lymphocytes. Transl Lung Cancer Res. 2018;7(Suppl 4):S336-S40.

168. Hiraoka K, Miyamoto M, Cho Y, Suzuoki M, Oshikiri T, Nakakubo Y, et al. Concurrent infiltration by CD8+ T cells and CD4+ T cells is a favourable prognostic factor in non-small-cell lung carcinoma. Br J Cancer. 2006;94(2):275-80.

169. Ohri CM, Shikotra A, Green RH, Waller DA, Bradding P. Macrophages within NSCLC tumour islets are predominantly of a cytotoxic M1 phenotype associated with extended survival. Eur Respir J. 2009;33(1):118-26.

170. Jackute J, Zemaitis M, Pranys D, Sitkauskiene B, Miliauskas S, Vaitkiene S, et al. Distribution of M1 and M2 macrophages in tumor islets and stroma in relation to prognosis of non-small cell lung cancer. BMC Immunol. 2018;19(1):3.

171. Torres-Duran M, Ruano-Ravina A, Kelsey KT, Parente-Lamelas I, Leiro-Fernandez V, Abdulkader I, et al. Environmental tobacco smoke exposure and EGFR and ALK alterations in never smokers' lung cancer. Results from the LCRINS study. Cancer Lett. 2017;411:130-5.

172. Salvatore V, Teti G, Focaroli S, Mazzotti MC, Mazzotti A, Falconi M. The tumor microenvironment promotes cancer progression and cell migration. Oncotarget. 2017;8(6):9608-16.

173. Kim Y, Kang H, Powathil G, Kim H, Trucu D, Lee W, et al. Role of extracellular matrix and microenvironment in regulation of tumor growth and LAR-mediated invasion in glioblastoma. PLoS One. 2018;13(10):e0204865.

174. Embgenbroich M, Burgdorf S. Current Concepts of Antigen Cross-Presentation. Front Immunol. 2018;9:1643.

175. Cerezo-Wallis D, Soengas MS. Understanding Tumor-Antigen Presentation in the New Era of Cancer Immunotherapy. Curr Pharm Des. 2016;22(41):6234-50.

176. Escors D. Tumour immunogenicity, antigen presentation and immunological barriers in cancer immunotherapy. New J Sci. 2014;2014.

177. Dieu-Nosjean MC, Antoine M, Danel C, Heudes D, Wislez M, Poulot V, et al. Long-term survival for patients with non-small-cell lung cancer with intratumoral lymphoid structures. J Clin Oncol. 2008;26(27):4410-7.

178. Suzuki K, Kachala SS, Kadota K, Shen R, Mo Q, Beer DG, et al. Prognostic immune markers in non-small cell lung cancer. Clin Cancer Res. 2011;17(16):5247-56.

179. Schernberg A, Mezquita L, Boros A, Botticella A, Caramella C, Besse B, et al. Neutrophilia as prognostic biomarker in locally advanced stage III lung cancer. PLoS One. 2018;13(10):e0204490.

180. Phan TT, Ho TT, Nguyen HT, Nguyen HT, Tran TB, Nguyen ST. The prognostic impact of neutrophil to lymphocyte ratio in advanced non-small cell lung cancer patients treated with EGFR TKI. Int J Gen Med. 2018;11:423-30.

181. Tao H, Mimura Y, Aoe K, Kobayashi S, Yamamoto H, Matsuda E, et al. Prognostic potential of FOXP3 expression in non-small cell lung cancer cells combined with tumor-infiltrating regulatory T cells. Lung Cancer. 2012;75(1):95-101.

182. Punt S, Langenhoff JM, Putter H, Fleuren GJ, Gorter A, Jordanova ES. The correlations between IL-17 vs. Th17 cells and cancer patient survival: a systematic review. Oncoimmunology. 2015;4(2):e984547.

183. Tian C, Lu S, Fan Q, Zhang W, Jiao S, Zhao X, et al. Prognostic significance of tumor-infiltrating CD8(+) or CD3(+) T lymphocytes and interleukin-2 expression in radically resected non-small cell lung cancer. Chin Med J (Engl). 2015;128(1):105-10.

184. Ito N, Suzuki Y, Taniguchi Y, Ishiguro K, Nakamura H, Ohgi S. Prognostic significance of T helper 1 and 2 and T cytotoxic 1 and 2 cells in patients with non-small cell lung cancer. Anticancer Res. 2005;25(3B):2027-31.

185. Miotto D, Lo Cascio N, Stendardo M, Querzoli P, Pedriali M, De Rosa E, et al. CD8+ T cells expressing IL-10 are associated with a favourable prognosis in lung cancer. Lung Cancer. 2010;69(3):355-60.

186. Yuan A, Hsiao YJ, Chen HY, Chen HW, Ho CC, Chen YY, et al. Opposite Effects of M1 and M2 Macrophage Subtypes on Lung Cancer Progression. Sci Rep. 2015;5:14273.

187. Wang TT, Zhao YL, Peng LS, Chen N, Chen W, Lv YP, et al. Tumour-activated neutrophils in gastric cancer foster immune suppression and disease progression through GM-CSF-PD-L1 pathway. Gut. 2017;66(11):1900-11.

188. Eruslanov EB. Phenotype and function of tumor-associated neutrophils and their subsets in early-stage human lung cancer. Cancer Immunol Immunother. 2017;66(8):997-1006.

189. Lemos HP, Grespan R, Vieira SM, Cunha TM, Verri WA, Jr., Fernandes KS, et al. Prostaglandin mediates IL-23/IL-17-induced neutrophil migration in inflammation by inhibiting IL-12 and IFNgamma production. Proc Natl Acad Sci U S A. 2009;106(14):5954-9.

190. Kargl J, Busch SE, Yang GH, Kim KH, Hanke ML, Metz HE, et al. Neutrophils dominate the immune cell composition in non-small cell lung cancer. Nat Commun. 2017;8:14381.

191. Yin Y, Wang J, Wang X, Gu L, Pei H, Kuai S, et al. Prognostic value of the neutrophil to lymphocyte ratio in lung cancer: A meta-analysis. Clinics. 2015;70(7):524-30.

192. Esendagli G, Bruderek K, Goldmann T, Busche A, Branscheid D, Vollmer E, et al. Malignant and non-malignant lung tissue areas are differentially populated by natural killer cells and regulatory T cells in non-small cell lung cancer. Lung Cancer. 2008;59(1):32-40.

193. Kiriu T, Yamamoto M, Nagano T, Hazama D, Sekiya R, Katsurada M, et al. The time-series behavior of neutrophil-to-lymphocyte ratio is useful as a predictive marker in non-small cell lung cancer. PLoS One. 2018;13(2):e0193018.

194. Nguyen HH, Kim T, Song SY, Park S, Cho HH, Jung SH, et al. Naive CD8(+) T cell derived tumor-specific cytotoxic effectors as a potential remedy for overcoming TGF-beta immunosuppression in the tumor microenvironment. Sci Rep. 2016;6:28208.

195. Trojan A, Urosevic M, Dummer R, Giger R, Weder W, Stahel RA. Immune activation status of CD8+ T cells infiltrating non-small cell lung cancer. Lung Cancer. 2004;44(2):143-7.

196. Appleman LJ, Boussiotis VA. T cell anergy and costimulation. Immunol Rev. 2003;192:161-80.

197. Esensten JH, Helou YA, Chopra G, Weiss A, Bluestone JA. CD28 Costimulation: From Mechanism to Therapy. Immunity. 2016;44(5):973-88.

198. Gong J, Chehrazi-Raffle A, Reddi S, Salgia R. Development of PD-1 and PD-L1 inhibitors as a form of cancer immunotherapy: a comprehensive review of registration trials and future considerations. J Immunother Cancer. 2018;6(1):8.

199. Spranger S, Spaapen RM, Zha Y, Williams J, Meng Y, Ha TT, et al. Up-regulation of PD-L1, IDO, and T(regs) in the melanoma tumor microenvironment is driven by CD8(+) T cells. Sci Transl Med. 2013;5(200):200ra116.

200. Miura Y, Sunaga N. Role of Immunotherapy for Oncogene-Driven Non-Small Cell Lung Cancer. Cancers (Basel). 2018;10(8).

201. Gong K, Guo G, Gerber DE, Gao B, Peyton M, Huang C, et al. TNF-driven adaptive response mediates resistance to EGFR inhibition in lung cancer. J Clin Invest. 2018;128(6):2500-18.

202. Thumallapally N, Parylo S, Vennepureddy A, Ibrahim U, Sokoloff A. Synchronous Presence of EGFR, ALK Driver Mutations Along With PD L1 Overexpression in a Resected Early Stage Non-Small Cell Lung Cancer: A Case Report and Review of Literature. World J Oncol. 2018;9(2):50-5.

203. Sheng J, Fang W, Yu J, Chen N, Zhan J, Ma Y, et al. Expression of programmed death ligand-1 on tumor cells varies pre and post chemotherapy in non-small cell lung cancer. Sci Rep. 2016;6:20090.

204. Berge EM, Doebele RC. Targeted therapies in non-small cell lung cancer: emerging oncogene targets following the success of epidermal growth factor receptor. Semin Oncol. 2014;41(1):110-25.

205. Mooradian MJ, Gainor JF. Putting the brakes on CTLA-4 inhibition in lung cancer? Transl Lung Cancer Res. 2018;7(Suppl 1):S35-S8.

206. Rieth J, Subramanian S. Mechanisms of Intrinsic Tumor Resistance to Immunotherapy. Int J Mol Sci. 2018;19(5).

207. Mulder C, Prust N, van Doorn S, Reinecke M, Kuster B, van Bergen En Henegouwen P, et al. Adaptive Resistance to EGFR-Targeted Therapy by Calcium Signaling in NSCLC Cells. Mol Cancer Res. 2018;16(11):1773-84.

208. Wang P, Huang B, Gao Y, Yang J, Liang Z, Zhang N, et al. CD103(+)CD8(+) T lymphocytes in non-small cell lung cancer are phenotypically and functionally primed to respond to PD-1 blockade. Cell Immunol. 2018;325:48-55.

209. Lu Y, Hong B, Li H, Zheng Y, Zhang M, Wang S, et al. Tumor-specific IL-9-producing CD8+ Tc9 cells are superior effector than type-I cytotoxic Tc1 cells for adoptive immunotherapy of cancers. Proc Natl Acad Sci U S A. 2014;111(6):2265-70.

210. Flores-Santibanez F, Cuadra B, Fernandez D, Rosemblatt MV, Nunez S, Cruz P, et al. In Vitro-Generated Tc17 Cells Present a Memory Phenotype and Serve As a Reservoir of Tc1 Cells In Vivo. Front Immunol. 2018;9:209.

211. Dobrzanski MJ, Reome JB, Hollenbaugh JA, Dutton RW. Tc1 and Tc2 effector cell therapy elicit long-term tumor immunity by contrasting mechanisms that result in complementary endogenous type 1 antitumor responses. J Immunol. 2004;172(3):1380-90.

212. Yu Y, Cho HI, Wang D, Kaosaard K, Anasetti C, Celis E, et al. Adoptive transfer of Tc1 or Tc17 cells elicits antitumor immunity against established melanoma through distinct mechanisms. J Immunol. 2013;190(4):1873-81.

213. Murata M. Inflammation and cancer. Environ Health Prev Med. 2018;23(1):50.

214. Multhoff G, Molls M, Radons J. Chronic inflammation in cancer development. Front Immunol. 2011;2:98.

215. Lizotte PH, Ivanova EV, Awad MM, Jones RE, Keogh L, Liu H, et al. Multiparametric profiling of non-small-cell lung cancers reveals distinct immunophenotypes. JCI Insight. 2016;1(14):e89014.

216. Olazabal IM, Martin-Cofreces NB, Mittelbrunn M, Martinez del Hoyo G, Alarcon B, Sanchez-Madrid F. Activation outcomes induced in naive CD8 T-cells by macrophages primed via "phagocytic" and nonphagocytic pathways. Mol Biol Cell. 2008;19(2):701-10.

217. Kimura S, Sone S, Takahashi K, Uyama T, Ogura T, Monden Y. Antitumour potential of pleural cavity macrophages in lung cancer patients without malignant effusion. Br J Cancer. 1989;59(4):535-9.

218. Siziopikou KP, Harris JE, Casey L, Nawas Y, Braun DP. Impaired tumoricidal function of alveolar macrophages from patients with non-small cell lung cancer. Cancer. 1991;68(5):1035-44.

219. Conway EM, Pikor LA, Kung SH, Hamilton MJ, Lam S, Lam WL, et al. Macrophages, Inflammation, and Lung Cancer. Am J Respir Crit Care Med. 2016;193(2):116-30.

220. Jin S, Deng Y, Hao JW, Li Y, Liu B, Yu Y, et al. NK cell phenotypic modulation in lung cancer environment. PLoS One. 2014;9(10):e109976.

221. Zhang H, Li ZL, Ye SB, Ouyang LY, Chen YS, He J, et al. Myeloid-derived suppressor cells inhibit T cell proliferation in human extranodal NK/T cell lymphoma: a novel prognostic indicator. Cancer Immunol Immunother. 2015;64(12):1587-99.

222. Ito H, Seishima M. Regulation of the induction and function of cytotoxic T lymphocytes by natural killer T cell. J Biomed Biotechnol. 2010;2010:641757.

223. Ladanyi A, Kiss J, Somlai B, Gilde K, Fejos Z, Mohos A, et al. Density of DC-LAMP(+) mature dendritic cells in combination with activated T lymphocytes infiltrating primary cutaneous melanoma is a strong independent prognostic factor. Cancer Immunol Immunother. 2007;56(9):1459-69.

224. Colbeck EJ, Ager A, Gallimore A, Jones GW. Tertiary Lymphoid Structures in Cancer: Drivers of Antitumor Immunity, Immunosuppression, or Bystander Sentinels in Disease? Front Immunol. 2017;8:1830.

225. Zhang L, Yang X, Sun Z, Li J, Zhu H, Li J, et al. Dendritic cell vaccine and cytokine-induced killer cell therapy for the treatment of advanced non-small cell lung cancer. Oncol Lett. 2016;11(4):2605-10.

226. Perrot I, Blanchard D, Freymond N, Isaac S, Guibert B, Pacheco Y, et al. Dendritic cells infiltrating human non-small cell lung cancer are blocked at immature stage. J Immunol. 2007;178(5):2763-9.

227. Bergeron A, El-Hage F, Kambouchner M, Lecossier D, Tazi A. Characterisation of dendritic cell subsets in lung cancer micro-environments. Eur Respir J. 2006;28(6):1170-7.

228. Wang SS, Liu W, Ly D, Xu H, Qu L, Zhang L. Tumor-infiltrating B cells: their role and application in anti-tumor immunity in lung cancer. Cell Mol Immunol. 2019;16(1):6-18.

229. Bruno TC, Ebner PJ, Moore BL, Squalls OG, Waugh KA, Eruslanov EB, et al. Antigen-Presenting Intratumoral B Cells Affect CD4(+) TIL Phenotypes in Non-Small Cell Lung Cancer Patients. Cancer Immunol Res. 2017;5(10):898-907.

230. Nelson BH. CD20+ B cells: the other tumor-infiltrating lymphocytes. J Immunol. 2010;185(9):4977-82.

231. Liu J, Wang H, Yu Q, Zheng S, Jiang Y, Liu Y, et al. Aberrant frequency of IL-10-producing B cells and its association with Treg and MDSC cells in Non Small Cell Lung Carcinoma patients. Hum Immunol. 2016;77(1):84-9.

232. Carlini MJ, Dalurzo MC, Lastiri JM, Smith DE, Vasallo BC, Puricelli LI, et al. Mast cell phenotypes and microvessels in non-small cell lung cancer and its prognostic significance. Hum Pathol. 2010;41(5):697-705.

233. Welsh TJ, Green RH, Richardson D, Waller DA, O'Byrne KJ, Bradding P. Macrophage and mast-cell invasion of tumor cell islets confers a marked survival advantage in non-small-cell lung cancer. J Clin Oncol. 2005;23(35):8959-67.

234. Wolf BJ, Choi JE, Exley MA. Novel Approaches to Exploiting Invariant NKT Cells in Cancer Immunotherapy. Front Immunol. 2018;9:384.

235. Konishi J, Yamazaki K, Yokouchi H, Shinagawa N, Iwabuchi K, Nishimura M. The characteristics of human NKT cells in lung cancer--CD1d independent cytotoxicity against lung cancer cells by NKT cells and decreased human NKT cell response in lung cancer patients. Hum Immunol. 2004;65(11):1377-88.

236. Pandit R, Scholnik A, Wulfekuhler L, Dimitrov N. Non-small-cell lung cancer associated with excessive eosinophilia and secretion of interleukin-5 as a paraneoplastic syndrome. Am J Hematol. 2007;82(3):234-7.

237. Ellis TN, Beaman BL. Interferon-gamma activation of polymorphonuclear neutrophil function. Immunology. 2004;112(1):2-12.

238. Wittmann S, Frohlich D, Daniels S. Characterization of the human fMLP receptor in neutrophils and in Xenopus oocytes. Br J Pharmacol. 2002;135(6):1375-82.

239. Nguyen GT, Green ER, Mecsas J. Neutrophils to the ROScue: Mechanisms of NADPH Oxidase Activation and Bacterial Resistance. Front Cell Infect Microbiol. 2017;7:373.

240. Kinhult J, Egesten A, Benson M, Uddman R, Cardell LO. Increased expression of surface activation markers on neutrophils following migration into the nasal lumen. Clin Exp Allergy. 2003;33(8):1141-6.

241. Frauwirth KA, Thompson CB. Activation and inhibition of lymphocytes by costimulation. J Clin Invest. 2002;109(3):295-9.

242. Stoiber W, Obermayer A, Steinbacher P, Krautgartner WD. The Role of Reactive Oxygen Species (ROS) in the Formation of Extracellular Traps (ETs) in Humans. Biomolecules. 2015;5(2):702-23.

243. Ojlert AK, Halvorsen AR, Nebdal D, Lund-Iversen M, Solberg S, Brustugun OT, et al. The immune microenvironment in non-small cell lung cancer is predictive of prognosis after surgery. Mol Oncol. 2019;13(5):1166-79.

244. Leone K, Poggiana C, Zamarchi R. The Interplay between Circulating Tumor Cells and the Immune System: From Immune Escape to Cancer Immunotherapy. Diagnostics (Basel). 2018;8(3).

245. Heidenreich A, Rawal SK, Szkarlat K, Bogdanova N, Dirix L, Stenzl A, et al. A randomized, double-blind, multicenter, phase 2 study of a human monoclonal antibody to human alphanu integrins (intetumumab) in combination with docetaxel and prednisone for the first-line treatment of patients with metastatic castration-resistant prostate cancer. Ann Oncol. 2013;24(2):329-36.

246. Raab-Westphal S, Marshall JF, Goodman SL. Integrins as Therapeutic Targets: Successes and Cancers. Cancers (Basel). 2017;9(9).

247. Levitzki A. Targeting the Immune System to Fight Cancer Using Chemical Receptor Homing Vectors Carrying Polyinosine/Cytosine (PolyIC). Front Oncol. 2012;2:4.

248. Wang T, Liu G, Wang R. The Intercellular Metabolic Interplay between Tumor and Immune Cells. Front Immunol. 2014;5:358.

249. Uribe-Querol E, Rosales C. Neutrophils in Cancer: Two Sides of the Same Coin. J Immunol Res. 2015;2015:983698.

250. Selders GS, Fetz AE, Radic MZ, Bowlin GL. An overview of the role of neutrophils in innate immunity, inflammation and host-biomaterial integration. Regen Biomater. 2017;4(1):55-68.

251. Abdel-Salam BK, Ebaid H. Expression of CD11b and CD18 on polymorphonuclear neutrophils stimulated with interleukin-2. Cent Eur J Immunol. 2014;39(2):209-15.

252. Potts JR, Farahi N, Heard S, Chilvers ER, Verma S, Peters AM. Circulating granulocyte lifespan in compensated alcohol-related cirrhosis: a pilot study. Physiol Rep. 2016;4(17).

253. Souza LR, Silva E, Calloway E, Cabrera C, McLemore ML. G-CSF activation of AKT is not sufficient to prolong neutrophil survival. J Leukoc Biol. 2013;93(6):883-93.

254. Riyapa D, Buddhisa S, Korbsrisate S, Cuccui J, Wren BW, Stevens MP, et al. Neutrophil extracellular traps exhibit antibacterial activity against burkholderia pseudomallei and are influenced by bacterial and host factors. Infect Immun. 2012;80(11):3921-9.

255. Belikov AV, Schraven B, Simeoni L. T cells and reactive oxygen species. J Biomed Sci. 2015;22:85.

256. Yarosz EL, Chang CH. The Role of Reactive Oxygen Species in Regulating T Cell-mediated Immunity and Disease. Immune Netw. 2018;18(1):e14.

257. Barquero-Calvo E, Martirosyan A, Ordonez-Rueda D, Arce-Gorvel V, Alfaro-Alarcon A, Lepidi H, et al. Neutrophils exert a suppressive effect on Th1

responses to intracellular pathogen Brucella abortus. PLoS Pathog. 2013;9(2):e1003167.

258. de Kleijn S, Langereis JD, Leentjens J, Kox M, Netea MG, Koenderman L, et al. IFN-gamma-stimulated neutrophils suppress lymphocyte proliferation through expression of PD-L1. PLoS One. 2013;8(8):e72249.

259. Shi H, Bi H, Sun X, Dong H, Jiang Y, Mu H, et al. Antitumor effects of Tubeimoside-1 in NCI-H1299 cells are mediated by microRNA-126-5p-induced inactivation of VEGF-A/VEGFR-2/ERK signaling pathway. Mol Med Rep. 2018;17(3):4327-36.

260. Foster KA, Oster CG, Mayer MM, Avery ML, Audus KL. Characterization of the A549 cell line as a type II pulmonary epithelial cell model for drug metabolism. Exp Cell Res. 1998;243(2):359-66.

261. Salomon JJ, Muchitsch VE, Gausterer JC, Schwagerus E, Huwer H, Daum N, et al. The cell line NCl-H441 is a useful in vitro model for transport studies of human distal lung epithelial barrier. Mol Pharm. 2014;11(3):995-1006.

262. Gazdar AF, Girard L, Lockwood WW, Lam WL, Minna JD. Lung cancer cell lines as tools for biomedical discovery and research. J Natl Cancer Inst. 2010;102(17):1310-21.

263. Wistuba, II, Bryant D, Behrens C, Milchgrub S, Virmani AK, Ashfaq R, et al. Comparison of features of human lung cancer cell lines and their corresponding tumors. Clin Cancer Res. 1999;5(5):991-1000.

264. Parsonage G, Filer A, Bik M, Hardie D, Lax S, Howlett K, et al. Prolonged, granulocyte-macrophage colony-stimulating factor-dependent, neutrophil survival following rheumatoid synovial fibroblast activation by IL-17 and TNFalpha. Arthritis Res Ther. 2008;10(2):R47.

265. Wang X, Qiu L, Li Z, Wang XY, Yi H. Understanding the Multifaceted Role of Neutrophils in Cancer and Autoimmune Diseases. Front Immunol. 2018;9:2456.

266. Shaul ME, Levy L, Sun J, Mishalian I, Singhal S, Kapoor V, et al. Tumor-associated neutrophils display a distinct N1 profile following TGFbeta modulation: A transcriptomics analysis of pro- vs. antitumor TANs. Oncoimmunology. 2016;5(11):e1232221.

267. Ma Z, Finkel TH. T cell receptor triggering by force. Trends Immunol. 2010;31(1):1-6.

268. Schmidt D, Joyce EJ, Kao WJ. Fetal bovine serum xenoproteins modulate human monocyte adhesion and protein release on biomaterials in vitro. Acta Biomater. 2011;7(2):515-25.

269. Mortha A, Burrows K. Cytokine Networks between Innate Lymphoid Cells and Myeloid Cells. Front Immunol. 2018;9:191.

270. Chen L, Flies DB. Molecular mechanisms of T cell co-stimulation and co-inhibition. Nat Rev Immunol. 2013;13(4):227-42.

271. Hernandez-Chacon JA, Li Y, Wu RC, Bernatchez C, Wang Y, Weber JS, et al. Costimulation through the CD137/4-1BB pathway protects human melanoma

tumor-infiltrating lymphocytes from activation-induced cell death and enhances antitumor effector function. J Immunother. 2011;34(3):236-50.

272. Ren F, Zhao T, Liu B, Pan L. Neutrophil-lymphocyte ratio (NLR) predicted prognosis for advanced non-small-cell lung cancer (NSCLC) patients who received immune checkpoint blockade (ICB). Onco Targets Ther. 2019;12:4235-44.

273. Yang HB, Xing M, Ma LN, Feng LX, Yu Z. Prognostic significance of neutrophil-lymphocyteratio/platelet-lymphocyteratioin lung cancers: a meta-analysis. Oncotarget. 2016;7(47):76769-78.

274. Li H, Huang N, Zhu W, Wu J, Yang X, Teng W, et al. Modulation the crosstalk between tumor-associated macrophages and non-small cell lung cancer to inhibit tumor migration and invasion by ginsenoside Rh2. BMC Cancer. 2018;18(1):579.

275. Roussos ET, Condeelis JS, Patsialou A. Chemotaxis in cancer. Nat Rev Cancer. 2011;11(8):573-87.

276. Spicer JD, McDonald B, Cools-Lartigue JJ, Chow SC, Giannias B, Kubes P, et al. Neutrophils promote liver metastasis via Mac-1-mediated interactions with circulating tumor cells. Cancer Res. 2012;72(16):3919-27.

277. Kawahara T, Furuya K, Nakamura M, Sakamaki K, Osaka K, Ito H, et al. Neutrophil-to-lymphocyte ratio is a prognostic marker in bladder cancer patients after radical cystectomy. BMC Cancer. 2016;16:185.

278. Schreiner J, Thommen DS, Herzig P, Bacac M, Klein C, Roller A, et al. Expression of inhibitory receptors on intratumoral T cells modulates the activity of a T cell-bispecific antibody targeting folate receptor. Oncoimmunology. 2016;5(2):e1062969.

279. Joller N, Kuchroo VK. Tim-3, Lag-3, and TIGIT. Curr Top Microbiol Immunol. 2017;410:127-56.

280. Anderson AC, Joller N, Kuchroo VK. Lag-3, Tim-3, and TIGIT: Co-inhibitory Receptors with Specialized Functions in Immune Regulation. Immunity. 2016;44(5):989-1004.

281. Legat A, Speiser DE, Pircher H, Zehn D, Fuertes Marraco SA. Inhibitory Receptor Expression Depends More Dominantly on Differentiation and Activation than "Exhaustion" of Human CD8 T Cells. Front Immunol. 2013;4:455.

282. Sabins NC, Chornoguz O, Leander K, Kaplan F, Carter R, Kinder M, et al. TIM-3 Engagement Promotes Effector Memory T Cell Differentiation of Human Antigen-Specific CD8 T Cells by Activating mTORC1. J Immunol. 2017;199(12):4091-102.

283. Yoon SH, Yun SO, Park JY, Won HY, Kim EK, Sohn HJ, et al. Selective addition of CXCR3(+) CCR4(-) CD4(+) Th1 cells enhances generation of cytotoxic T cells by dendritic cells in vitro. Exp Mol Med. 2009;41(3):161-70.

284. Wu X, Zhang H, Xing Q, Cui J, Li J, Li Y, et al. PD-1(+) CD8(+) T cells are exhausted in tumours and functional in draining lymph nodes of colorectal cancer patients. Br J Cancer. 2014;111(7):1391-9.

285. Turnis ME, Andrews LP, Vignali DA. Inhibitory receptors as targets for cancer immunotherapy. Eur J Immunol. 2015;45(7):1892-905.

286. Lee S, Margolin K. Cytokines in cancer immunotherapy. Cancers (Basel). 2011;3(4):3856-93.

287. Ribas A. Adaptive Immune Resistance: How Cancer Protects from Immune Attack. Cancer Discov. 2015;5(9):915-9.

288. Chauhan P, Lokensgard JR. Glial Cell Expression of PD-L1. Int J Mol Sci. 2019;20(7).

289. Kansy BA, Concha-Benavente F, Srivastava RM, Jie HB, Shayan G, Lei Y, et al. PD-1 Status in CD8(+) T Cells Associates with Survival and Anti-PD-1 Therapeutic Outcomes in Head and Neck Cancer. Cancer Res. 2017;77(22):6353-64.

290. Anderson KG, Stromnes IM, Greenberg PD. Obstacles Posed by the Tumor Microenvironment to T cell Activity: A Case for Synergistic Therapies. Cancer Cell. 2017;31(3):311-25.

291. Fujita K, Iwama H, Oura K, Tadokoro T, Samukawa E, Sakamoto T, et al. Cancer Therapy Due to Apoptosis: Galectin-9. Int J Mol Sci. 2017;18(1).

292. Jiang J, Jin MS, Kong F, Cao D, Ma HX, Jia Z, et al. Decreased galectin-9 and increased Tim-3 expression are related to poor prognosis in gastric cancer. PLoS One. 2013;8(12):e81799.

293. Das M, Zhu C, Kuchroo VK. Tim-3 and its role in regulating anti-tumor immunity. Immunol Rev. 2017;276(1):97-111.

294. Du W, Yang M, Turner A, Xu C, Ferris RL, Huang J, et al. TIM-3 as a Target for Cancer Immunotherapy and Mechanisms of Action. Int J Mol Sci. 2017;18(3).

295. Long L, Zhang X, Chen F, Pan Q, Phiphatwatchara P, Zeng Y, et al. The promising immune checkpoint LAG-3: from tumor microenvironment to cancer immunotherapy. Genes Cancer. 2018;9(5-6):176-89.

296. Huang RY, Eppolito C, Lele S, Shrikant P, Matsuzaki J, Odunsi K. LAG3 and PD1 co-inhibitory molecules collaborate to limit CD8+ T cell signaling and dampen antitumor immunity in a murine ovarian cancer model. Oncotarget. 2015;6(29):27359-77.

297. Buchbinder EI, Desai A. CTLA-4 and PD-1 Pathways: Similarities, Differences, and Implications of Their Inhibition. Am J Clin Oncol. 2016;39(1):98-106.

298. Seidel JA, Otsuka A, Kabashima K. Anti-PD-1 and Anti-CTLA-4 Therapies in Cancer: Mechanisms of Action, Efficacy, and Limitations. Front Oncol. 2018;8:86.

299. Silva EM, Mariano VS, Pastrez PRA, Pinto MC, Castro AG, Syrjanen KJ, et al. High systemic IL-6 is associated with worse prognosis in patients with non-small cell lung cancer. PLoS One. 2017;12(7):e0181125.

300. Yang R, Masters AR, Fortner KA, Champagne DP, Yanguas-Casas N, Silberger DJ, et al. IL-6 promotes the differentiation of a subset of naive CD8+ T cells into IL-21-producing B helper CD8+ T cells. J Exp Med. 2016;213(11):2281-91.

301. Nowacki TM, Kuerten S, Zhang W, Shive CL, Kreher CR, Boehm BO, et al. Granzyme B production distinguishes recently activated CD8(+) memory cells from resting memory cells. Cell Immunol. 2007;247(1):36-48.

302. Bhat P, Leggatt G, Waterhouse N, Frazer IH. Interferon-gamma derived from cytotoxic lymphocytes directly enhances their motility and cytotoxicity. Cell Death Dis. 2017;8(6):e2836.

303. Zelinskyy G, Robertson SJ, Schimmer S, Messer RJ, Hasenkrug KJ, Dittmer U. CD8+ T-cell dysfunction due to cytolytic granule deficiency in persistent Friend retrovirus infection. J Virol. 2005;79(16):10619-26.

304. O'Brien S, Thomas RM, Wertheim GB, Zhang F, Shen H, Wells AD. Ikaros imposes a barrier to CD8+ T cell differentiation by restricting autocrine IL-2 production. J Immunol. 2014;192(11):5118-29.

305. Tau GZ, Cowan SN, Weisburg J, Braunstein NS, Rothman PB. Regulation of IFN-gamma signaling is essential for the cytotoxic activity of CD8(+) T cells. J Immunol. 2001;167(10):5574-82.

306. Governa V, Trella E, Mele V, Tornillo L, Amicarella F, Cremonesi E, et al. The Interplay Between Neutrophils and CD8(+) T Cells Improves Survival in Human Colorectal Cancer. Clin Cancer Res. 2017;23(14):3847-58.

307. Sharpe AH. Mechanisms of costimulation. Immunol Rev. 2009;229(1):5-11.

308. Capece D, Verzella D, Fischietti M, Zazzeroni F, Alesse E. Targeting costimulatory molecules to improve antitumor immunity. J Biomed Biotechnol. 2012;2012:926321.

309. Bandyopadhyay S, Long M, Qui HZ, Hagymasi AT, Slaiby AM, Mihalyo MA, et al. Self-antigen prevents CD8 T cell effector differentiation by CD134 and CD137 dual costimulation. J Immunol. 2008;181(11):7728-37.

310. Bartkowiak T, Curran MA. 4-1BB Agonists: Multi-Potent Potentiators of Tumor Immunity. Front Oncol. 2015;5:117.

311. Alari-Pahissa E, Notario L, Lorente E, Vega-Ramos J, Justel A, Lopez D, et al. CD69 does not affect the extent of T cell priming. PLoS One. 2012;7(10):e48593.

312. Werfel TA, Cook RS. Efferocytosis in the tumor microenvironment. Semin Immunopathol. 2018;40(6):545-54.

313. Barrera L, Montes-Servin E, Hernandez-Martinez JM, Garcia-Vicente MLA, Montes-Servin E, Herrera-Martinez M, et al. CD47 overexpression is associated with decreased neutrophil apoptosis/phagocytosis and poor prognosis in non-small-cell lung cancer patients. Br J Cancer. 2017;117(3):385-97.

314. Urlaub D, Hofer K, Muller ML, Watzl C. LFA-1 Activation in NK Cells and Their Subsets: Influence of Receptors, Maturation, and Cytokine Stimulation. J Immunol. 2017;198(5):1944-51.

315. Kelly CP, O'Keane JC, Orellana J, Schroy PC, 3rd, Yang S, LaMont JT, et al. Human colon cancer cells express ICAM-1 in vivo and support LFA-1-dependent lymphocyte adhesion in vitro. Am J Physiol. 1992;263(6 Pt 1):G864-70.

316. Reina M, Espel E. Role of LFA-1 and ICAM-1 in Cancer. Cancers (Basel). 2017;9(11).

317. Sun B, Qin W, Song M, Liu L, Yu Y, Qi X, et al. Neutrophil Suppresses Tumor Cell Proliferation via Fas /Fas Ligand Pathway Mediated Cell Cycle Arrested. Int J Biol Sci. 2018;14(14):2103-13.

318. Edmondson R, Broglie JJ, Adcock AF, Yang L. Three-dimensional cell culture systems and their applications in drug discovery and cell-based biosensors. Assay Drug Dev Technol. 2014;12(4):207-18.

8.APPENDICES

APPENDIX 1: Ethics Committee Approval

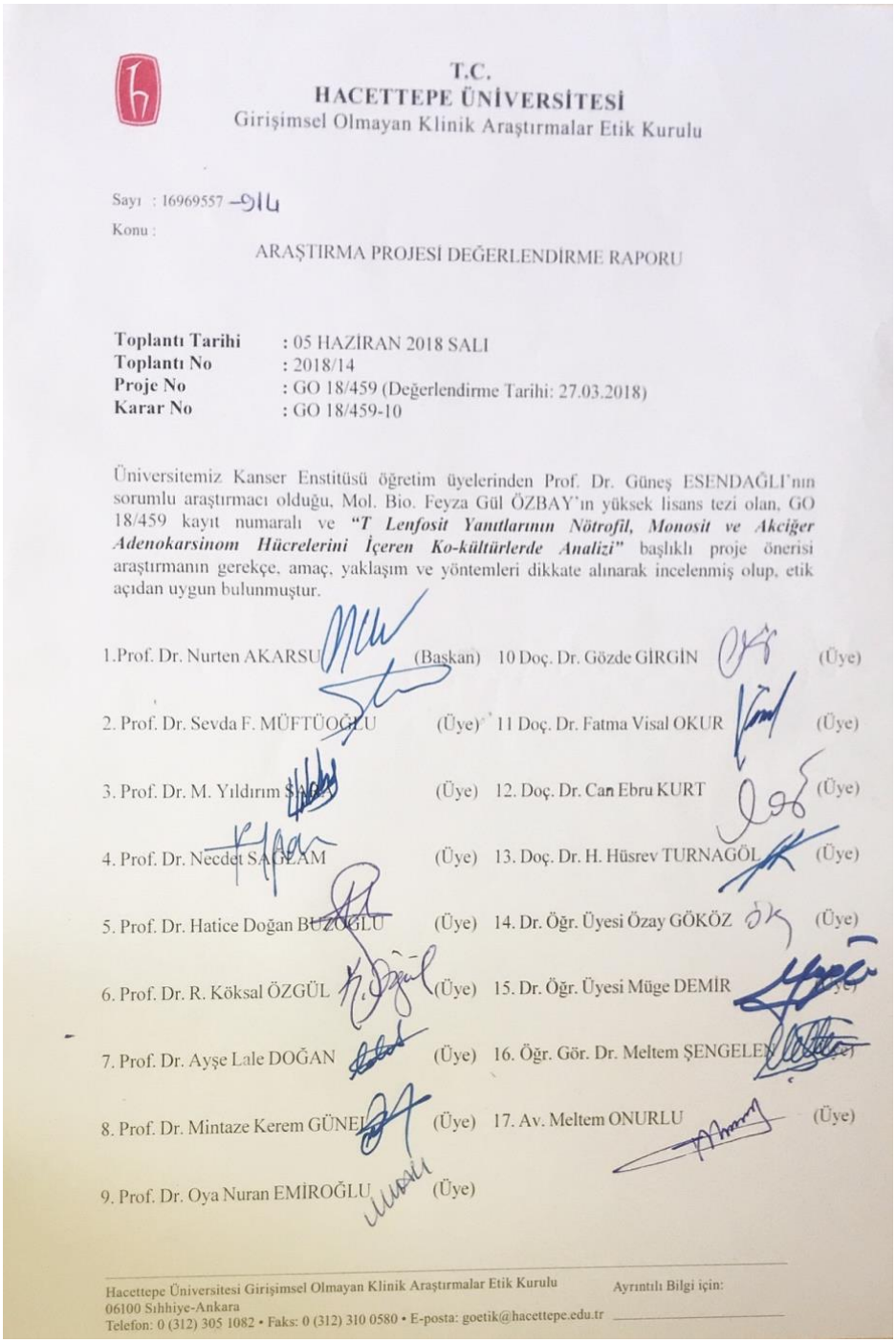

T.C.
HACETTEPE ÜNİVERSİTESİ
Girişimsel Olmayan Klinik Araştırmalar Etik Kurulu

Sayı : 16969557 -911
Konu :

ARAŞTIRMA PROJESİ DEĞERLENDİRME RAPORU

Toplantı Tarihi : 05 HAZİRAN 2018 SALI
Toplantı No : 2018/14
Proje No : GO 18/459 (Değerlendirme Tarihi: 27.03.2018)
Karar No : GO 18/459-10

Üniversitemiz Kanser Enstitüsü öğretim üyelerinden Prof. Dr. Güneş ESENDAĞLI'nın sorumlu araştırmacı olduğu, Mol. Bio. Feyza Gül ÖZBAY'ın yüksek lisans tezi olan, GO 18/459 kayıt numaralı ve ***"T Lenfosit Yanıtlarının Nötrofil, Monosit ve Akciğer Adenokarsinom Hücrelerini İçeren Ko-kültürlerde Analizi"*** başlıklı proje önerisi araştırmanın gerekçe, amaç, yaklaşım ve yöntemleri dikkate alınarak incelenmiş olup, etik açıdan uygun bulunmuştur.

1.Prof. Dr. Nurten AKARSU (Başkan)
2. Prof. Dr. Sevda F. MÜFTÜOĞLU (Üye)
3. Prof. Dr. M. Yıldırım SAĞ (Üye)
4. Prof. Dr. Necdet SAĞLAM (Üye)
5. Prof. Dr. Hatice Doğan BUZOĞLU (Üye)
6. Prof. Dr. R. Köksal ÖZGÜL (Üye)
7. Prof. Dr. Ayşe Lale DOĞAN (Üye)
8. Prof. Dr. Mintaze Kerem GÜNEL (Üye)
9. Prof. Dr. Oya Nuran EMİROĞLU (Üye)
10 Doç. Dr. Gözde GİRGİN (Üye)
11 Doç. Dr. Fatma Visal OKUR (Üye)
12. Doç. Dr. Can Ebru KURT (Üye)
13. Doç. Dr. H. Hüsrev TURNAGÖL (Üye)
14. Dr. Öğr. Üyesi Özay GÖKÖZ (Üye)
15. Dr. Öğr. Üyesi Müge DEMİR (Üye)
16. Öğr. Gör. Dr. Meltem ŞENGELEN (Üye)
17. Av. Meltem ONURLU (Üye)

Hacettepe Üniversitesi Girişimsel Olmayan Klinik Araştırmalar Etik Kurulu
06100 Sıhhiye-Ankara
Telefon: 0 (312) 305 1082 • Faks: 0 (312) 310 0580 • E-posta: goetik@hacettepe.edu.tr

Ayrıntılı Bilgi için:

APPENDIX 2: Scientific meetings where the data of this thesis were presented.

Poster Presentation:

Feyza Gul Ozbay, Gunes Esendagli (2018). Evaluation of helper T cell proliferation in the co-cultures of lung adenocarcinoma cells, neutrophils and monocytes. European Congress of Immunology (ECI 2018), 2-5 September, Amsterdam, Netherland, P.B4.03.12

Feyza Gul Ozbay, Gunes Esendagli (2018). Evaluation of cytotoxic T cell responses in a co-culture model employing neutrophils, monocytes and lung cancer cells. 1st European Symposium on Myeloid Regulatory Cells in Health and Disease (ESMRC), 1-3 November, Essen, Germany.

Feyza Gul Ozbay, Gunes Esendagli (2019). Neutrophils reinforce cytotoxic T cell responses in a co-culture model mimicking tumor microenvironment in lung cancer. International Molecular Immunology and Immunogenetics Congress (MIMIC IV), 27-29 April, Bursa, Turkey.

APPENDIX 3: Thesis Orijinality Report.

TEZİN TAM BAŞLIĞI: EVALUATION OF T CELL RESPONSES IN THE CO-CULTURES ESTABLISHED WITH NEUTROPHILS, MONOCYTES, AND LUNG ADENOCARCINOMA CELLS

ÖĞRENCİNİN ADI SOYADI: FEYZA GÜL ÖZBAY

DOSYANIN TOPLAM SAYFA SAYISI:100

ORIJINALLIK RAPORU

%7	%2	%4	%5
BENZERLIK ENDEKSI	İNTERNET KAYNAKLARI	YAYINLAR	ÖĞRENCI ÖDEVLERI

BIRINCIL KAYNAKLAR

1	Submitted to National University of Singapore Öğrenci Ödevi	%1
2	The Tumor Immunoenvironment, 2013. Yayın	<%1
3	Eruslanov, Evgeniy B., Pratik S. Bhojnagarwala, Jon G. Quatromoni, Tom Li Stephen, Anjana Ranganathan, Charuhas Deshpande, Tatiana Akimova, Anil Vachani, Leslie Litzky, Wayne W. Hancock, José R. Conejo-Garcia, Michael Feldman, Steven M. Albelda, and Sunil Singhal. "Tumor-associated neutrophils stimulate T cell responses in early-stage human lung cancer", Journal of Clinical Investigation, 2014. Yayın	<%1
4	Submitted to University of Hong Kong Öğrenci Ödevi	<%1
5	Submitted to University of Birmingham Öğrenci Ödevi	<%1

APPENDIX 4: Digital Receipt

turnitin

Dijital Makbuz

Bu makbuz ödevinizin Turnitin'e ulaştığını bildirmektedir. Gönderiminize dair bilgiler şöyledir:

Gönderinizin ilk sayfası aşağıda gönderilmektedir.

Gönderen:	Feyza Gül Özbay
Ödev başlığı:	EVALUATION OF T CELL RESPON…
Gönderi Başlığı:	EVALUATION OF T CELL RESPON…
Dosya adı:	Dosya boyutu:23.08M
Sayfa sayısı:	101
Kelime sayısı:	26,223
Karakter sayısı:	155,651
Gönderim Tarihi:	31-Tem-2019 04:17PM (UTC+0300)
Gönderim Numarası:	1156494425

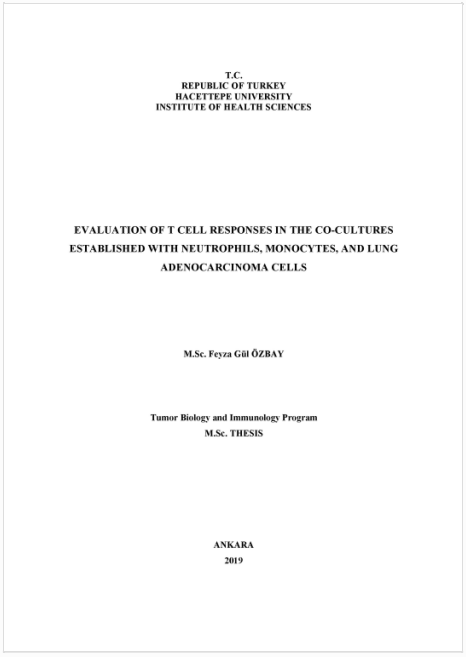

T.C.
REPUBLIC OF TURKEY
HACETTEPE UNIVERSITY
INSTITUTE OF HEALTH SCIENCES

EVALUATION OF T CELL RESPONSES IN THE CO-CULTURES ESTABLISHED WITH NEUTROPHILS, MONOCYTES, AND LUNG ADENOCARCINOMA CELLS

M.Sc. Feyza Gül ÖZBAY

Tumor Biology and Immunology Program
M.Sc. THESIS

ANKARA
2019

Copyright 2019 Turnitin. Tüm hakları saklıdır.

9. CURRICULUM VITAE

Feyza Gül Özbay

Address: 44.cadde 455.sokak 10/5 Aydoğan Apartmanı Çankaya/Ankara

Tel: +09 0506 5012508

E-mail: feyza.ozbay92@gmail.com

EDUCATION

2017-2019 July (Msc)	Hacettepe University Cancer Institute, Tumor Biology and Immunology, Ankara, Turkey
2010-2017 (Bsc)	Bilkent University, Molecular Biology and Genetics, Ankara, Turkey
2006-2010	Dr.Binnaz Ege Dr. Rıdvan Ege Anadolu Lisesi, Ankara, Turkey